DECLARATION

I hereby declare that this thesis has been composed by me, that the work of which it is a record has been carried out by me, and that it has not been accepted in any previous application for a Higher Degree. The work was conducted in the Physical Laboratories of the University of St. Andrews under the supervision of Professor J. F. Allen, F.R.S.

.....

David Watmough

CERTIFICATE

I certify that David John Watmough, B.Sc. (St. A.) has spent nine terms as Research Student in the United College of St. Salvator and St. Leonard, that he has fulfilled the conditions of Ordinance Number 16 of the University Court of St. Andrews and that he is qualified to submit the accompanying thesis in application for the Degree of Doctor of Philosophy.

.... ..

J. F. Allen, Supervisor

ACKNOWLEDGEMENTS

The author wishes to thank:

Professor J. F. Allen, F.R.S., not only for suggesting this research but also for much help and advice.

Professor D. V. Osborne, Dr. D. J. Griffiths, Dr. C. G. Kuper and Dr. J. Wilks for helpful discussions.

Mr. J. McNab for technical assistance.

Mr. R. H. Mitchell for providing a plentiful supply of liquid helium.

The Department of Scientific and Industrial Research for a Research Studentship.

C O N T E N T S

A B S T R A C T

Superflow of liquid helium II under a gravitational potential has been investigated by means of wire-filled tube superleaks[1] and three sizes of Millipore filter[2] in the temperature region 1.2°K to the λ-point. The superleaks, which ranged in size from 1.2×10^{-4} cm to 4×10^{-7} cm, were attached to relatively large reservoirs made partly of glass and partly of thin copper being thus designed to minimise thermal effects. Critical velocity v_c, channel size d, and pressure dependence $\frac{d \log v}{d \log p} = n$ were measured. The magnitude of v_c, 7 cm sec^{-1} for $d = 8.5 \times 10^{-5}$ cm rose to a maximum value of about 14 cm sec^{-1} for $d = 3 \times 10^{-6}$ cm then fell again, but over the whole range of d its magnitude was smaller than that predicted by Feynman's[3] equation $v_c = \frac{\hbar}{md} \ln \frac{d}{a}$.

Values of n together with certain of those obtained in previous investigations[4,5,6] when related to d suggested that there are two regimes of critical flow, the transition between them occurring when $d \sim 10^{-5}$ cm. In order to test this hypothesis pressure gradients were measured by placing manometer tubes at intermediate points along two of the wire-filled tubes, one of size $d = 8 \times 10^{-5}$ cm and the other of size $d = 4 \times 10^{-6}$ cm. In the larger tube an almost uniform pressure gradient extended throughout the channels but in the smaller

one the evidence pointed to the existence of a discontinuous pressure drop probably in the narrowest channel section.

The flow regime $n = 0.3$ in channels of size 10^{-3} cm $> d >$ 10^{-4} cm can be understood in terms of the Gorter-Mellink[7] mutual friction hypothesis. An attempt has been made to explain the transition to the regime $n = 0$. The basis of this argument stems from a theory already proposed by Vinen[8]. It is argued that the rapid decay of vortex lines when $d = 10^{-5}$ cm prevents their propagation into the channels, suppresses the growth of vortex line within the channel and hence also the appearance of the mutual friction force. It is therefore tentatively suggested that some other dissipative mechanism gives rise to the value $n = 0$ when $d < 10^{-5}$ cm.

Evidence obtained from gas flow tests, photomicrographs and in the case of the Millipore filters from electron micrographs indicates that each type of superleak contains not a uniform set of channels but a whole range of sizes. The effect of this spread on the magnitude of v_c was examined and it was concluded that the values of v_c would not be significantly lower than would have been observed using uniform channels. This spread of sizes also prevented the observation of well defined depressions of the onset temperature. However, by measuring the mean flow velocity $\bar{v}$ at temperatures between 1.2°K and the λ-point

indirect evidence was obtained in support of the onset effect.

Measurements of v_c using the filters showed that even in one size of filter the percentage open area varied from sample to sample, but the critical velocities were in fair agreement with those measured using the wire-filled tubes. The index n was generally independent of temperature but in the 1.2×10^{-4} cm size of filter its magnitude was lower than that for comparable sizes of wire-filled tube and n was found to increase with increasing temperature. A simple explanation of the index $n = 0.3$ in the 10^{-6} cm size of filter previously observed by Seki[9] is offered.

References

1. A channel making technique first devised by Allen and Misener (1939) Proc. Roy. Soc. (London) A172, 467.
2. Millipore filters are thin cellulosic porous membranes manufactured by the Millipore Filter Corporation of Bedford, Mass.
3. Feynman, R. P., (1959) Proc. Low Temp. Phys. I ch. II, 36, Ed. C. J. Gorter (North-Holland Publishing Co., Amsterdam).
4. Swim, R. T. and Rorschach, H. E., (1955) Phys. Rev. 97, 25.
5. Winkel, P., Delsing, A. M. J. and Gorter, C. J., (1955) Physica 21, 312.

6. van Alphen, N. M., Olijhoek, J. F. and de Bruyn Ouboter, R. Proc. St. Andrews Symposium on Superfluid Helium, (to be published).

7. Gorter, C. J. and Mellink, J. H., (1949) Physica 15, 285.

8. Vinen, W. P., (1957) Proc. Roy. Soc. (London) A242, 493.

9. Seki, H., (1962) Ph.D. Thesis University of Pennsylvania.

CHAPTER 1

INTRODUCTION

1.1 Some of the properties of liquid He^4

The stable isotopes of helium, He^3 and He^4, hold unique positions in the family of liquids. They are the only substances which exist as liquids in the temperature region close to the absolute zero. Under their respective vapour pressures they remain liquid down to the lowest temperatures so far attained and considerable pressure is required to solidify them.

At 2.18°K, the lambda temperature, the specific heat of liquid He^4 has a maximum and a discontinuity. This behaviour of the specific heat curve is reminiscent of order-disorder phenomena in general such as phase transitions in β-brass and magnetic disordering in ferromagnetics, but there is at present no completely satisfactory theory of this λ-point. Above the λ-point the liquid phase of He^4 is known as He I and below it as He II. He II, unlike He I and He^3, exhibits strange properties and in consequence is termed a superfluid.

The work reported in this thesis is connected with the flow property of He II in narrow channels. Before describing the purpose and design of the present experiments it is helpful first to outline briefly the properties and theories of the superfluid state.

The viscosity η of He II gave the first indication of the non-classical nature of the liquid. Keesom and MacWood (1938) who used the rotating disc method to measure η found it to decrease with decreasing temperature below the λ-point. The magnitude of η was comparable with that of He I. In their investigation of the flow of He II through narrow capillaries, Allen and Misener (1939) found that the viscosity was orders of magnitude smaller.

A further property of the superfluid was revealed when Allen and Jones (1938) discovered the fountain-effect. The essential feature of this phenomenon is that in He II a small temperature gradient results in a corresponding pressure gradient. The observation by Keesom and Keesom (1936) of an enormous internal heat conduction in He II suggested that the liquid was a thermal superconductor. Allen, Peierls and Uddin (1937) showed that the heat conductivity in He II could not be characterised by a large value of the classical thermal conductivity coefficient.

Taken together, the problems of viscosity, the fountain effect and the thermal conductivity suggest that the usual differential equations of macroscopic physics are inapplicable to a description of liquid helium below the λ-point.

1.2 The two fluid model of London, Tisza and Landau

This model, constructed to explain the non-classical behaviour exemplified by the phenomena described in the previous subsection,

remains, even at the present time, the basis of all theories descriptive of the superfluid state of He II. The main assumption is that the liquid consists of two interpenetrating fluids one with density ρ_s called the superfluid and the other with density ρ_n called the normal fluid. The total density of the liquid ρ is the sum of the densities of the two components. At the absolute zero He II is entirely superfluid and at the λ-point entirely normal fluid. The temperature dependence of ρ_n/ρ has been measured experimentally by Andronikashvili (1946). The superfluid corresponds to a single quantum state and as such does not contribute to the entropy of the liquid. The existence of the normal fluid is attributed to thermal excitations. On the basis of the two fluid model Tisza (1938) was able to predict the phenomenon of second sound. This is a temperature wave within the liquid in which total density and pressure remain constant.

In terms of the two fluid model the viscosity paradox is resolved. The rotating disc experiment measures the viscosity of the normal fluid. By way of contrast in narrow channels the normal fluid is immobilised and the flow property of the superfluid is observed. In this latter case the concept of a viscosity has little meaning. The fountain effect is also explained because the raising of the temperature inside a reservoir, connected to a He II bath by a capillary, increases the thermal

excitation of the liquid and so ρ_n/ρ. The superfluid flows into the reservoir until thermal equilibrium is re-established. The heat conduction is thought of rather as an internal convection process in which the normal and the superfluid flow in opposite directions.

1.3 Theories of liquid helium

Support for the two-fluid model stems from two important theories. The first was that of London (1938) based on Bose-Einstein statistics. London sought to explain the properties of liquid helium by considering it to be an ideal Bose-Einstein gas. At a temperature T_c such a gas of non-interacting particles should undergo a kind of condensation. The theoretical transition temperature is given by

$$T_c = (h^2/2\pi mk).(N/2.6)v^{2/3} \qquad (1)$$

and with the constants relevant to helium, equation (1) gives a value for T_c of approximately 3°K. The arguments in favour of this theory are that helium particles, with an even number of nucleons should obey Bose-Einstein statistics and also that since the atoms in the liquid are widely spaced the approximation to a gas should hold. It is an obvious next step to identify the excited particles with the normal fluid and the 'condensed' particles with superfluid. The fraction of molecules that have not

condensed at temperature T is given by

$$\frac{N - n_o}{N} = (T/T_\lambda)^{3/2}$$

It follows that

$$\rho_n/\rho = (T/T_\lambda)^{3/2} \qquad (2)$$

Unfavourable comparison of this equation with the measurements of Andronikashvili led London (1954) to introduce into the energy spectrum of the gas an energy gap Δ. The quantity ρ_n/ρ then becomes

$$\rho_n/\rho = (\frac{T}{T_\lambda})^{3/2} \exp(\Delta/k)(\frac{1}{T_\lambda} - \frac{1}{T}) \qquad (3)$$

Equation (3) has the virtue that it reproduces the measured dependence of ρ_n/ρ on temperature but this is probably to a degree fortuitous.

The second important theory was that of Landau (1941, 1947). He considered the liquid at 0°K as a single quantum state, and imagined the liquid at higher temperatures to be in a weakly excited state. This state he regarded as the net result of a number of individual excitations, thought of as quasi-particles occupying the volume of the liquid and having definite energy [ϵ] and momentum [p] characteristics. Like other liquids helium ought to support compression waves. Landau considered those waves in which the wavelength is large compared with the atomic spacing. These are the so called acoustic quanta (phonons) whose

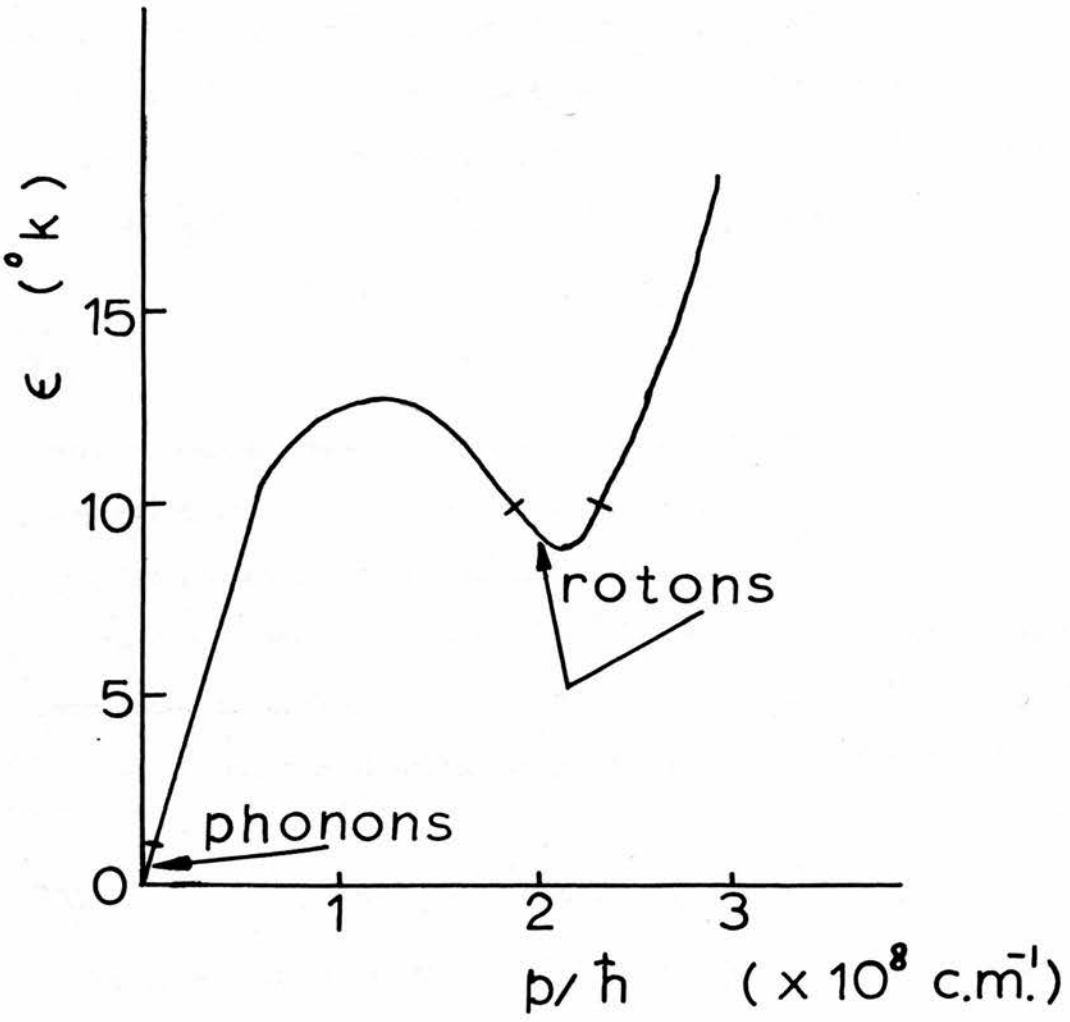

Figure 1.

energy is a linear function of momentum:

$$\varepsilon = cp \tag{4}$$

An analysis of the data on specific heat and the velocity of second sound shows that the temperature dependance of the thermodynamic functions can be explained if the excitation spectrum has the form of Fig 1.

c being the acoustic velocity. ~~For higher values of p experimental data on entropy and specific heat showed that the ε - p relation was similar to that of figure 1~~. In thermal equilibrium the excitations are distributed around the energy ~~minima~~ values $\varepsilon = 0$, $\varepsilon = \Delta$. Near the point $p = p_o$, $\varepsilon(p)$ can be expanded in a power series of terms in $(p - p_o)$. Since $\left(\frac{d\varepsilon}{dp}\right)_{p = p_o} = 0$ there is no linear term and to an approximation ε is given by

$$\varepsilon = \Delta + (p - p_o)^2/2\mu \tag{5}$$

where μ and Δ are constants. The elementary excitations in this second region are called rotons and μ is the roton effective mass.

Above 1.2°K the normal fluid fraction is determined mainly by the roton contribution and ρ_n/ρ can be calculated from the Landau theory if it is assumed that the rotons form an ideal gas. The free energy F of a gas with N particles in a volume V is given by

$$F = - NkT \ln \frac{eV}{N} \int e^{-\varepsilon/kT} \, d\tau_p/(2\pi\hbar)^3 \tag{6}$$

where $d\tau_p = dp_x \, dp_y \, dp_z$ and, $\int = \emptyset$ say. To find the number of particles in the roton gas we note that $(\partial F/\partial N) = 0$, whereupon differentiating (6) gives

$$N_r = V\emptyset \tag{7}$$

and thus for unit mass,

$$N_r = \frac{1}{\rho(2\pi\hbar)^3} \int e^{-\varepsilon/kT} \, d\tau_p \tag{8}$$

Since $d\tau_p = 4\pi p^2 dp$, N_r becomes

$$N_r = \frac{4\pi}{\rho(2\pi\hbar)^3} \left\{ \exp - \Delta/kT \right\} \int p^2 \exp\left\{ \frac{-(p - p_o)^2}{2\mu kT} \right\} dp \tag{9}$$

An approximate solution is obtained by putting $p = p_o$ in (9) in the term before the exponential. Thus, examining the integral only, it is found that

$$\int p_o^2 \exp\{ -(p - p_o)^2/2\mu kT \} \, dp$$

$$\simeq \; p_o^2 \int_{-\infty}^{+\infty} \exp\{ -\xi^2/2\mu kT \} \, d\xi = p_o^2 \sqrt{2\pi\mu kT} \tag{10}$$

Substitution in (9) gives the number of particles in the roton gas

$$N_r = \frac{2(\mu kT)^{\frac{1}{2}} p_o^2}{(2\pi)^{3/2} \rho \hbar^3} \exp(-\Delta/kT) \tag{11}$$

Consider now the distribution function for a gas which moves as a whole. It is obtained by replacing the particle energy ε by $\varepsilon - \underline{p}.\underline{v}$ where $\underline{p}$ is the particle momentum. Thus the total momentum for the gas $\underline{P}$ is

$$\underline{P} = \int \underline{p} \, n(\varepsilon - \underline{p}.\underline{v}) . d\tau_p \tag{12}$$

and for rotons $n(\varepsilon)$ is the Boltzmann distribution function. For small $\underline{v}$ the integrand can be expanded in powers of $\underline{p}\,\underline{v}$, whence

$$\underline{P} = -\int \underline{p}(\underline{p}.\underline{v}) \frac{\partial n(\varepsilon)}{\partial \varepsilon} \, d\tau_p \tag{13}$$

In the Boltzmann distribution

$$\frac{\partial n(\varepsilon)}{\partial \varepsilon} = -\frac{n}{kT} \tag{14}$$

Averaging the integrand in equation (13) over directions of p we have

$$\underline{P} = \frac{\underline{v}}{3kT} \int p^2 \, n(\varepsilon) d\tau_p = \underline{v} \, \frac{\bar{p}^2}{3kT} \rho \, N_r \tag{15}$$

so that ρ_n is given by

$$\rho_n = \frac{\bar{p}^2}{3kT} \rho \, N_r \tag{16}$$

so that from (18), (16) becomes

$$(\rho_n)_r = \frac{2\mu^{\frac{1}{2}} \, p_o^4}{3(2\pi)^{3/2}(kT)^{\frac{1}{2}} \hbar^3} \exp(-\Delta/kT) \tag{17}$$

If the theory were valid for high roton densities then at the λ-point

$$(\rho_n)_{roton} \rightarrow \rho \tag{18}$$

Substituting the condition (18) in (17) gives the variation of ρ_n/ρ with temperature as

$$\frac{\rho_n}{\rho} = \left(\frac{T}{T_\lambda}\right)^{-\frac{1}{2}} \exp \frac{\Delta}{k}\left(\frac{1}{T_\lambda} - \frac{1}{T}\right) \tag{19}$$

This equation is not altogether dissimilar from that obtained by London but the important point is that on both theories the magnitude of ρ_n/ρ is strongly dependent on the size of the energy gap. Kuper (1958) has predicted that Δ will be reduced in the neighbourhood of a solid wall. One consequence of this prediction

is that in sufficiently small channels the onset temperature for superflow will be lower than the λ-temperature.

Feynman (1955) has made the Landau theory more rigorous by showing from first principles why it is that there are no statistically important internal excitations other than those supposed by Landau, namely the phonons and rotons. He then goes on to consider the wave function which represents the state of the fluid when it is in motion. He gives plausibility arguments for assuming that

$$\Psi_{\text{flow}} = [\exp i(\sum_i s\ (\underline{R}_i)]\Phi \qquad (20)$$

where $s(\underline{R})$ is a function varying slowly over distances of a few Å units, and Φ is the ground state wave function of the system. This equation represents the helium flowing with velocity

$$\underline{v}_s = \hbar\, m^{-1} \nabla s \qquad (21)$$

Equation (21) implies that the motion is irrotational. In a simply connected region this means that the superfluid will not rotate. Since $\nabla \times \underline{v}_s = 0$ the circulation about any closed curve which can be shrunk to a point is zero. However in the case of a region enclosing a hole the circulation does not vanish and must have values in multiples of $2\pi\hbar/m$. Thus Feynman shows that the liquid can support vortex-type excitations and that for these

$$\oint \underline{v}_s \cdot \underline{dl} = 2\pi\hbar\, m^{-1} \qquad (22)$$

Although states represented by these lines are not numerous in comparison to the density of roton and phonon states it will be seen (in chapter 2) that they play an important role in determining the flow properties of the liquid.

CHAPTER 2

THE SUPERFLOW OF LIQUID HELIUM II

2.1 The thermohydrodynamic equations

The equations of motion which describe superflow, based on the two fluid model, are

$$\rho_s \frac{Dv_s}{Dt} = \rho_s S \text{ grad } T - \frac{\rho_s}{\rho} \text{ grad } P + F_{sn}(v_s - v_n) + F_s(v_s) \quad (23)$$

and

$$\rho_n \frac{Dv_n}{Dt} = -\rho_s S \text{ grad } T - \frac{\rho_n}{\rho} \text{ grad } P + \eta_n(\nabla^2 v_n + \frac{1}{3} \text{ grad div } v_n) - F_{sn}(v_s - v_n) \quad (24)$$

where D/Dt is an operator defined as

$$D/Dt = \partial/\partial t + v \text{ grad}.$$

In wide capillaries both equations are necessary to specify the flow of He II but in narrow channels where the normal fluid is immobilised by viscous forces equation (23) should provide an adequate description of superflow.

Gorter and Mellink (1949) proposed the existence of a mutual friction force, F_{sn}, between the normal and the superfluid. This was suggested to account for dissipative effects other than those due to normal fluid viscosity. The magnitude of the relative velocity $|v_s - v_n|$ determines the size of this force, which is given

by

$$F_{sn} = A\rho_s/\rho_n |v_s - v_n|^2 (v_s - v_n) \quad v > v_c$$

$$= 0 \qquad\qquad\qquad\qquad v < v_c \qquad (25)$$

where A is constant but depends on temperature and channel size. The velocity at which friction forces, indicated by the terms F_{sn} and $F_s(v_s)$, first appear is called the critical velocity, v_c. There is conflicting evidence on the question of whether it is the quantity $|v_s|$ or $|v_s - v_n|$ which becomes critical. Kidder and Fairbank (1960) found that at supercritical velocities friction occurred between the superfluid and the walls. Vinen (1957) found that it was the relative velocity of the two fluids which determined the onset of dissipative effects. Evidence obtained by Kramers et al (1960) also supports this view. The nature of the mutual friction force was not understood when it was first proposed, but the work of Hall, Vinen, Feynman and Critchlow has led to the belief that it arises from the interaction of phonons and rotons with vortex lines. The theory of mutual friction is more fully discussed in 2.2.

A second friction term $F_s(v_s)$ was introduced into the thermohydrodynamic equations by Atkins (1959). The experiments of Hung et al (1955) suggested the presence, apart from a mutual force, of a minute force proportional to the superfluid velocity. This was not inconsistent with the earlier observation of Allen and Misener

(1939) who found that, at temperatures above 1.7°K and at low pressures, the mean velocity of superflow was proportional to the hydrostatic pressure. Recent work by Bhagat and Mendelssohn (1960) on gravitational flow in capillaries of size ranging down to 88μ indicated the existence of a large linear force but no mutual force. These authors found the mean flow velocity $\bar{v}$ to be a linear function of pressure gradient;

$$\bar{v} = v_c + k(h_i) \text{ grad } p$$

where k is a function of initial level difference. Their interpretation of this regime of flow was based on the concept of an eddy viscosity η_s associated with the superfluid. The pressure dependent part of $\bar{v}$ they wrote as

$$v_p = \frac{a^2}{8} \left\{ \left(\frac{\rho n}{\rho}\right)^2 \frac{1}{\eta_n} + \left(\frac{\rho s}{\rho}\right)^2 \frac{1}{\eta_s} \right\} \text{grad } p \qquad (26)$$

where a is the radius. These authors replaced $F_s(v_s)$ by $\eta_s \nabla^2 v_s$ and in doing so ascribed an eddy viscosity to the superfluid. This complex phenomenon has been discussed by Staas (1961) in terms of normal fluid turbulence but this argument appears to be inapplicable since at 1.3°K, $\rho_n/\rho \ll \rho_s/\rho$ and $\eta_n \sim \eta_s$, which means that the flow is almost entirely that of the superfluid component. Allen and Watmough (1965) have shown that if thermal effects are not minimised a regime resembling laminar flow of a classical liquid can be observed.

ANNULAR SUPERLEAK

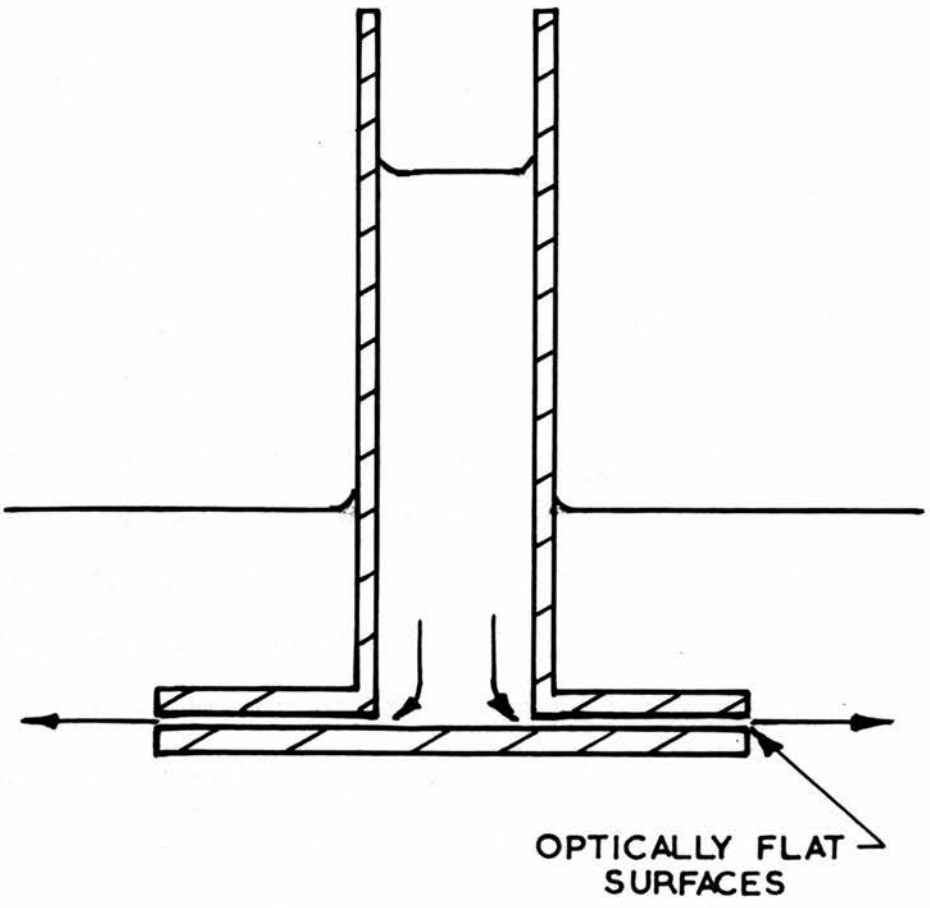

Figure 2.

The flow property of He II in channels smaller than 10^{-4} cm is not well understood and there have been relatively few attempts to make quantitative measurements. The reason for this is partly due to the lack of techniques for making such small channels and also to the difficulty of estimating their size. The Rollin film has however been extensively investigated, and it is often considered in the context of channel flow.

When an empty beaker is filled by means of film transfer it is found that the rate of filling is almost independent of level difference (Atkins 1948). Similar behaviour in channel flow gave rise to the concept of critical velocity and also to the belief that the pressure dependence, $\frac{d \log v}{d \log p} = n$, fell to zero in small channels. A recent investigation (Seki 1962) showed no consistent trend in the relation between n and channel size d, and no evidence of a critical velocity. A regime suggestive of a mutual friction force was observed in a filter of pore size 10^{-6} cm. The flow of He II through Vycor glass and jewellers rouge was also found to depend on pressure head. Work reported in this thesis together with that of van Alphen et al (1965) suggests that pressure dependence in very narrow channels arises from small temperature differences caused by the mechano-caloric effect.

2.2 Mutual Friction

Quantised vortex lines were first proposed by Onsager (1949)

to account for the onset of dissipative processes in Rollin film transfer. This vortex line concept was later developed to account for the observation (Osborne 1951) that He II rotates as if it were a solid body. According to Landau's system of non-linear hydrodynamical equations curl $v_s = 0$. If the superfluid is restricted by this condition then in a simply connected region it should be impossible to bring it into rotation. This difficulty was overcome by assuming that within the superfluid there are regions of vorticity. In this case the liquid itself forms a multiply-connected region and rotation becomes possible without violation of the restriction.

Hall and Vinen (1957) have measured the attenuation of second sound, propagating it both radially across and also along the axis of a rotating vessel. The attenuation coefficient was much higher in the first case as would be expected if the liquid contained an array of vortex lines parallel to the axis of rotation.

Vinen (1957a) has investigated thermally induced flow in wide capillaries ($d \sim 6$ mm). The flow was studied by propagating and receiving second sound in a direction at right angles to the heat current. The results indicated that above a certain heat current the superfluid became turbulent. The onset of this dissipative mechanism depended on the initial state of the liquid. For example if a heat current had been switched on previously the build-up of turbulence was made more rapid. When the heat current was switched

off, measurements of the attenuation coefficient gave information concerning the decay of turbulence. The rate of decay depended on the dimensions of the channel. Having thus established strong experimental evidence to connect dissipative effects with the onset of turbulence in the superfluid Vinen (1957b) developed theoretical arguments to explain the mutual friction force in terms of turbulence, thought of as a tangled mass of quantised vortex lines.

Critchlow (1960) has also investigated thermally induced flow in capillaries of smaller diameter using resistance thermometers to measure the propagation velocity of turbulent fronts. A striking result of these experiments was the observation that turbulence invariably propagates from the ends of the channel and not from the channel walls.

Qualitatively it is easy to visualise the mutual friction force as arising from the collisions of rotons and phonons with vortex lines in the superfluid. In order to understand how equation (25) arises it is necessary to follow through the Vinen theory.

Let L be the total length of vortex line per unit volume at any instant. Then

$$l = L^{-\frac{1}{2}}$$

is a measure of the average distance between adjacent vortex lines. Also let u_s be the velocity due to an isolated rectilinear vortex line at a perpendicular distance l from it. This velocity is

related to the root mean square turbulent velocity measured relative to the bulk motion of the superfluid. Since the circulation, $\oint v.dr$, round a vortex line is $\hbar/m$, κ_s and l are related by the equation

$$2\pi\, l\kappa_s = h/m, \text{ or } l\kappa_s = \hbar/m \tag{27}$$

Assuming that turbulence is isotropic, that vortex lines move on average with velocity v_s and that the force on unit length of line is

$$f = \frac{B}{2}\frac{\rho_s\rho_n}{\rho}\frac{h}{m}(v_n - v_s) \tag{28}$$

then the friction force must be of the form

$$F_{sn} = G.(v_s - v_n) \tag{29}$$

It follows that G is given by

$$G = \frac{2}{3}\left(\frac{B}{2}\frac{\rho_s\rho_n}{\rho}\frac{h}{m}.L\right) \tag{30}$$

Replacing L by $\kappa_s^2 m^2/\hbar^2$, from equation (27) we obtain,

$$G = \frac{2\pi}{3} B .\frac{\rho_s\rho_n}{\rho}\frac{m}{\hbar}\kappa_s^2 \tag{31}$$

Vinen shows that it is plausible to put κ_s equal to $\alpha|\overline{v_s - v_n}|$ and so finally obtains an expression for F_{sn} of the form

$$F_{sn} = \frac{2\pi}{3} B \frac{\rho_s\rho_n}{\rho}\frac{m}{\hbar}\alpha^2|v_s - v_n|^2 .(v_s - v_n) \tag{32}$$

Equation (32) has the required form to explain the type of force proposed by Gorter and Mellink and it also relates F_{sn} to the presence of vortex lines in the superfluid.

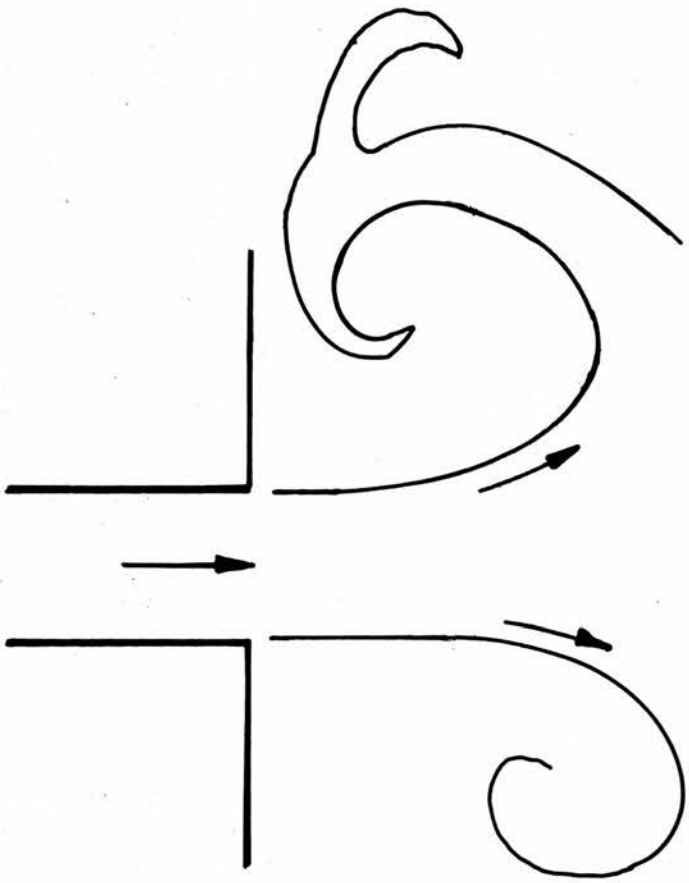

CLASSICAL FLOW FROM AN ORIFICE

Figure 3.

2.3 Theories of critical velocity in channels

The mechanism of critical velocity has been explained by Landau (1941). Consider the superfluid at 0°K flowing through a slit with velocity $\underline{v}_y$. The only way in which the liquid can be slowed down is by the creation of elementary excitations having energy ε and momentum $\underline{p}$ relative to a reference frame moving with the liquid. The energy ε' of such an excitation with respect to fixed walls is given by

$$\varepsilon' = \varepsilon + \underline{p}_y . \underline{v}_y \tag{33}$$

If the kinetic energy is to be reduced ε' must be negative so

$$\varepsilon + \underline{p}_y . \underline{v}_y < 0 \tag{34}$$

and thus

$$v_y < \varepsilon / p_y \tag{35}$$

No excitations can be created and the flow will be frictionless if the velocity v is less than a critical value defined by

$$v_c < \left| \frac{\varepsilon}{p} \right|_{\text{minimum}} \tag{36}$$

The magnitude of the critical velocity is thus determined by the excitation spectrum of the liquid. The low values of observed critical velocity ($\sim$ 10 cm/sec) rule out roton creation which requires a velocity of 60 m sec^{-1}. The ratio ε/p for phonons is also too high.

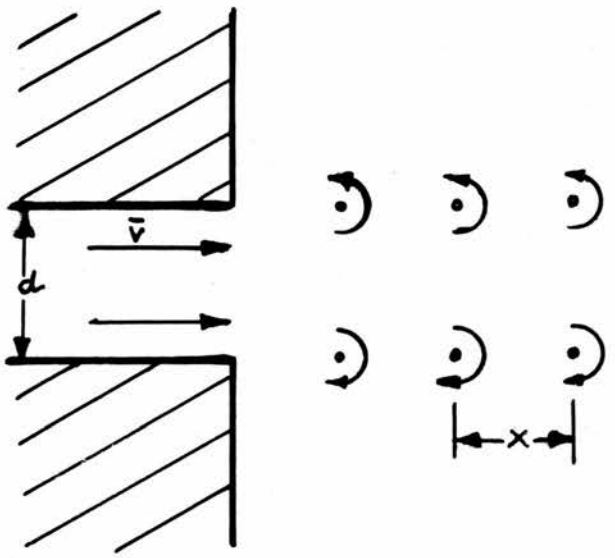

FORMATION OF VORTEX RINGS AT A CHANNEL EXIT

Ginsburg (1949) suggested that there must be other forms of excitation having ratios ε/p lower than those of rotons and phonons. Feynman (1955) has developed this suggestion by considering the possibility that vortices are formed at the exit of a capillary. He first pictures the situation for a classical fluid as indicated in figure 3. He next considers superflow by examining the circulation between the effusing jet and the stationary liquid outside it (figure 4). He shows that the number of lines per cm is

$$\frac{1}{x} = v/(2\pi \hbar m^{-1}). \tag{37}$$

Now the kinetic energy per cm^3 per sec of the liquid is

$$dm \rho_0 v^3/2 \tag{38}$$

where ρ_0 is the number density,

and the energy required to produce the lines is

$$(v^2/2\pi\hbar m^{-1}) \rho_0 \pi\hbar^2 m^{-1} \ln d/a \tag{39}$$

Equating these quantities, the velocity v_0 at which there is just sufficient energy to produce lines is given by

$$v_0 = \frac{\hbar}{md} \ln \frac{d}{a} \tag{40}$$

where a is the vortex core diameter. If this quantity is assumed to be about 4 Å, the size of predicted critical velocities is still too high, since, taking $m/\hbar = 6 \times 10^3$, $d = 10^{-5}$ cm and $\ln d/a = 6$, v_0 is about 100 cm/sec. Feynman goes on to point out that non-uniformity of channel size can lead to lower values of critical

velocity.

Atkins (1959) has also treated the problem of critical velocity by considering the possibility that the vorticity in a capillary is initiated in the form of closed vortex rings. The ring is regarded as a particular form of elementary excitation so that the Landau condition can be applied. In this case the critical velocity is given by the smallest ratio $\mathcal{E}/I$ of such a ring, where $\mathcal{E}$ is the energy and I the impulse required to create it. From classical hydrodynamics the expressions for $\mathcal{E}$ and I are

$$\mathcal{E} = \tfrac{1}{2}\rho k^2 r \ln \left(\frac{8r}{a_o} - 7/4\right) \tag{41}$$

and

$$I = \pi \rho k r^2 \ . \tag{42}$$

When $k = h/m$, the expression for the critical velocity is given by

$$v_c \sim \frac{\hbar}{mR} \ln \frac{8R}{a} \ . \tag{43}$$

This expression, like that of Feynman, has the correct form for explaining critical velocities but it does not contain a temperature dependence. Experiments such as that of Staas (1961) indicate that v_c does depend on temperature. Another difficulty is that the creation of a vortex ring whose diameter approaches the tube size (e.g. 1 mm) requires an enormous co-operative effect.

Another problem which Kuper (1965) discusses in this context, is that the critical rate associated with film transfer rises below

1°K. Theories which predict the creation of an unique form of low energy excitation would appear to be inconsistent with such a trend. van Alphen (1965), investigating critical velocities in superleaks has found v_c to be constant down to 0.5°K. This suggests that film phenomena must be treated separately from those associated with narrow channels. For example it is possible that surface excitations (ripplons) are important in the case of film flow.

2.4 Experimental measurements of critical velocity

The gravitational flow of helium II in narrow channels was first comprehensively investigated by Allen and Misener (1939). In a channel† of width d estimated to be 1.2×10^{-5} cm they observed a type of flow where the velocity did not depend on the driving pressure. Daunt and Mendelssohn (1938) found evidence of a critical transfer rate associated with the Rollin film. This non-classical behaviour gave rise to the concept of critical velocity. There have been many subsequent investigations of critical phenomena.

Swim and Rorschach (1955) have investigated gravitational flow through radial superleaks, similar to the one shown in figure 2. They found that the flow could be understood by assuming a friction force F_{sn} proportional to $(v_s - v_n)^n$. For d = 4.3 μ they found n = 3 but when d = 2.3 μ, n rose to around 3.7. In both cases n was

†A wire-filled tube superleak. A technique for producing these is described in Chapter 3.

practically independent of temperature.

Hung, Hunt and Winkel (1952) investigated thermally induced flow in slits of similar geometry and were also able to interpret their observations in terms of a friction force with n = 3, in the range 5 μ > d > 1 μ. The critical velocity which they observed was around 20 cm sec^{-1}, but their measurements of slit size were made at room temperature. Winkel, Delsing and Poll (1955), using the overshoot procedure, obtained values of v_c of about 10 cm/sec in superleaks of comparable size.

Winkel, Delsing and Gorter (1955) in a similar experiment using a somewhat shorter slit found evidence to favour a mutual friction force (n = 3) when d was greater than 1 μ. They found that when d = 0.43 μ n increased to a value of 5. These authors were also able to deduce that the friction occurred throughout the entire slit and not only at the narrowest section or on the walls or indeed at the outlet.

Seki (1962) has carried out an extensive investigation of flow via the Rollin film, Vycor glass, jewellers rouge and Millipore filters†. There was no evidence to favour the idea of a critical velocity. Whereas the temperature dependence of mean velocity had previously been found to be roughly that of ρ_s/ρ Seki found a significantly different dependence in the case of flow through Millipore

---

†These are described in Chapter 3.6

filters and jewellers rouge.

Another investigation of critical phenomena in capillaries (Bhagat and Mendelssohn, 1961) indicated the existence of a critical velocity but this depended on the initial level difference in the reservoir. In capillaries of comparable size Atkins (1951) had previously found that the mutual friction force was all-important.

The experimental results obtained in investigations using a wide variety of channel geometries and techniques have not so far allowed the construction of a comprehensive theory of the processes underlying critical phenomena. The critical velocities are generally found to increase with decreasing channel size but whereas Allen and Misener (1939) observed pressure independent flow Seki (1962) does not. The mutual friction hypothesis while accounting for values of $n = 3$ does not explain why values of 4 and 5 are observed. There is at present no understanding of the mechanism which causes the disappearance of the mutual friction force.

CHAPTER 3

THE CHANNELS

3.1 Techniques previously employed

The flow of liquid helium II in narrow channels has been investigated by a number of authors using a variety of channel techniques. Bowers and Mendelssohn (1952) and Kapitza (1941) have used radial superleaks made by pressing together optically polished flat discs. Wansink et al (1955) produced a superleak by embedding a gold wire into glass; the differential contraction was sufficient to permit superflow through the resulting gap. Seki (1962) has studied flow through Vycor porous glass which has interconnecting pores of mean diameter about 40 Å. He has also investigated superflow using a leak made by pressing jewellers rouge powder into a tube. The channels formed in this way were estimated to be of the same order as the particle size of the rouge. Seki has also investigated flow through Millipore filters. A detailed account of the pore structure of these filters is given in 3.6 since three sizes of filter have been investigated by the present author. Flow through the helium film, which can be considered as a special case of channel flow, has been extensively investigated, (see for instance Atkins (1952)). Allen and Misener (1939), Manchester and Brown (1957) and Chopra (1957) have all investigated channel flow by means of wire-filled tubes. These tubes devised by Allen

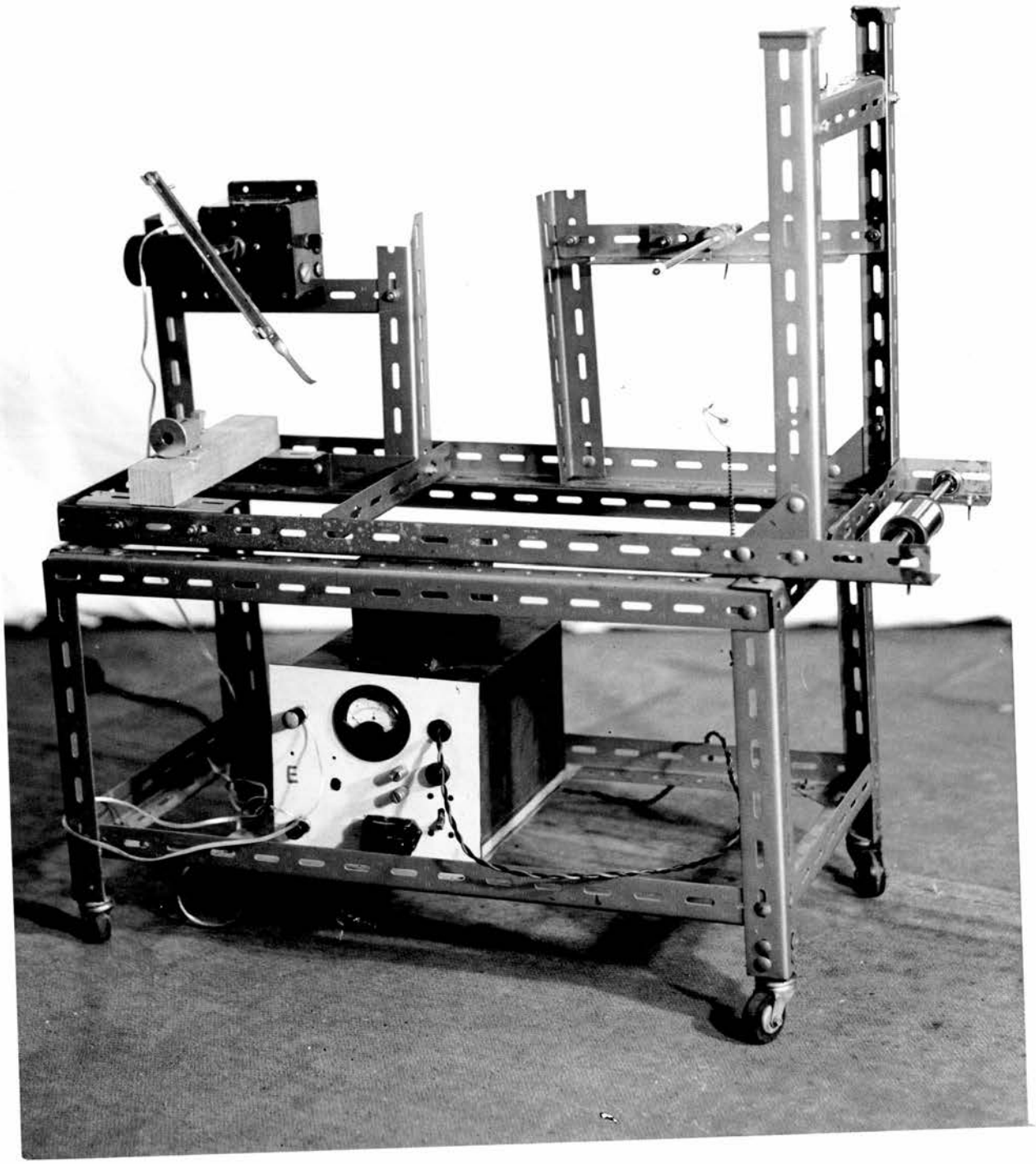

Figure 5

and Misener have a number of advantages over those already mentioned. Despite the fact that wire-filled tubes do not provide a single uniform channel nevertheless they allow quantitative measurements of channel size to be made. An estimate of the effect of the distribution of channel sizes on measured critical velocity is reported in this thesis. The non-uniformity of width is not a property associated only with wire-filled tubes but is common to all channels where the width is less than 10^{-4} cm.

3.2 The wire-filled tubes

The wire-filled tubes constitute the bulk of the flow channels used in the present investigation. The essence of the method is to fill a tube with a known number of wires and draw the tube (and contents) until the wires are deformed into regular hexagons. Continued drawing then reduces the gap (which forms the channel) between adjacent hexagons. The detailed procedure is outlined below. To produce the tubes a length of wire was wound by means of a rotating former powered by a small electric motor. The wire was caused to move over a system of teflon pulleys and through a pad of tissue which removed all grease. The number of turns and hence the number of wires was recorded on a counter clipped on to the former. The former was so constructed that after winding the wire the removal of a single nut caused the former to 'collapse', whereupon the wires (which were being kept in a state of continuous

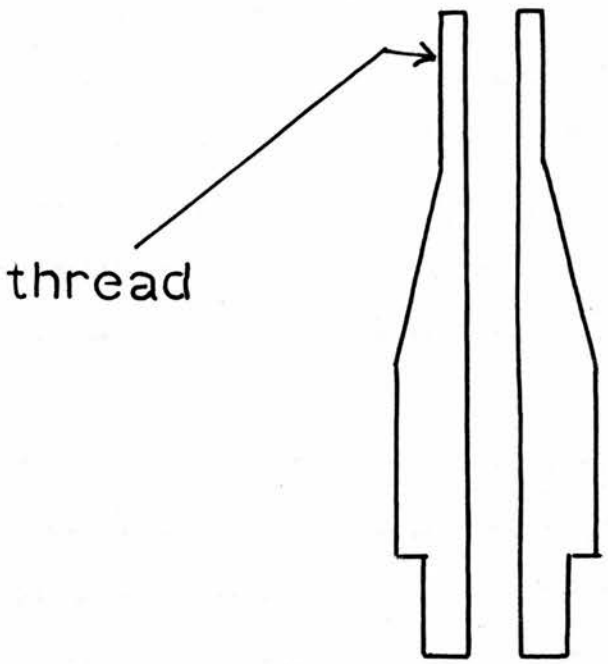

steel draw piece

Figure 6.

tension) came off as a parallel bundle. This bundle was carefully introduced into a highly polished copper-nickel tube internally tapered at the mouth to facilitate entry of the wires. The length of the tube was chosen so that when the wires were inside, the bundle was at least 10 cm from one end. At this end a steel drawing piece, shown in figure 6, was hard soldered on to the tube. Before a tube could be drawn it was first placed in the collet of a lathe and the soldered joint coned down and polished. The tube was then inserted into the first die plate and the winch started. After each draw the length of the wires within the tube was measured - thus permitting calculation of the wire perimeter after drawing. The total channel perimeter was the sum of the lengths of all the hexagonal sides.

Each wire-filled tube consisted of approximately six thousand copper† wires, electrolytically pure, 50 microns in diameter (0.002 inch) inside a copper-nickel* tube of 5 mm internal diameter and of 6.6 mm outer diameter. This gave an initial wire perimeter of about 90 cm and thus an initial channel path 45 cm wide after deformation but before significant elongation had taken place. The path width diminishes on continued drawing by an amount proportional to the wire elongation. The gap or channel width between the

---

†manufactured by Fredrick Smith, London.

*manufactured by Johnson Matthey.

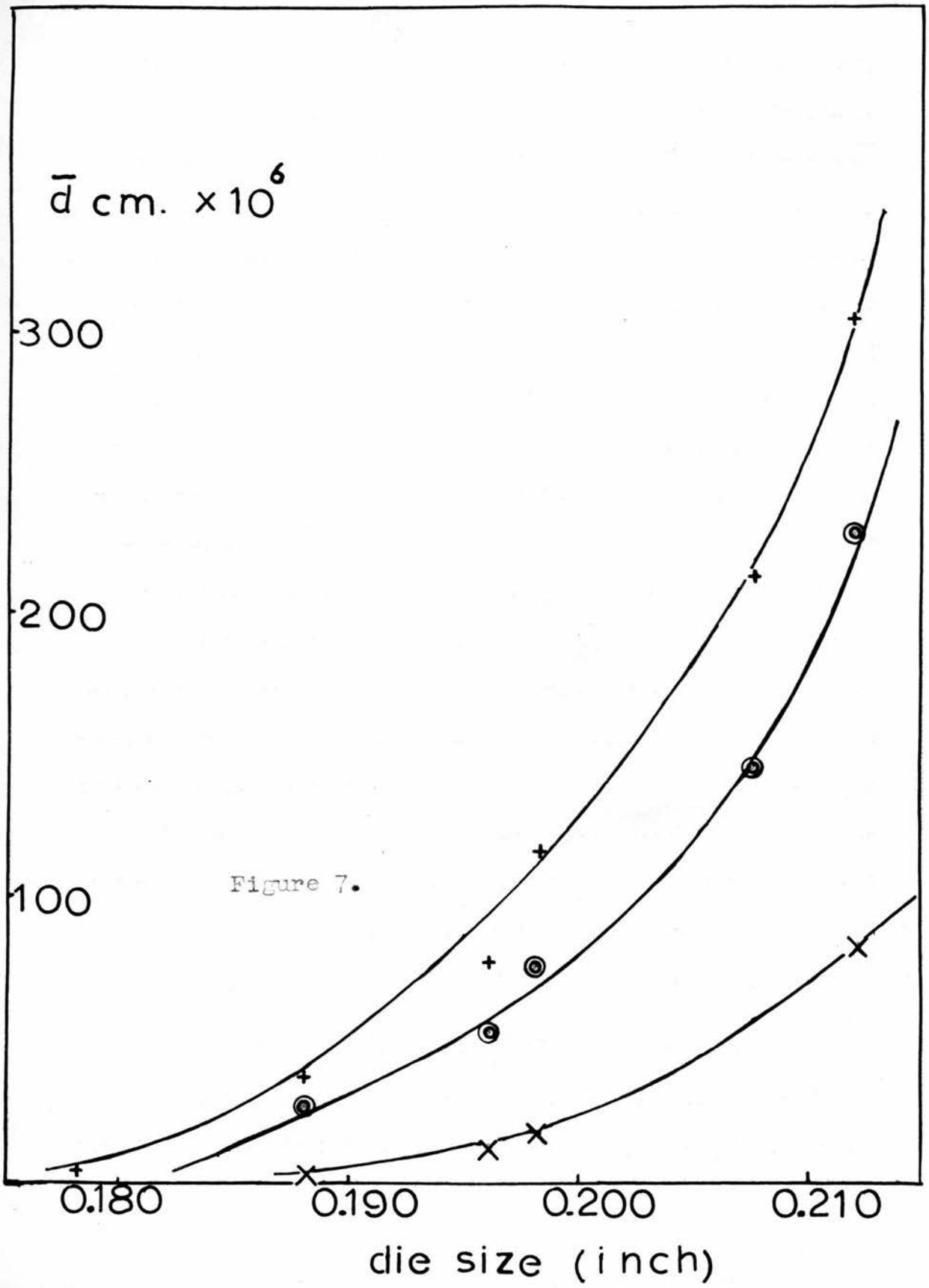
$\bar{d}$ cm. $\times 10^6$
300
200
100
0.180
0.190
0.200
0.210
die size (inch)

Figure 7.

wires also diminishes with continued drawing but careful control of die size was found to give fairly predictable and reproducible channels. The elastic properties of the two materials copper and copper-nickel, i.e., the elastic limit and Poisson's ratio, were favourable for the leaving of open channels after the draw process, while the integrated expansion coefficient caused the channels to increase in size as the temperature dropped. The drawing process was extremely lengthy, often taking several days, and the smallest channel that could be obtained was governed mainly by the amount of drawing the tubes could tolerate before they broke. At the outset of this research we examined the possibility of using steel wires, but found that they did not deform so readily as copper and also that after deformation there remained a number of relatively large triangular gaps at the corners of the hexagons. The length of the wire bundle before drawing was always about 16 cm and since the length after drawing was not much more than 20 cm, no more than two superleaks 10 cm long could be produced at one time. The length of superleak used in helium II flow measurements was about 10 cm except in one or two experiments where other lengths were more appropriate.

3.3 The channel perimeter in the wire-filled tubes

The channel path formed by each tube could be determined in two ways. Suppose a_1 to be the area of an individual wire initially

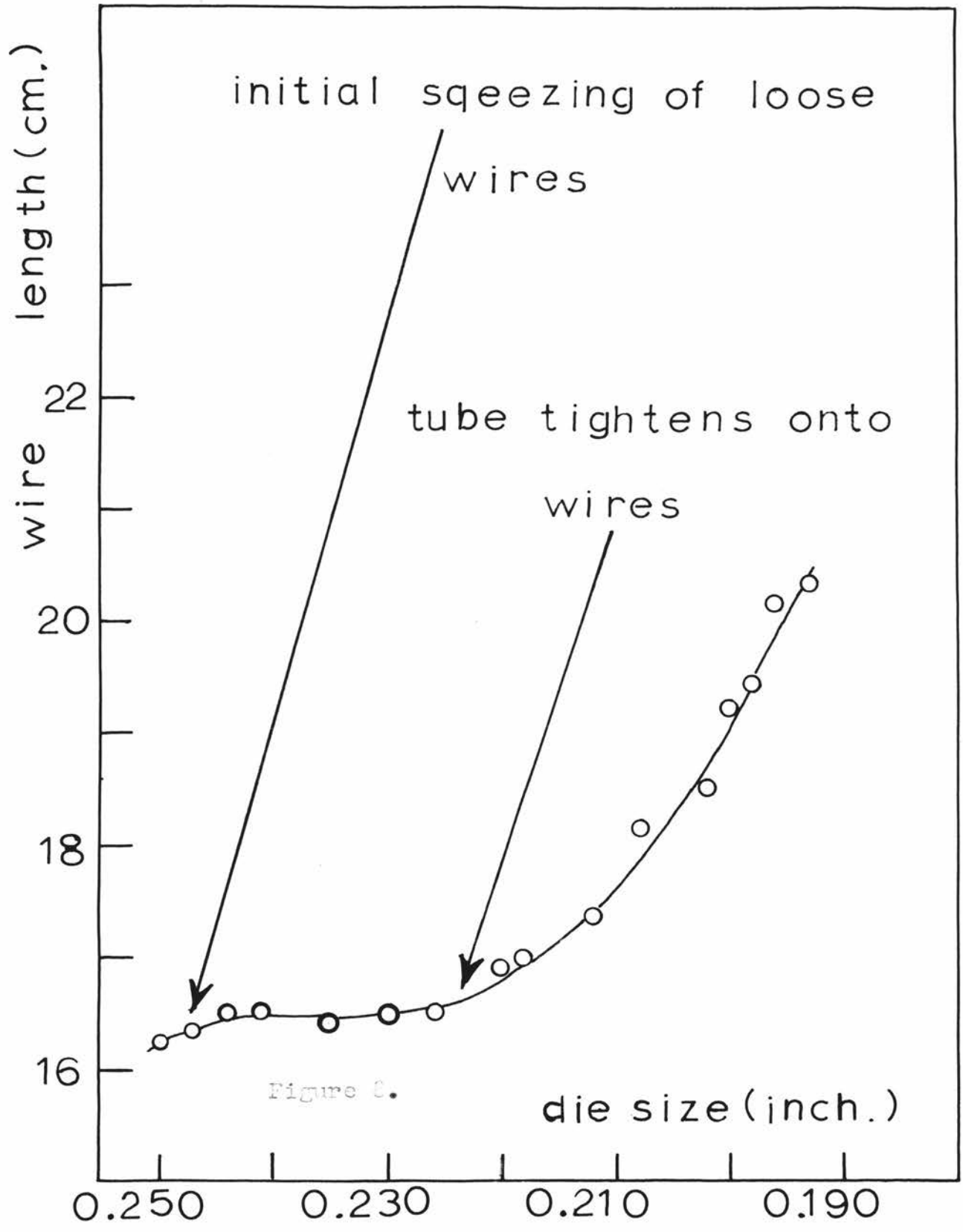
initial sqeezing of loose wires
tube tightens onto wires
wire length (cm.)
22
20
18
16
0.250
0.230
0.210
0.190
die size (inch.)

Figure 8.

and a_2 to be the area after drawing and also that during the draw process its length changes from a value l_1 to a value l_2.

If we denote the perimeter before and after drawing by p_1 and p_2 then,

$$p_1 = k\, a_1 \text{ and } p_2 = k\, a_2 \tag{44}$$

where k is a constant.

Since $a_1 l_1 = a_2 l_2$ we finally obtain

$$\frac{p_1}{p_2} = \frac{l_2}{l_1} \quad . \tag{45}$$

The length of the wire bundle was measured after passage of the tube through each die plate by means of a feeler inserted from each end of the tube. Figure (8) shows how the length of a typical wire bundle changed during the draw process. Equation (45) gives the channel perimeter after drawing. There is, however, some error in applying equation (45) because the initial perimeter is calculated for circular wires whereas finally the wires are hexagonal. The error introduced arises in equation (44) where it is assumed that the constant k is the same for both wire cross-sections. One can see this problem in another way: one does not know the value of l_1 for which the deformation is just complete. If we did, (45) would give p_2 exactly. To avoid these difficulties the following method has been used.

When the tube had been drawn through the final die a short length (~ 3 mm) was sawn off. The wires were extracted by drilling a small hole through the wires and scraping out the remainder. The internal diameter of the tube was measured with a microscope and the tube area (A) calculated. The area of a regular hexagon of side $\underline{a}$ is $3\sqrt{3}\,\underline{a}^2/2$ so that the area (A') of n close packed wires is

$$A' = 3n\sqrt{3}\,a^2/2 \ .$$

But A' is also the area of the tube. This allowed us to calculate the length of a side $\underline{a}$ and hence the total channel path q, given by,

$$q = 3\underline{a}\ n. \qquad (46)$$

3.4 The channel structure of wire-filled tubes

In order to choose suitable wire for the production of very small channels we examined the cross-section of a tube formed by steel wires drawn inside a copper-nickel tube. After a considerable number of draws we found that triangular gaps still remained. These would have affected the flow of helium II by allowing the flow of normal fluid and since their fractional area was relatively large and impossible to calculate we were obliged to choose another material[†]. We therefore drew down a tube containing copper wires. A section of this tube was sawn off but the tube then had the appearance of a section through a copper rod, no channels being

[†]Steel had the further disadvantage that the force required to squeeze the wires finally caused the copper-nickel tube to fracture.

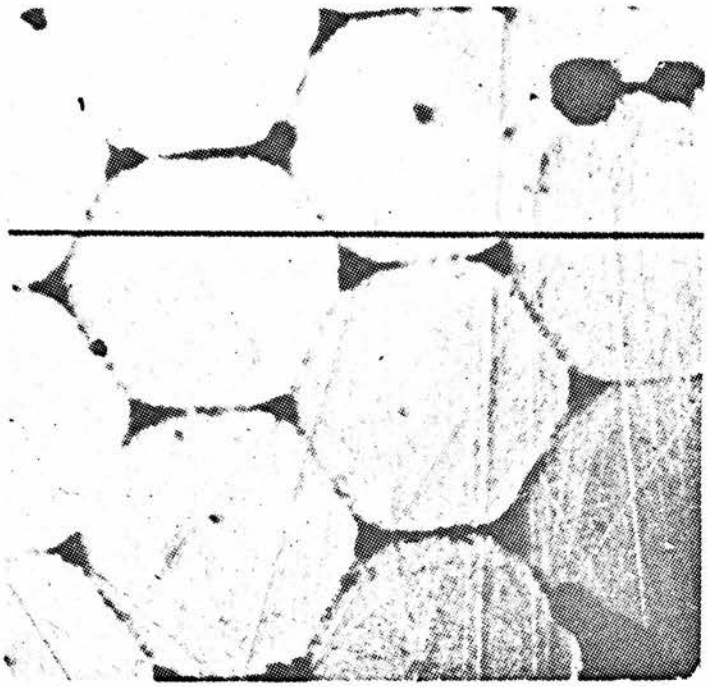

Figure 9.

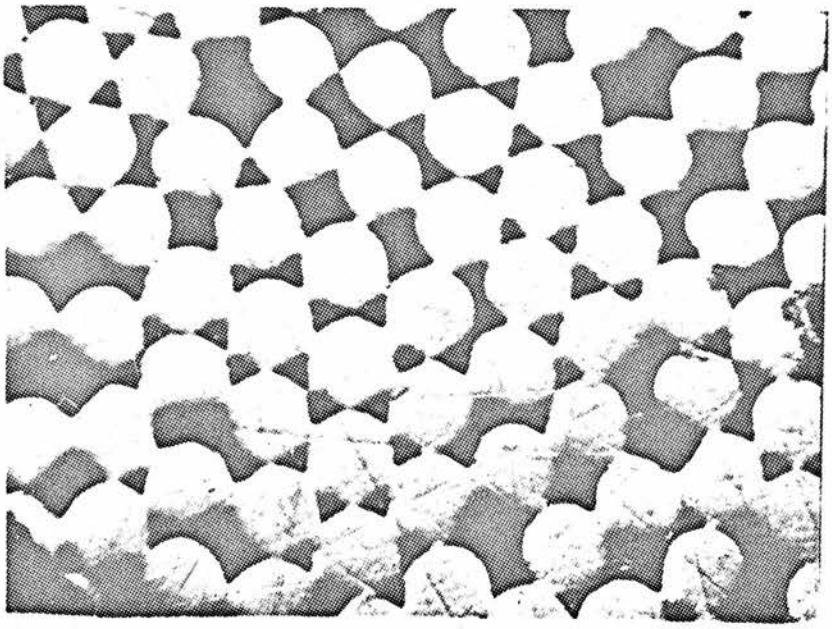

Figure 10.

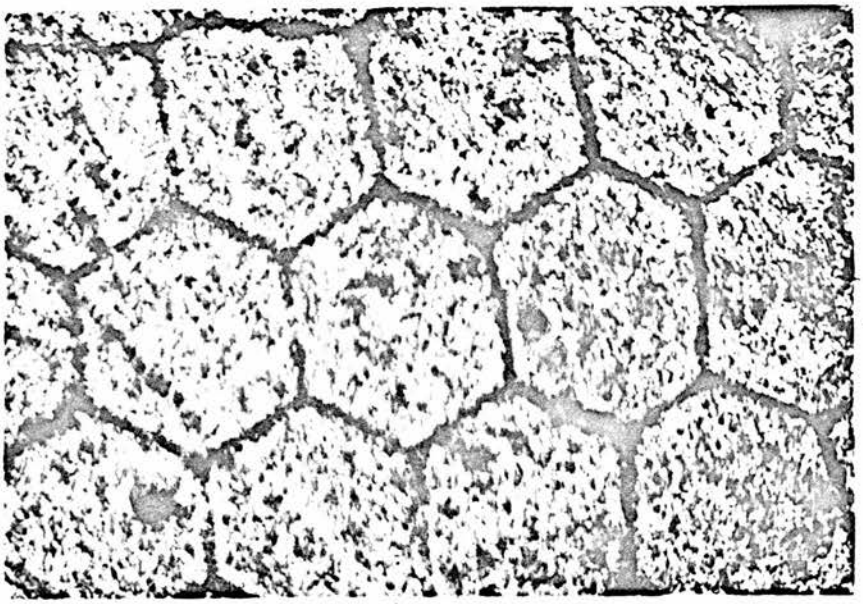

Figure 11.

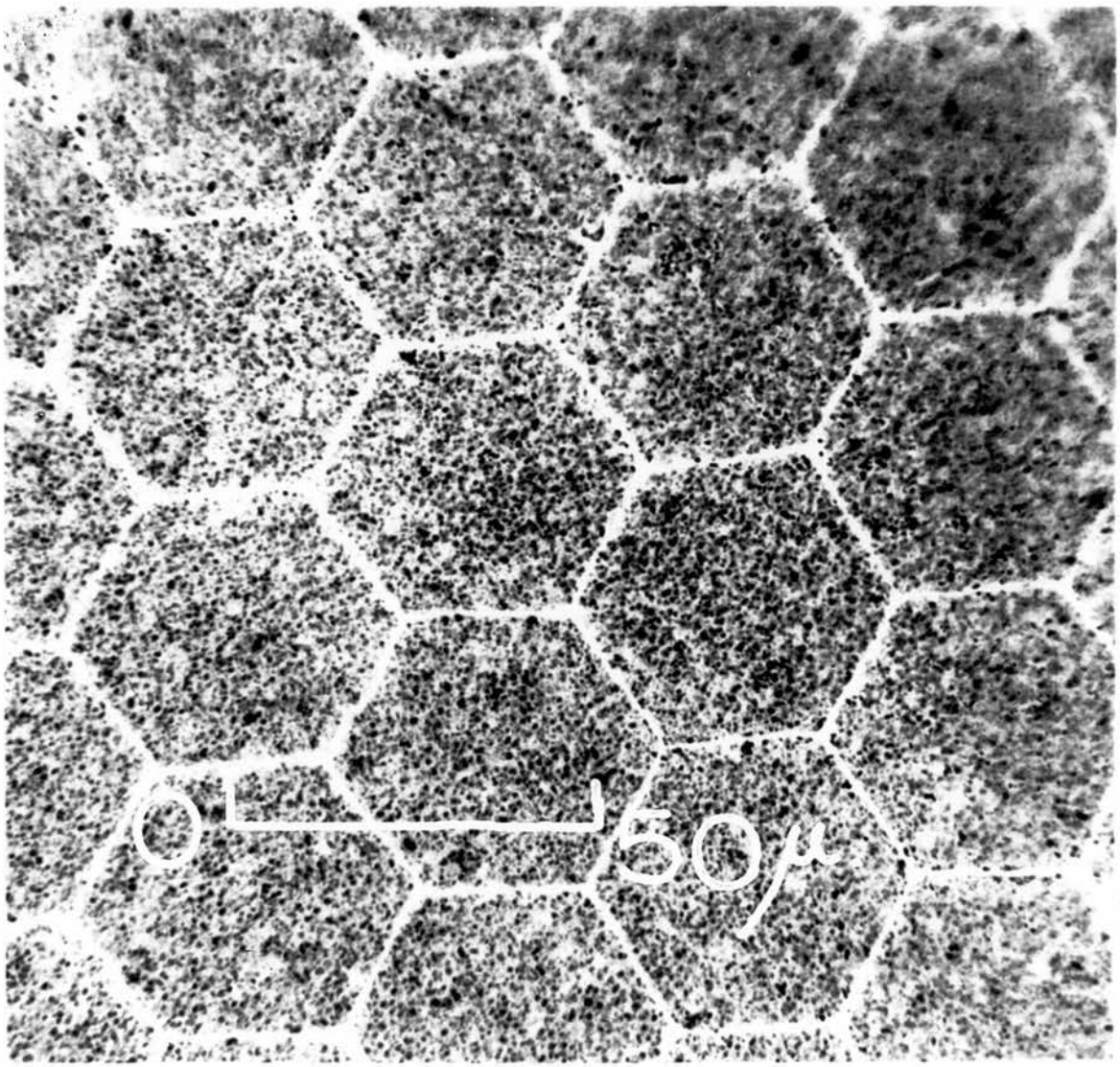

Figure 12

visible. In order to examine the channel structure, the tube was set into a brass block and machined flat after which this surface was polished with several grades of emery powder and finally with rouge. The unit was dipped for a few seconds into concentrated acid then taken out, thoroughly washed and dried. The acid attacked the copper at interfaces of the wires thus bringing out the hexagonal pattern. Figure (11) shows a photomicrograph obtained in this way using the copper wire. Figure (9) shows the unwanted triangular pores obtained using steel wire - in this case the surface was not polished. Figure (10) shows the result of drawing copper wires in a copper tube. Both wires and tube in this latter case probably have the same Poisson's ratio, thus no hexagonal deformation occurs and therefore no superleaks are formed.

3.5 The cross-section for flow through wire-filled tubes

Two methods have been employed to determine the open cross-section available for flow. The less accurate of the two depends on measuring the quantity of helium gas which passed down the tubes under a given pressure and this method is described here. The other method is discussed in 4.1.

The gas flow technique was used mainly to estimate the channel size of a given tube before it was prepared for a helium run. In order to obtain a reasonable estimate we made the measurements at

the temperature of liquid air. This was necessary because of the increase in open cross-section which occurred as the tubes were cooled. For the purpose of measuring S_p at these temperatures the cryostat shown schematically in figure (13) was constructed. The wire-filled tubes were sealed into the cryostat by means of two indium seals. Before any measurements were made the entire system was pumped down to 10^{-2} mm Hg and left pumping for several hours until all traces of water vapour were removed. A narrow spiral tube which formed part of the inlet to the high pressure side (not shown in the diagram) ensured that the gas was cooled to the temperature of liquid air and also served to remove any traces of water vapour from the helium gas. The volume of gas emerging from the wire-filled tube at the low pressure side was measured by timing the motion of a soap film as it traversed the graduated marks of the flow tube. This tube was made from a burette by removing its tap. On the high pressure side of the cryostat there were cylinders, one containing hydrogen and the other helium, thus enabling measurements to be made with either gas. The pressure was adjusted so that the bubble moved at a conveniently measurable rate; this also determined the minimum inlet pressure. Whenever the seals were remade there was no significant change in the flow rate and it was concluded that the seals were impervious to both hydrogen and helium. The open cross-section S_p was deter-

Figure 13.

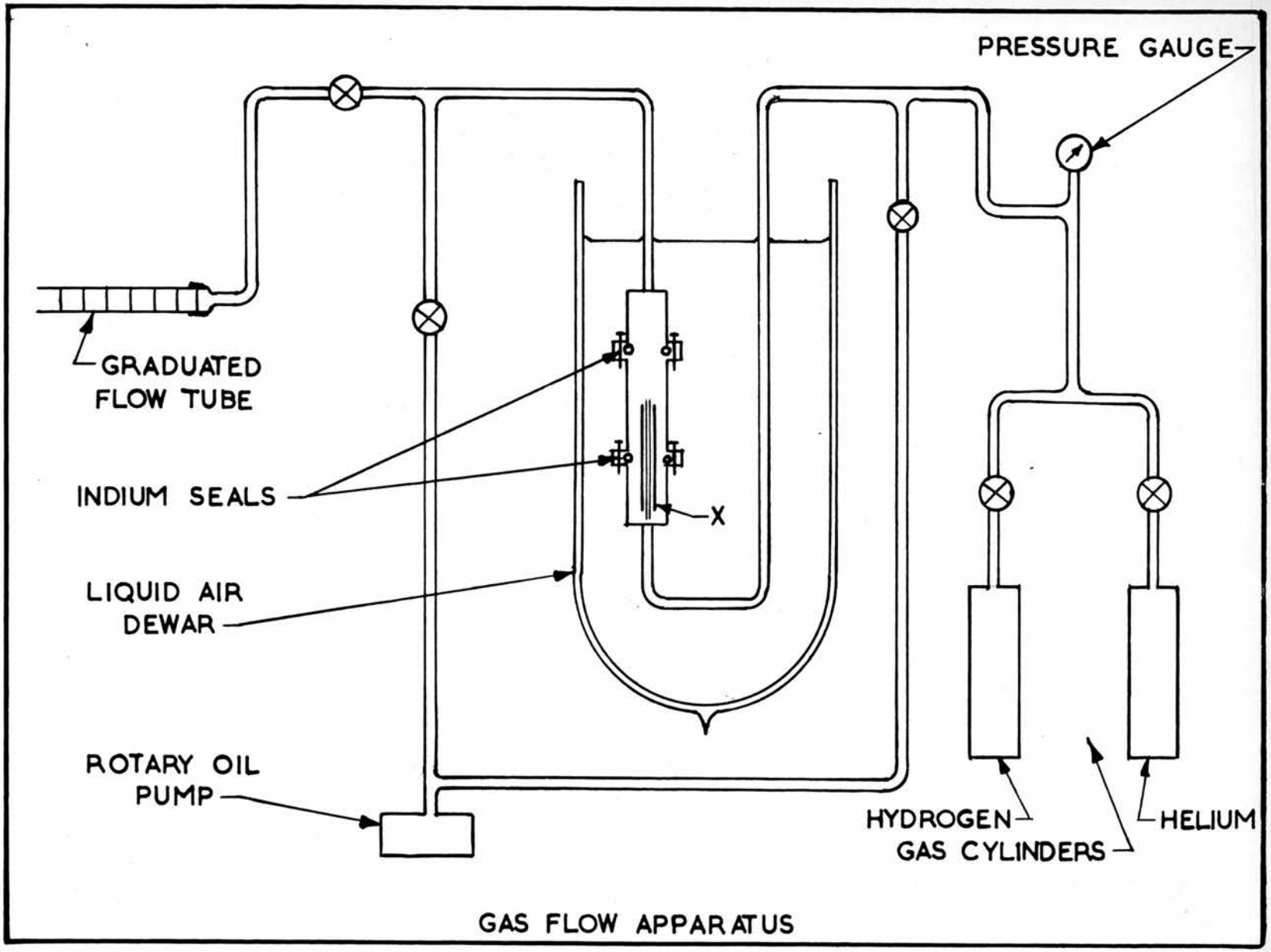

GAS FLOW APPARATUS

mined from the Poiseuille formula derived for flow of a compressible gas between parallel plates. The volume/sec, Q, is given by

$$Q = \frac{d^3 q(p_2^2 - p_1^2)}{24 \eta l p_1} \qquad (47)$$

where d is the channel width, q its total length through any cross-section of tube, p_2 is the inlet pressure, p_1 the pressure at the outlet, η the viscosity of the gas at liquid air temperature and l the tube length.

Measurement of Q and a knowledge of q and the other constants permits d to be calculated. In order to establish the applicability of equation (47) to the flow through the tubes, Q was measured over a range of pressure differences. In the wider channels Q was proportional to the square of the inlet pressure. In the narrower tube Q was proportional to the pressure difference and in sizes where $d \sim 10^{-5}$ cm there was an intermediate pressure dependence. From the point of view of He II measurements, the most interesting region of channel diameters is where the flow of gas cannot be described by either the Poiseuille or Knudsen formulae. We concluded that since there is no quantitative theory for flow when the channel size and mean free path are comparable, it would be better to rely entirely on a second method. This latter has the added advantage that the measurements are made at helium

temperatures. In 4.2 we shall discuss the question of channel uniformity and its effect on the channel diameter derived from the Poiseuille formula.

Apart from providing an indication of channel size and open cross-sectional area the gas flow cryostat also enabled us to flush the wire-filled tubes with helium gas thus removing air which could have led to the formation of a solid air substrate and hence to irreproducible results when the flow of He II was investigated. We point out in this context that the flow rate of the Rollin film is affected by deposits of solid air (Atkins 1948).

3.6 Millipore Filters

A second type of superleak, the Millipore filter, was also used in the present investigation. The filters manufactured by the Millipore Filter Corporation of Bedford, Mass., are described as highly porous cellulose ester structures containing numerous uniform and submicroscopic channels whose pore size can be controlled by the manufacturing process. The filters, 150 micron thick, are manufactured in various sizes ranging from 5 micron to 10 milli-micron. The pores are reported by Seki (1962) to be cone shaped, all the wide ends being situated on one side and the narrow ends on the other. After some calculation Seki determined the value of r, the radius at the narrow end of the conical channel in terms of r_o, a mean radius, obtaining finally,

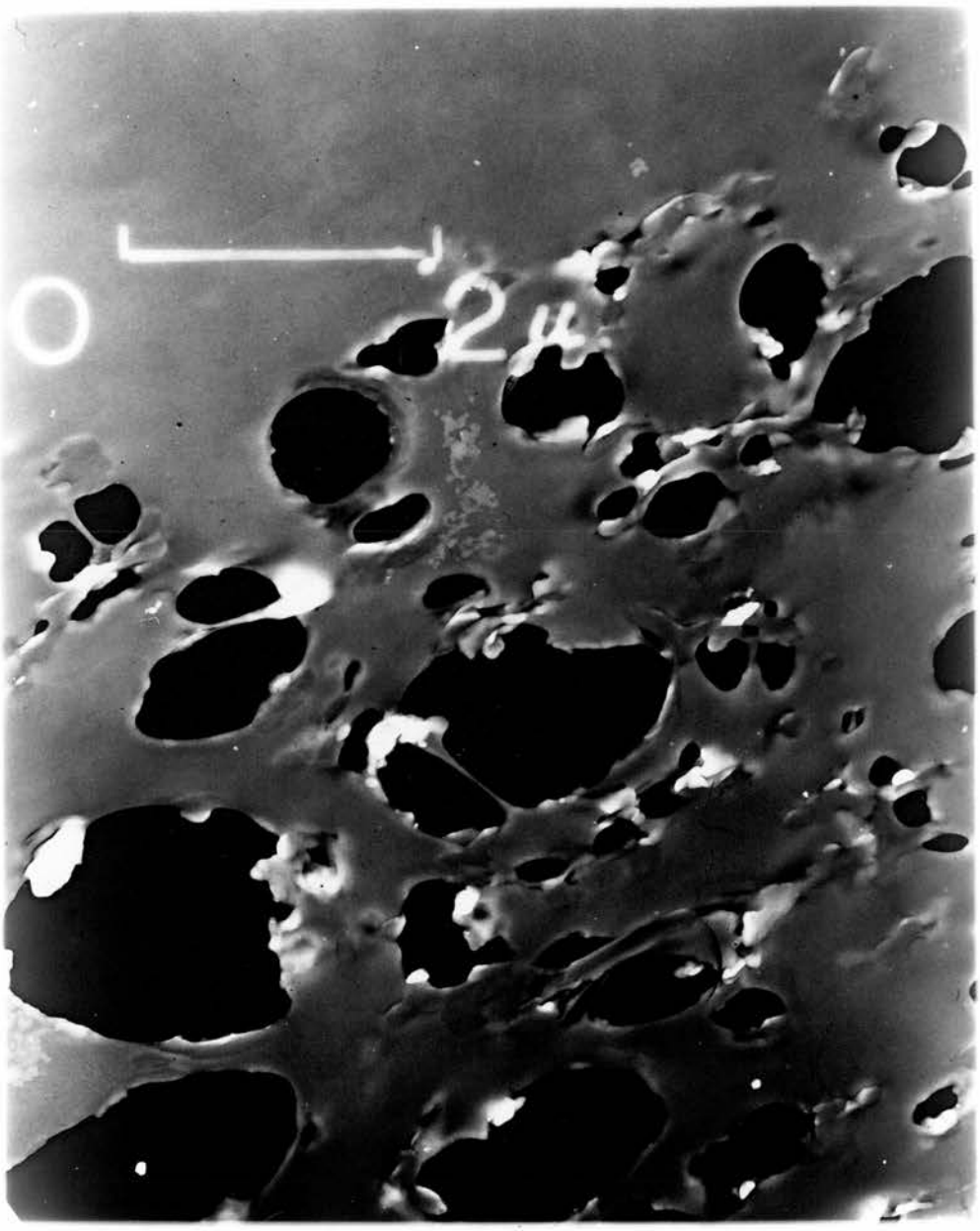

Figure 14

$$r^2 = 0.825\, r_o^2 .$$

Since the highest flow velocity occurs at the point where the channel has its minimum cross-sectional area Seki used the reduced radius in order to calculate the total area available for flow, S_o.

Electron micrographs which we have made of samples supplied to us, shown in figure (14), have been interpreted as showing that the filters are probably sponge-like. In calculating the open area, the author has assumed that the channels are right circular cylinders with diameters as quoted by the Millipore Filter Corporation. S_o was obtained by multiplying the total exposed area by a factor α (the percentage pore volume), which was obtained from data sheets provided by the Millipore Corporation. It must be pointed out that when the reduced radius is used the mean values quoted by the Corporation ought for consistency to be similarly reduced. In this case the smallest pore size provided by the filters instead of being taken as 10^{-6} cm should be taken as 6.8×10^{-7} cm, and similarly for the other sizes. The measurement of pore size and pore size distribution were made by the Company using the Skau Ruska high pressure mercury intrusion method by filtration tests with particles of known size. The porosity of the filters is so great that the exposed area through which flow occurred had to be restricted to a circle of diameter $\sim$ 0.1 mm. Details of the mercury intrusion method are given in a paper by

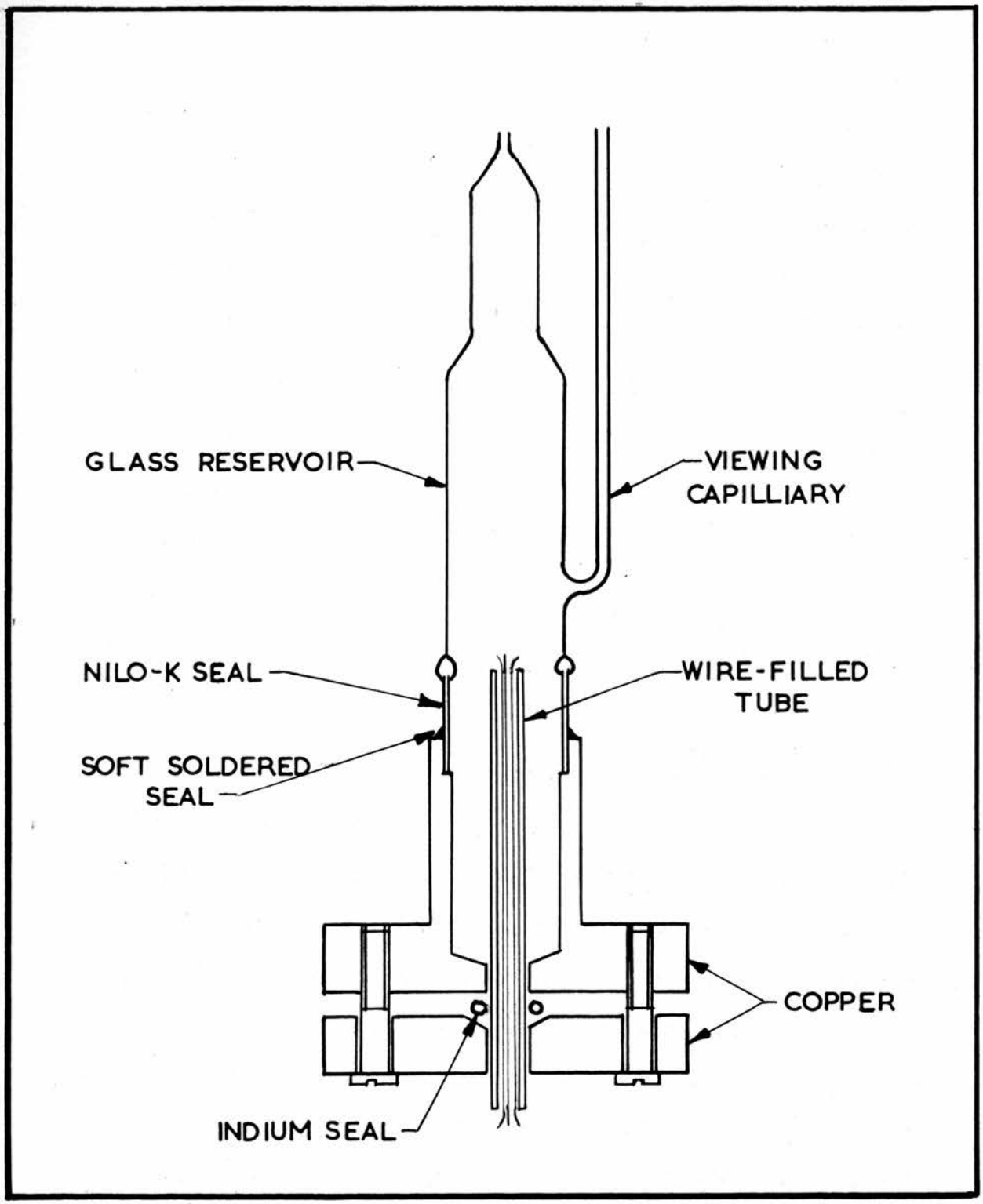
GLASS RESERVOIR
VIEWING CAPILLIARY
NILO-K SEAL
WIRE-FILLED TUBE
SOFT SOLDERED SEAL
COPPER
INDIUM SEAL

Figure 15.

Honold and Skau (1954). The pressure required to force mercury, a non wetting liquid, into the pores against the force of surface tension is measured. The filters are submerged in mercury and the total volume of mercury in the system appears to change by the amount which enters the pores. The following equation was used to find the mean pore size,

$$pr = -2\sigma\cos\theta$$

where p is the applied pressure, r the mean radius, σ the surface tension of mercury and θ its angle of contact with respect to the filter. Honold and Skau (1954) showed that a 0.5 micron filter had pores ranging in size from 0.8 to 0.1 micron. The distribution of channel sizes can therefore be taken to range over an order of magnitude.

3.7 The mounting arrangement for the wire-filled tubes

The form of apparatus used for measuring the flow of He II through the wire-filled tubes is shown in figure (15). Each tube was attached to a reservoir by means of indium seals, since there was a danger that solder and soldering flux would cause blockage of the channels. In order to test the indium seals a single wire-filled tube was cut in half, one length being attached to a reservoir by means of a soldered seal and the other by means of an indium seal. The flow of He II from the two reservoirs was the same to within 2%. This result not only showed that the seals

were equally good but also that the variation of channel diameter averaged over macroscopic lengths was small. The indium seals were all tested for flow of helium I. Further, whenever the seals were remade no detectable change in the flow rate of He II at a given temperature could be detected. We were thus satisfied that the seals were impervious to He II.

The lower half of the reservoir was made of copper and the walls were about ten thousandths of an inch thick, this being the thinnest section to which they could easily be machined.* The glass reservoirs were attached to the copper tubes by means of a nilo-k soft soldered seal. The latter were made before the wire-filled tubes were sealed in place. The virtue of a viewing capillary lies in the fact that surface tension causes the liquid level in it to rise above the meniscus of the bath and this makes for easier observation. The glass reservoirs were themselves made with two or, in some cases, three sections of different diameter so as to be able to cope with the wide range of volume flow rates encountered over the temperature range between the λ-point and 1.2°K, and as will be seen in 4.1 to give conveniently measurable periods of inertial oscillation of reservoir level.

After assembling and cleaning the reservoir system a wire-filled tube was placed in its holder, a ring of indium wire being

---

*The purpose of the copper wall is to minimise the mechano-caloric effect - this will be discussed in 5.2.

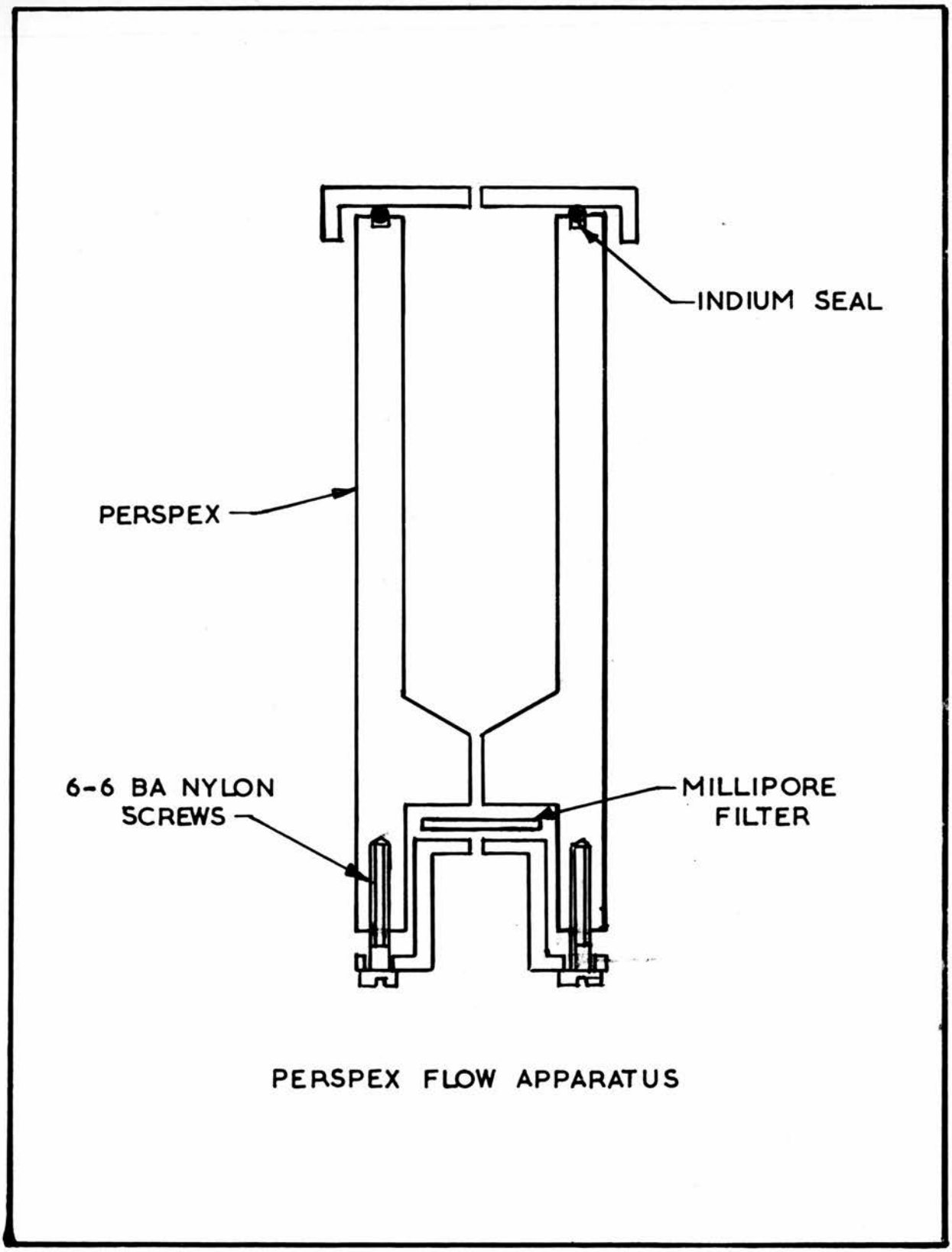

PERSPEX FLOW APPARATUS

Figure 16.

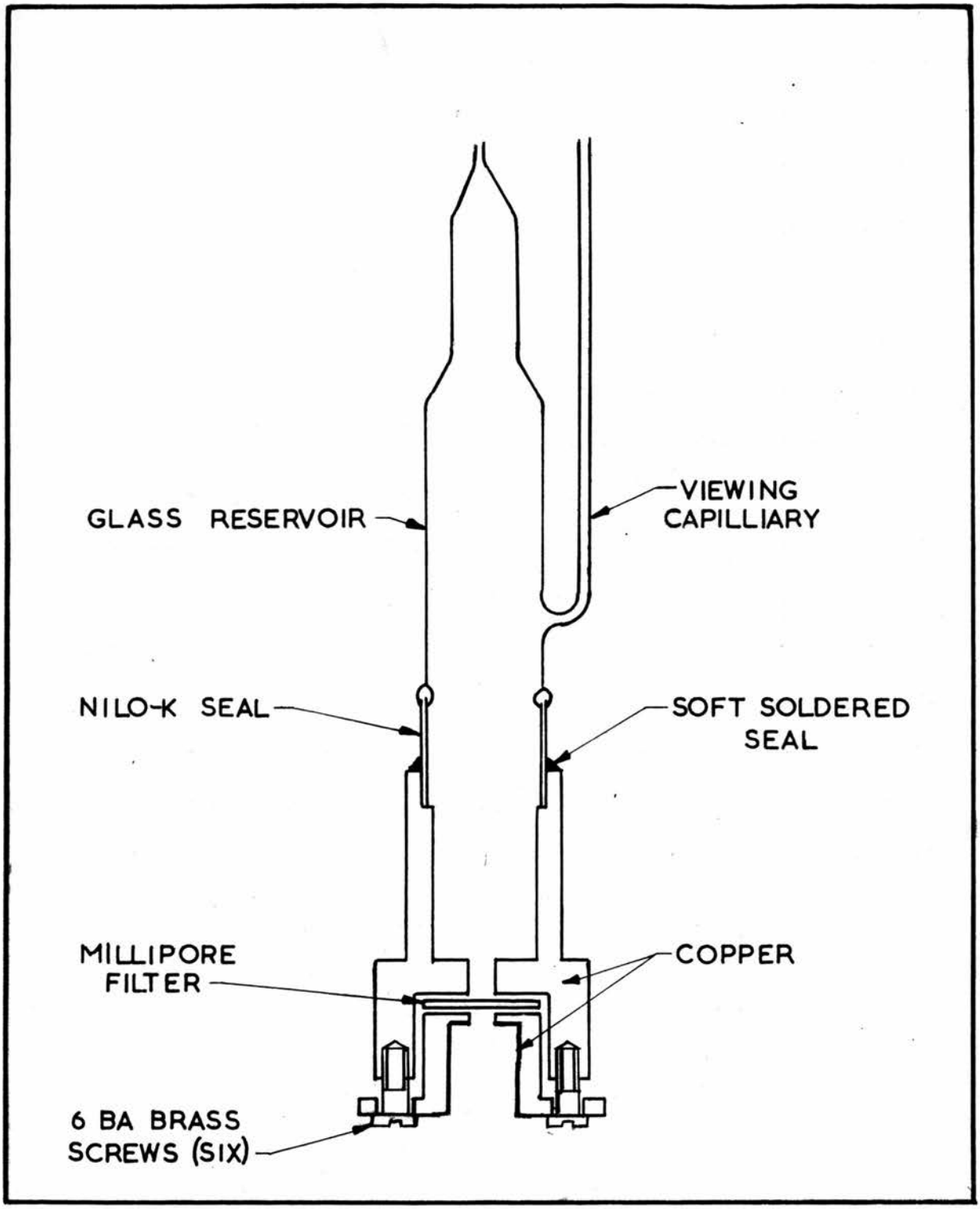
GLASS RESERVOIR
VIEWING CAPILLIARY
NILO-K SEAL
SOFT SOLDERED SEAL
MILLIPORE FILTER
COPPER
6 BA BRASS SCREWS (SIX)

Figure 17.

inserted between the sealing groove and the lower plate. The plate was then tightened by three screws thereby squeezing the indium outwards between the plates and also around the tube itself.

3.8 The mounting arrangement used for the Millipore filters

Figure (16) shows an apparatus which was used in our early experiments with the filters. The apparatus was machined from a perspex rod and the Millipore filters were held in place by contact pressure. Nylon screws were used in order to minimise slackening due to differential contraction. Because of the possibility of thermal effects arising due to the poor thermal contact of perspex we redesigned these reservoirs incorporating in the lower half a thin copper wall. This together with contact via the vapour phase minimises temperature differences between reservoir and bath caused by the flow process. Figure (17) shows the type of reservoir used for the latter part of the Millipore investigation.

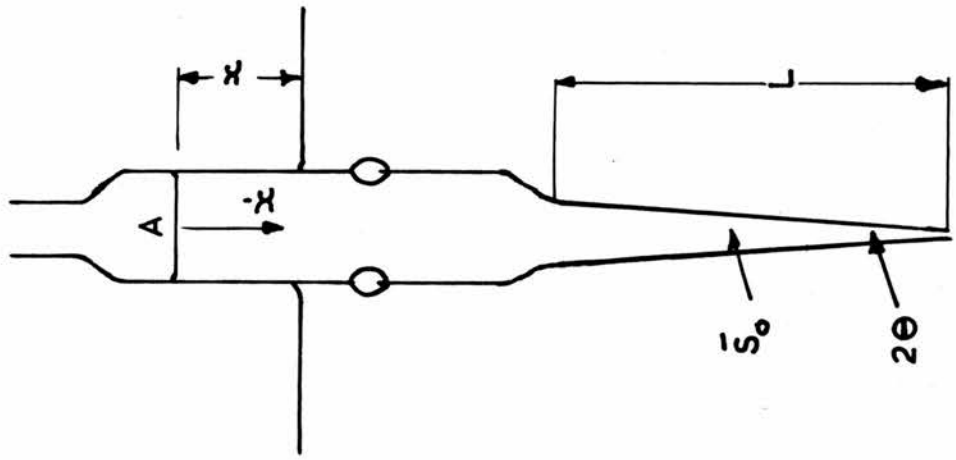

Figure 18 (b).

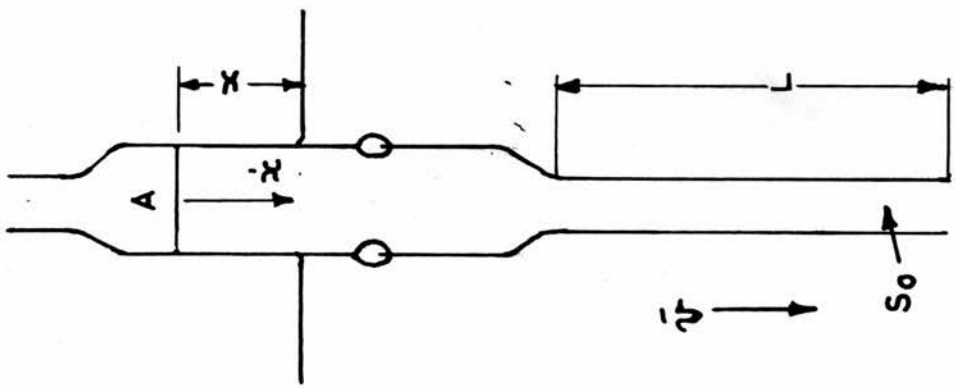

Figure 18 (a).

CHAPTER 4

4.1 The Theory of the Experiment

It will be convenient in this section to refer to the schematic diagram of figure 18(a). When the reservoir is raised above the bath the gravitational potential causes liquid to flow from reservoir to bath. Flow via the wire-filled tubes is entirely superfluid, since viscous forces prevent normal fluid motion. The level in the reservoir falls at a rate $\dot{x}$ and approaching the bath level with finite velocity oscillates about it with measurable amplitude. Isothermal oscillations of this type were first observed by Allen and Misener (1939) and treated theoretically by Robinson (1951). Since they provide a basis for determining superfluid critical velocity and mean channel width they will be discussed in some detail.

The period τ of oscillation, with the notation of figure 18(a), is given by

$$\tau = 2\pi \sqrt{\left\{ AL\rho/S_o\, g\rho_s \right\}} \qquad (48)$$

where g is the acceleration due to gravity. Upon rearrangement equation (48) yields

$$S_o = \phi.\rho/\rho_s \text{ where } \phi = 4\pi^2 AL/\tau^2 g \ . \qquad (49)$$

Now at some temperature T, since only the superfluid is flowing, the mean velocity v and the mean superfluid velocity v_s are related

by

$$\rho_s v_s = \rho v \tag{50}$$

The continuity equation gives

$$A\dot{x} = S_o v \tag{51}$$

so that from (49), (50) and (51), one finds that v_s, the superfluid velocity, becomes

$$v_s = \rho/\rho_s \cdot A\dot{x}/S_o = A\dot{x}/\emptyset \tag{52}$$

The mean channel diameter d was obtained from the relation

$$d = S_o/q \tag{53}$$

Measurement of A, L, $\dot{x}$ and τ for each of a series of wire-filled tubes enabled us to relate the magnitude of critical velocity to channel width. The experimental results are shown and discussed in 6.1. It is noteworthy that equation (52) permits calculation of v_s without a knowledge of either ρ_s/ρ or the microscopic perimeter of the channels.

4.2 The geometry of channels provided by the wire-filled tubes

It is necessary and will be profitable to give consideration to the geometry of channels formed by the wire-filled tube technique. The channel shape may have a pronounced effect not only on the absolute magnitude of critical velocity but also on the pressure dependence of flow and on such phenomena as onset depres-

sions. Examination of figure (7) reveals that the cross-section available for superflow depends on the method of measurement. When the gas flow technique was employed the cross-sectional area of a given tube was found to be S_p, say, whereas using the oscillation method a different value, S_o, was found. In every case S_p was significantly greater than S_o. In this section we shall examine ways in which the channel geometry of the wire-filled tubes can give rise to values of S_o smaller than S_p and consequently to values of $d(S_o)$ less than $d(S_p)$. Modification of the simple Poiseuille formula to take account of mean free path effects would reduce the divergence of S_o and S_p for small sizes of channel but would be a negligible correction in the wider sizes.

We start by considering the effect of variations in channel width through a cross-section of tube and to simplify calculation, assume all sections through a single tube to be identical.

1(a) <u>The effect on Poiseuille flow</u>

Let l be the total channel circumference and the channel width d, a random variable, with probability f(d). Then the circumference of channel of width d to $d + dd$ is just $lf(d)dd/2$ and this piece of channel may be considered parallel sided to a good approximation provided that the variation in d is slow, as would be the case if all the channels were wedge shaped. In this latter case the distribution function f(d) would be that shown below, d_1 being

the largest size of channel.

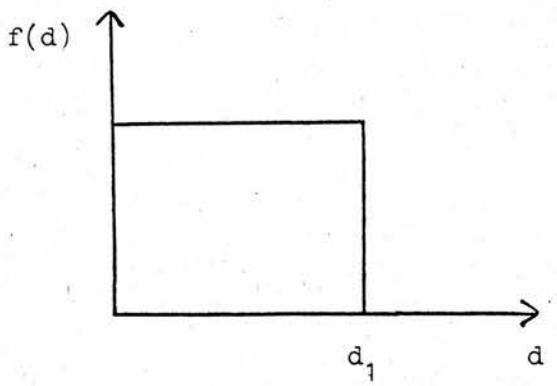

If $f(d) = 1/d_1$ then,

$$\frac{1}{2} \cdot \int_{\circ}^{d_1} f(d)\, dd = 1/2 \qquad (54)$$

So, in other words, f(d) is correctly normalised. Another choice for the distribution function would be

$$f(d) = 3(d - d_1)^2/d_1^3$$

which corresponds to rather more small channels. Now the volume of gas per second flowing $\dot{v}$ is given by

$$\dot{v} = 1/2 \int_{\circ}^{\infty} v_p(d) \,.\, d.f(d)dd^{\dagger} \qquad (55)$$

If the channels are treated as parallel sided over each length then

$$v_p(d) \propto d^2$$

---

†suffix p denotes Poiseuille

and

$$\dot{v} = v_p(\bar{d}_p).\bar{d}_p \cdot 1/2$$

by definition of $\bar{d}_p$. It follows that

$$\bar{d}_p \; v_p(\bar{d}_p) = \int_0^\infty d.v_p(d) \cdot f(d)dd \qquad (56)$$

and thus that

$$\bar{d}_p^3 = \int_0^\infty d^3 \, f(d)dd$$

If we take f(d) as

$$f(d) = \frac{1}{d_1} \;, \; 0 < d < d_1$$

$$= 0, \text{ otherwise} \qquad (57)$$

equation (56) yields

$$\bar{d}_p = d_o/3\sqrt{4} \qquad (58)$$

Thus we see that the magnitude of the channel width as measured by Poiseuille flow will for the distribution function of (57) be about 0.63 $d_,, d_1$ being the diameter of the widest channel or the maximum channel width.

1(b) The effect on inertial oscillations

Consider d as before to be a random variable. With the notation of figure 18(a) conservation of mass flow gives

$$A\dot{x} = \int_0^\infty \frac{1}{2} f(d)\, v_m(d)\, dd \,. \tag{59}$$

Conservation of energy leads to

$$\text{constant} = \tfrac{1}{2} A \rho g x^2 + \tfrac{1}{4} \rho_s Ll \int_0^\infty d\, f(d)\, v_m^2(d)\, dd \tag{60}$$

which upon differentiation yields

$$0 = A\rho g x\dot{x} + (\rho_s/2) Ll \int_0^\infty df(d) v_m(d) \dot{v}_m(d)\, dd \tag{61}$$

Now assume that

$$\frac{\partial}{\partial t} (v_m(d)/\dot{x}) = 0$$

since otherwise the motion is not, in general, simple harmonic.

Then

$$v_m(d) = k(d)\dot{x}, \quad \dot{v}_m(d) = k(d)\ddot{x}$$

leading to

$$\dot{v}_m(d) = (\ddot{x}/\dot{x}) v_m(d)$$

We can rewrite equation (61) as

$$0 = A\rho g x\dot{x} + (\rho_s/2) Ll \int_0^\infty df(d)\, v_m^2(d)\, \frac{\ddot{x}}{\dot{x}}\, dd$$

which gives

$$\ddot{x} = -\left\{ 2A\rho g \Phi / Ll \rho_s \right\} . x \tag{62}$$

where $$\Phi = x^2 / \int_0^\infty df(d) v_m^2(d) dd$$

Substituting from the continuity equation we find

$$o = L^2/4A^2 \frac{\left(\int_0^\infty df(d) v_m(d) dd\right)^2}{\int_0^\infty df(d)\, v_m^2(d) dd} = \frac{L^2}{4A^2} \cdot R$$

From the simple theory of Robinson (1951), which relates to a uniform channel, the mean channel width $\bar{d}_m$ is defined by

$$S_o = L/2 \cdot \bar{d}_m$$

we find

$$\ddot{x} = - \left\{ g S_o \rho / AL \rho_s \right\} \cdot x$$

Comparison of this equation with (62) shows that

$$\bar{d}_m = R = \frac{\left(\int_0^\infty df(d) v_m(d) dd \right)^2}{\int_0^\infty df(d) v_m^2(d) dd}$$

which is the general relation assuming the motion remains simple harmonic. If we choose the distribution function of equation (57) then $\bar{d}_m$ is given by

$$\bar{d}_m = \frac{\left(1/d_1 \int_0^{d_1} d\, v_m(d) dd\right)^2}{1/d_1 \int_0^{d_1} d\, v_m^2(d) dd} \qquad (63)$$

In order to compare $\bar{d}_m$ and $\tilde{d}_p$ we must assume a trial function for $v_m(d)$. Suppose that v_m is related to d thus:

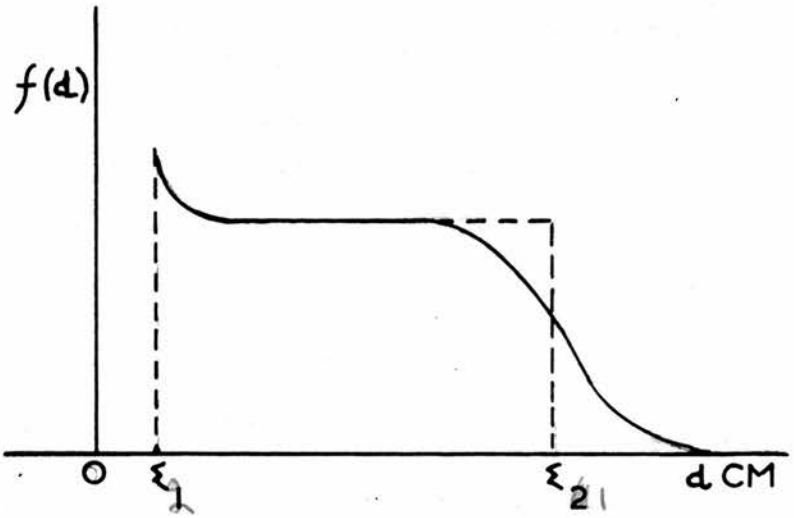

Figure 10 (a).

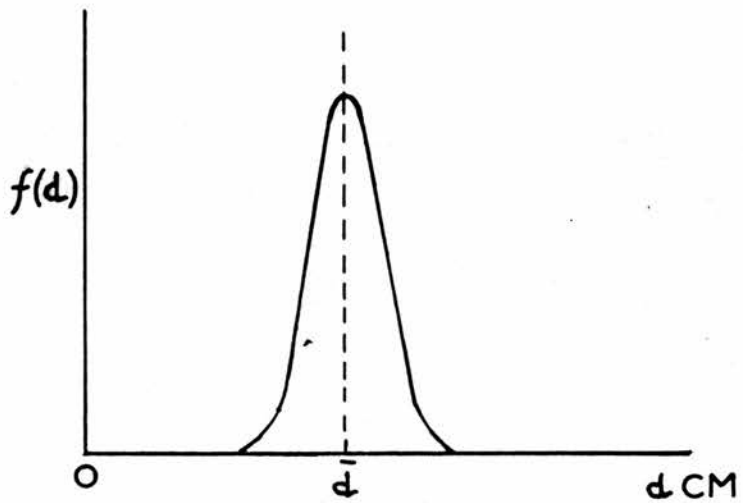

Figure 10 (b).

$$v_m \propto d^n \tag{64}$$

then

$$\bar{d}_m = 1/d_1(1/n+2) \cdot d_1^{n+2})/ \frac{1}{2n+2} \cdot d_1^{2n+2}$$

$$= [(2n+2)/(n+2)^2] . d_1 = d_1/2 \quad \text{for } n = 0$$

$$= (4/9)d_1 \quad \text{for } n = 1$$

$$= (3/8)d_1 \quad \text{for } n = 2$$

$$= (8/25)d_1 \quad \text{for } n = 3, \text{ etc.}$$

Another possibility is that $v_m(d) \propto 1/d$ in other words $n = -1$. To consider this case we must assume a lower cut-off for $d = \varepsilon$, and the distribution function must be that shown in figure 19(a).

We now find that $\bar{d}_m = d_1/\ln d_1/\varepsilon$ and that if $d_1/\varepsilon_1 \sim 10$ then $\bar{d}_m = d_1/2.3$. Similarly for $n = -2$,

$$\bar{d}_m = \frac{2\varepsilon^2}{d_1} [\ln d_1/\varepsilon]^2 . d_1$$

so that if $d_1/\varepsilon \sim 10$, $\bar{d}_m \sim d_1/10$. In the general case $v_m(d) \propto \frac{1}{d}n$, $n > 2$ one finds that

$$\bar{d}_m \approx \frac{(2n-2)}{(n-2)^2} \cdot \frac{\varepsilon^2}{d_1^2} \cdot d_1$$

and this gives for $n = 3$ and $\varepsilon/d_1 \sim 10$

$$\bar{d}_m = d_1/25$$

The maximum value of d_m namely $d_1/2$ is less than that of d_p which

is $d_1/3\sqrt{4}$. Thus the theory outlined above for flow through "wedge shape" channels leads to values of $\bar{d}_m < \bar{d}_p$ and is consistent with the results shown in figure 10. In conclusion, it is assumed that if the wire-filled tubes form a channel system with a random distribution of sizes but with a maximum size d_1, dependent on the number of draws, then theory suggests that the two methods of measuring $\bar{d}$ will lead to differing values. Before going on in Chapter 6 to assess the effect of such a distribution of channel sizes on the magnitude of observed critical velocities we first consider a second type of geometrical variation.

2(a) Variation in channel width in the direction of flow

Reference will be made to the notations of figure 18(b) and 19(a). First we calculate the period of inertial oscillation in a tapered channel noting that

$$v(d) = k/d .$$

Let the maximum channel size be ε_1 and the minimum size be ε_2, then

$$\tan\theta = (\varepsilon_1 - \varepsilon_2)/21 . \qquad (65)$$

Consider the flow through a strip dy of width d (see figure 20(a)).

The area of the strip dy is σ d and thus the volume/sec $\dot{v}$ is

$$\dot{v} = \sigma d\ k/d = \sigma k = A\dot{x} .$$

The kinetic energy of the element may be written as

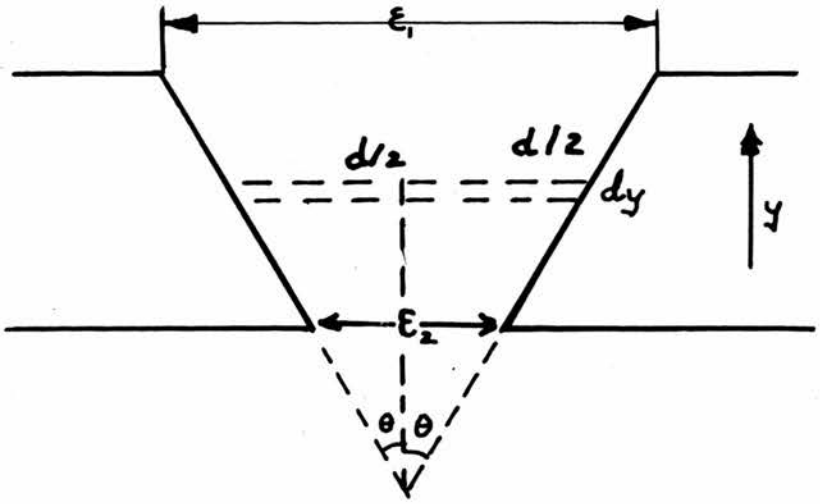

Figure 20 (a).

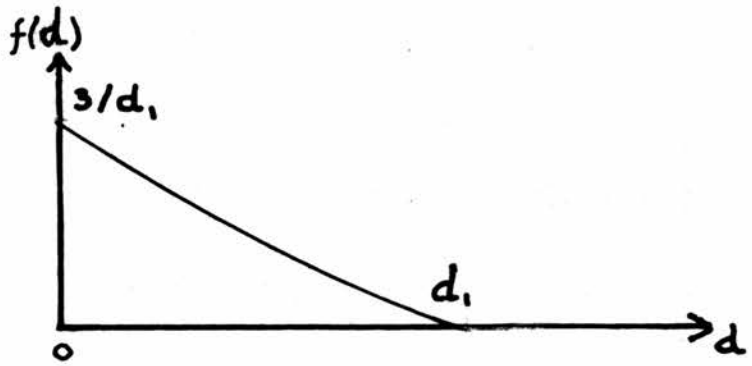

Figure 20 (b)

$$\tfrac{1}{2}\left\{\sigma d \rho_s \, dy\right\}\left\{\frac{k}{d}\right\}^2 .$$

Thus the total kinetic energy T in the channel is

$$\frac{\sigma}{2} \rho_s \, k^2 \int_{\varepsilon_1}^{\varepsilon_2} \frac{dy}{d}$$

but since $y = \frac{d}{2} \cot \theta$, we get

$$T = -\frac{1}{4} \sigma \rho_s k^2 \cot \theta \ln \frac{\varepsilon_2}{\varepsilon_1}$$

$$= -\frac{1}{4} \sigma \rho_s \left(\frac{A}{\sigma}\right)^2 \cot \theta \left(\ln \frac{\varepsilon_2}{\varepsilon_1}\right) \dot{x}^2$$

The potential energy V of the liquid above the bath is given by

$$A\rho g \, x^2/2 .$$

Thus by energy conservation for frictionless or superflow

$$A\rho g x^2/2 + \left\{(\rho_s A^2 \cot \theta . \ln \varepsilon_1/\varepsilon_2)/4\sigma\right\} . \dot{x}^2$$

$$= \text{constant.}$$

Partial differentiation with respect to time gives

$$0 = A\rho g \, x\dot{x} + \left\{\rho_s A^2 \cot \theta \ln \varepsilon_1/\varepsilon_2)/2\sigma\right\} \dot{x}\ddot{x} .$$

Thus the oscillations are still simple harmonic but their period is now given by

$$T = 2\pi \sqrt{\left\{\left[A \cot \theta \ln \varepsilon_1/\varepsilon_2)/(2g\sigma)\right] . \rho_s/\rho\right\}}. \qquad (66)$$

Since we have introduced no approximations in this already simple model, the theory should go over into the simple form, equation (48), when $\varepsilon_1 = \varepsilon_2$.

From (65) we find

$$(\ln \varepsilon_1/\varepsilon_2) \cot \theta = (2L \ln \varepsilon_1/\varepsilon_2)/(\varepsilon_1 - \varepsilon_2) \qquad (67)$$

so putting

$$u = \varepsilon_1 - \varepsilon_2$$

equation (67) becomes,

$$\frac{2L \ln \frac{u+\varepsilon_2}{\varepsilon_2}}{u} = \left\{2L \ln\left(1 + \frac{u}{\varepsilon_2}\right)\right\}/u$$

$$= 2L/\varepsilon_2, \text{ Lim } u \to 0.$$

Comparison of equations (66) and (48) shows that

$$\bar{d}_{oscill} = \frac{\bar{S}_o}{\sigma} = [(\varepsilon_1 - \varepsilon_2)/\ln \varepsilon_1/\varepsilon_2] \qquad (68)$$

Thus $\bar{S}_o$, the effective open cross-section in a tapered channel, is expressed in terms of ε_1 and ε_2 only and we notice that for $\varepsilon_1 \gg \varepsilon_2$ this depends strongly on ε_1.

2(b) Poiseuille flow in a uniformly tapering channel

Consider a channel of unit width as shown in figure (21). For the velocity profile we write

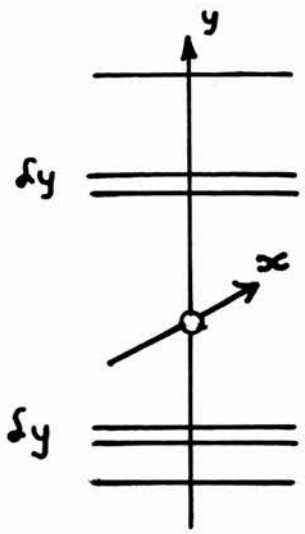

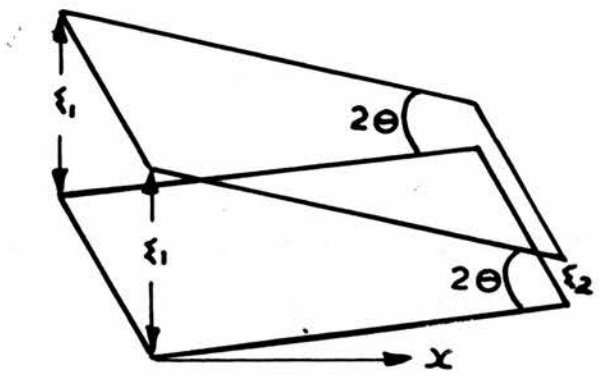

Figure 21.

$$y\ dp + 2dx\,\eta\,\frac{du}{dy} = 0$$

and hence that

$$du = -\left\{y\ dy/2\eta\right\}\frac{dp}{dx}$$

and thus,

$$u = \left(\frac{d^2}{4} - y^2\right) \cdot \frac{1}{4\eta} \cdot \frac{dp}{dx} \ .$$

Integrating, we find that the volume flowing/sec to be given by

$$v = \int_0^{d/2} 2u\,dy$$

$$= \frac{\eta^{-1}}{2}\ dp/dx \int_0^{d/2} \left(\frac{d^2}{4} - y^2\right)dy$$

or
$$v = \frac{\eta^{-1}}{2}\ dp/dx \cdot d^3/12 \ . \qquad (69)$$

Now $d = \varepsilon_1 - x/l(\varepsilon_1 - \varepsilon_2)$ since this equation (70) satisfies

$$d = \varepsilon_1 \quad \text{for } x = 0$$

$$d = \varepsilon_2 \quad \text{for } x = l \ .$$

We note that for an ideal gas PV = constant. Thus, from equation (69) we find, multiplying by P, that

$$PV \int_0^l \frac{dx}{d^3(x)} = \frac{\eta^{-1}}{24} \int_{p_1}^{p_2} p\ dp$$

and so

$$(p_2^2 - p_1^2)/48\eta p_1 V_1 = \int_0^1 \frac{dx}{d^3(x)}$$

$$= \frac{1}{\varepsilon_1 - \varepsilon_2} \int_1^2 dd/d^3(x) = \omega, \text{ say.}$$

Since $dd = 0 - \frac{(\varepsilon_1 - \varepsilon_2)}{1} dx$, by differentiation of (70), ω becomes

$$\omega = \{1/2(\varepsilon_1 - \varepsilon_2)\} . \{(\varepsilon_1^2 - \varepsilon_2^2)/\varepsilon_1^2 \varepsilon_2^2\} .$$

We note that for a uniform channel of width d,

$$d^3 = 24\eta l\, p_1 V_1/(p_2^2 - p_1^2) .$$

Thus

$$\bar{d}^3_p = \varepsilon_1^2 \varepsilon_2^2/\varepsilon_1 + \varepsilon_2$$

and that for $\varepsilon_1 \gg \varepsilon_2$

$$\bar{d}_p = \sqrt[3]{(\varepsilon_1 \varepsilon_2^2)} .$$

This value (from Poiseuille flow) depends on ε_2 more strongly than on ε_1 and thus one would expect that $\bar{d}_{eff}$ would be small, being influenced strongly by the constricting diameter.

Having now obtained two values of d, namely $\bar{d}_p$ and $\bar{d}_{oscill}$ both being expressed in terms of ε_1 and ε_2, we compare these and find

$$\bar{d}_p^3/\bar{d}_{oscill}^3 = \frac{\varepsilon_1^2\varepsilon_2^2}{\varepsilon_1+\varepsilon_2}\ \frac{(\ln \varepsilon_1/\varepsilon_2)^3}{(\varepsilon_1-\varepsilon_2)^3}\ .$$

If we take $\varepsilon_1/\varepsilon_2 \gg 1$, 10:1 say, then

$$\frac{\bar{d}_p^3}{d_{oscill}^3} = \frac{\varepsilon_1^2\varepsilon_2^2}{\varepsilon_1\varepsilon_1^3}.(\ln\frac{\varepsilon_1}{\varepsilon_2})^3$$

$$= \frac{\varepsilon_2^2}{\varepsilon_1^2}(\ln\frac{\varepsilon_1}{\varepsilon_2})^3 \approx 1/10\,. \qquad (71)$$

It follows that a constricted channel would lead to a value of d from oscillations about twice that obtained from Poiseuille flow. In fact this is contrary to the results of figure (7) and we conclude that the channels are moderately uniform in the direction of flow.

4.3 Onset depressions in wire-filled tubes

We consider now how onset depressions might affect the temperature dependence of mean flow velocity. It is clear at the outset that since each tube most probably contains a distribution of channel sizes that no clearly defined onset temperature will be

seen. The few large sizes of channel will contribute to the flow for all temperatures $T < T_\lambda$.

The total length of channel with separation d to d + dd is (c.f. equation (57))

$$\frac{1}{2} f(d)dd$$

Thus the area of this channel is

$$\frac{1}{2} d\, f(d)dd \tag{72}$$

The mean velocity at a temperature T is

$$v = v_s \, (\rho_s/\rho)_{T,d} \tag{73}$$

and we shall assume that v_s depends upon d as

$$v_s = k/d$$

being independent of temperature, so that

$$\bar{v}_{d,T} = k/d \, (\rho_s/\rho)_{T,d} \, . \tag{74}$$

Assume a distribution function f(d) of the form

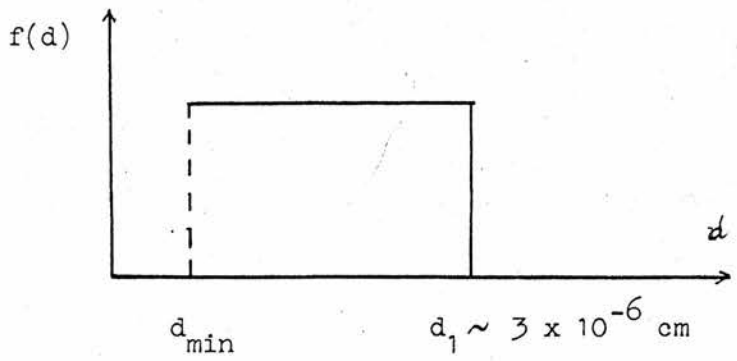

At a temperature T, only tubes with a separation larger than d_T will permit flow to take place. In order to calculate d_T we use a theoretical result of Ginsburg and Pitaevskii (1958) which relates the onset depression T_λ to the radius of the channel d, which is

$$\Delta T_\lambda = T_\lambda - T_o(d) = \beta^2/d^2 \tag{75}$$

where $\beta = 2 \times 10^{-7}$ for a parallel-sided channel.

It follows from equation (75) that d_T is given by

$$d_T = \beta \cdot \sqrt{\frac{1}{T_\lambda - T}} \cdot \tag{76}$$

The total flow at temperature T will therefore depend on how many channels are contributing and this will be

$$Q_T = \int_{d_T}^{d_1} \bar{v}_{d,T} \cdot 1/2 \, df(d)dd \tag{77}$$

which becomes

$$Q_T = \frac{kl}{2} \int_{d_T}^{d_1} (\rho_s/\rho)_{T,d} \cdot f(d)dd \, . \tag{78}$$

If the superfluid fraction for a channel with onset temperature T_o is taken to vary as

$$\rho_s/\rho = 1 - (T/T_o)^{\sigma} \tag{79}$$

where $\sigma = 5.6$ (Andronikashvili), we can evaluate equation (78) if we neglect second order terms, which will give a sufficiently good approximation. The equation becomes

$$Q_T = \frac{kl}{2(d_1 - d_{min})} \int_{d_T}^{d_o} 1 - T^{\sigma}/(T_\lambda - \frac{\beta^2}{d^2})^{\sigma} \; . \; dd \qquad (80)$$

$$= \frac{kl}{2(d_1 - d_{min})} [d]_{d_T}^{d_1} - \frac{kl(T/T_\lambda)^{\sigma}}{2(d_1 - d_{min})} \int_{d_T}^{d_o} \frac{dd}{(1 - \frac{\beta^2}{T_\lambda d^2})^{\sigma}} \qquad (81)$$

$$= A - B \text{ , say.}$$

The first term A is given by

$$A = \frac{kl}{2d_1} (d_1 - d_T), \text{ if } d_{min} \approx 0 \; .$$

Substituting from equation (76) for d_T one finds

$$A = \frac{kl}{2} - \frac{kl}{2d_1} \frac{\beta}{(T_\lambda - T)^{\frac{1}{2}}}$$

$$= \frac{kl}{2} \left\{ 1 - \frac{\beta}{d_1 \sqrt{T_\lambda}} (1 - T/T_\lambda)^{-\frac{1}{2}} \right\}$$

$$= \frac{kl}{2} \left\{ 1 - \frac{\beta}{d_1 \sqrt{T_\lambda}} (1 + T/2T_\lambda) \right\}$$

$$\frac{kl}{2} \left\{ 1 - f - f/2 \; (T/T_\lambda) \right\}, \text{ where } f = \beta/d_1 \sqrt{T_\lambda} \; .$$

In order to evaluate B we see that the absolute magnitude of

$$\frac{T_\lambda - T}{T_\lambda} \quad \text{for } T > 0$$

is $$\left| \frac{T_\lambda - T}{T_\lambda} \right| = \beta^2/d^2 T_\lambda < 1$$

thus,

$$B = \frac{1k}{2d_1} \int_{d_T}^{d_1} \left(\frac{T}{T_\lambda}\right)^\sigma \frac{dd}{(1 - \beta^2/d^2 T_\lambda)^\sigma}$$

can be rewritten as,

$$B \doteq \frac{1k}{2d_1} \left(\frac{T}{T_\lambda}\right)^\sigma \int_{d_T}^{d_1} \left(1 + \frac{\sigma\beta^2}{d^2 T_\lambda}\right) dd$$

$$= \frac{1k}{2d_1} \left(\frac{T}{T_\lambda}\right)^\sigma \int_{d_T}^{d_1} \left(1 + \frac{\sigma\beta^2}{d^2 T_\lambda}\right) dd$$

$$= \frac{1k}{2d_1} \left(\frac{T}{T_\lambda}\right)^\sigma \left\{ (d_1 - d_T) + \frac{\sigma\beta^2}{T_\lambda} \left(\frac{1}{d_1} - \frac{1}{d_T}\right) \right\}$$

$$= \frac{1k}{2} \left(\frac{T}{T_\lambda}\right)^\sigma \left\{ \left(1 - \frac{d_T}{d_1}\right) + \frac{\sigma\beta^2}{d^2 T_\lambda} \left(1 - \frac{d_1}{d_T}\right) \right\}$$

$$= \frac{1k}{2} \left(\frac{T}{T_\lambda}\right)^\sigma \left\{ \frac{(d_1 - d_T)}{d_1} - \frac{\sigma\beta^2}{d^2 T_\lambda} \frac{(d_1 - d_T)}{d_T} \right\}$$

$$= \frac{1k}{2} \left(\frac{T}{T_\lambda}\right)^{\sigma} \frac{(d_1 - d_T)}{d_1} \left\{ 1 - \frac{\sigma \beta^2}{d_1 d_T T_\lambda} \right\}$$

hence

$$Q_T = \frac{kl}{2d_1} (d_1 - d_T) \left\{ 1 - \left(\frac{T}{T_\lambda}\right)^{\sigma} \left(1 - \sigma f^2 \frac{d_1}{d_T}\right) \right\} .$$

But from equation (76)

$$d_T = \sqrt{\frac{\beta}{T_\lambda}} \left\{ 1 - \frac{T}{T_\lambda} \right\}^{-\frac{1}{2}}$$

thus

$$\frac{d_T}{d_1} = \frac{\beta}{d_1 \sqrt{T_\lambda}} \left\{ 1 - \frac{T}{T_\lambda} \right\}^{-\frac{1}{2}} = f \left\{ 1 - \frac{T}{T_\lambda} \right\}^{-\frac{1}{2}} .$$

It follows that to a rough approximation

$$Q_T = \frac{kl}{2} \left\{ 1 - f \left(1 - \frac{T}{T_\lambda} \right)^{-\frac{1}{2}} \right\} . \left\{ 1 - \left(\frac{T}{T_\lambda}\right)^{\sigma} \left(1 - \sigma f \left(1 - \frac{T}{T_\lambda}\right)^{\frac{1}{2}}\right) \right\} . \quad (82)$$

For small values of f this reduces to the usual equation

$$Q_T = \frac{kl}{2} \left(1 - \left(\frac{T}{T_\lambda}\right)^{\sigma}\right) .$$

When f cannot be neglected then at low temperatures where

$$\left(1 - \frac{T}{T_\lambda}\right)^{-\frac{1}{2}} \approx 1 + \frac{T}{2T_\lambda}$$

the flow velocity Q_T increases linearly, approaching a value given by

$$Q_T = \frac{kl}{2} (1 - f) .$$

These ideas do not explain the fact that the flow rate through Millipore filters increases almost linearly with temperature over the range $1.4 < T < T_\lambda$ (see for example Seki, 1962).

We refer again to equation (77) and suppose that the filters contain a high proportion of very small channels. Suppose

$$f(d) = \phi/d^3$$

$$v(d) = k/d$$

and for simplicity that $(\rho_s/\rho)_{d,T} = 1 \quad d_1 > d > d_T$

$$= 0 \quad d < d_T .$$

Then

$$Q_T = \phi k \frac{1}{2} \int_{d_T}^{d_1} d \cdot \frac{1}{d^3} \cdot \frac{1}{d}\, dd$$

$$= \frac{\phi k l}{2 d_1^2} \left\{ \left(\frac{d_1}{d_T}\right)^2 - 1 \right\}$$

$$= \frac{\phi k l}{2 d_1^2} \left\{ \frac{d_1^2 T_\lambda}{\beta^2} \left(1 - \frac{T}{T_\lambda}\right) - 1 \right\}$$

$$= \frac{\phi k l}{2 d_1^2} \left\{ \frac{1}{f^2} - 1 - \frac{1}{f^2} \cdot \frac{T}{T_\lambda} \right\}$$

$$\doteq \frac{\phi k l}{2 d_1 f^2} \left\{ 1 - \frac{T}{T_\lambda} \right\} \text{ for } f^2 \ll 1 \,.$$

Thus we see that a suitable choice of $v(d)$ and $(\rho_s/\rho)_{d,T}$ can give

rise to a linear variation of Q consistent with the results already obtained by Seki. It is possible that the mercury intrusion method which has been used to measure the mean pore size of the filters does not show the presence of pores much smaller than 10^{-6} cm. Such small pores could lead to the observed behaviour of Q_T via the onset mechanism. Allen and Watmough (1965) reported that flow through wire-filled tubes showed no evidence of onset depressions. In the light of this present analysis it would appear that their conclusions might be wrong since their measurements of mean velocity as a function of temperature showed a significant change of temperature dependence similar to that predicted by equation (82). The effect of onset depressions is to give an effective value of $\alpha < 5.6$. Supposing the above arguments to be correct we infer the validity of our previous discussions where we introduced the concept of a distribution function.

CHAPTER 5

THE EXPERIMENTS

5.1 Introduction

In order to investigate the relationship between superfluid critical velocity and channel width, a number of wire-filled tubes similar to those used by Allen and Misener (1939) and Brown and Mendelssohn (1947) were made as described in Chapter 3. Reservoirs made partly of glass and partly of copper were attached to these tubes by means of nilo-k and indium seals. In helium below the λ-point gravitationally induced flow via the channels formed by the tubes took place. The flow rates from the reservoirs were measured at stabilized temperatures between 1.2°K and a few millidegrees of the lambda temperature.

In channels smaller than 10^{-5} cm the only quantitative measurements of critical velocity so far reported are those through Millipore filters (Seki 1962) and those of the saturated and unsaturated film. The main obstacles to quantitative measurement of critical velocity are avoidance of the mechano-caloric effect and the production of small channels of well defined size. Thermal effects can affect both the magnitude and pressure dependence of flow. We can see how this arises. Consider flow occurring from a reservoir via a superleak. Since the superfluid carries no entropy there will be a tendency for the entropy per unit volume to increase.

On the other hand the heat Q will flow out of the system via the walls and some will cause evaporation. The degree of contact will govern the temperature rise in the reservoir.

Assume the heat flow Q is given by

$$Q = c \Delta T$$

At equilibrium the entropy per unit volume of the liquid is constant, due to the heat flowing away as fast as the entropy is increased. Therefore the entropy per unit volume produced by the flow is

$$\frac{ds}{dt} = - \frac{s}{v} \frac{dv}{dt} ,$$

i.e., the fractional change in entropy per unit volume is due to the fractional change in volume. The heat flow is

$$Q = TV \frac{ds}{dt} = c \Delta T$$

and so,

$$c \Delta T = - \frac{TVs}{V} \cdot \frac{dv}{dt}$$

$$= - ST \frac{dv}{dt}$$

Therefore we find

$$\Delta T = - \frac{ST}{c} \frac{dv}{dt}$$

and the difference in temperature gives rise to a fountain pressure of

$$\Delta p = - S \Delta T \quad (S \text{ is entropy/unit volume})$$

$$= - \frac{S^2 T}{c} \frac{dv}{dt} .$$

Suppose the thermal contact is so poor that the fountain pressure becomes equal to the hydrostatic pressure. Then,

$$\rho g x = \frac{S^2 T}{c} \frac{dv}{dt}$$

where x is the level difference between bath and reservoir. But $\frac{dv}{dt}$ is given by,

$$\frac{dv}{dt} = A\dot{x} \text{ since } v = A(X + l)$$

where l is the reservoir length below the bath. It follows that in these circumstances the flow becomes a "thermal relaxation" process and the equation of motion is

$$\rho g x = \frac{S^2 T}{c} A\dot{x} \ .$$

In other words the pressure is proportional to the velocity. Allen and Misener (1939) observed precisely this pressure dependence with one of their tubes at low pressures. Clearly it is desirable to avoid such thermal effects; also, as we show in Chapter 6, the mechano-caloric effect can cause the damping of inertial oscillations which are used to measure v_c and d.

There has so far been no completely satisfactory theory of flow in narrow channels. The reason probably lies partly in the curious behaviour of liquid helium but also in the difficulty of deciding whether in particular experiments thermal contact was achieved. Also as we have seen in Chapter 4 the distribution of

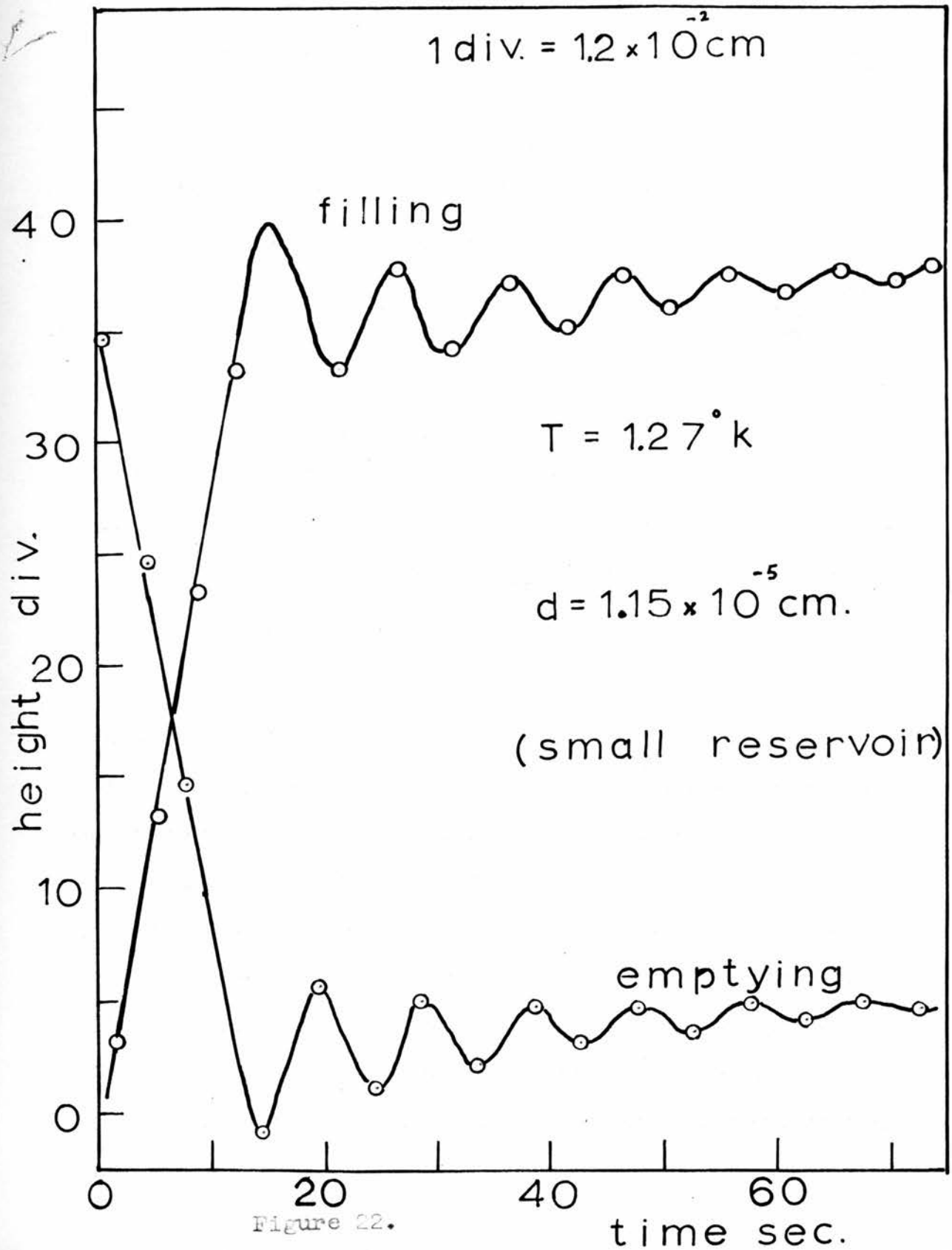
1 div. = 1.2 x 10^-2 cm
filling
T = 1.27° k
d = 1.15 x 10^-5 cm.
(small reservoir)
emptying
height div.
0
10
20
30
40
0
20
40
60
time sec.

Figure 22.

channel sizes (or width in the case of annular superleaks) is a factor influencing the measured value of d. Neglect of this consideration causes some error in relating critical velocity to channel size. Despite the fact that wire-filled tubes do not provide a single length of uniform channel nevertheless their area available for flow can be measured at helium temperatures and also they do provide a means of varying d over a wide range of channel sizes.

In the present work care was taken to ensure thermal contact so that at low temperatures the flow was almost isothermal. This was achieved by means of vapour contact between bath and reservoir and also by means of a copper cylinder built into the reservoir.

5.2 Experimental

Each experiment was performed by moving the reservoir with respect to the bath and measuring as a function of time the liquid level in a narrow side arm connected to the reservoir. The reservoir level approached the bath with a finite velocity and oscillated about it, owing to the inertia of the liquid in the channels provided by the long wire-filled tubes. Tube lengths of $\sim$ 10 cm were necessary in order to obtain oscillations of conveniently measurable amplitude. The amplitude was of the order of 1 mm and periods of up to 20 seconds were observed. The oscillations, see figure (22), persisted for up to several minutes in the narrower sizes of channel

at the lowest temperatures but were more heavily damped at higher temperatures and also at all temperatures in the larger sizes of channel which exhibited pressure dependent flow. The damping introduces a correction term which tends to make S_o larger and v_c smaller but since the magnitude of the correction was generally less than 2%, this effect was neglected. The damping of oscillations is more fully discussed in Chapter 6. The velocity in the widest channel might have been as much as 5% lower than the value calculated from equation (52) of 4.1, but other factors such as uncertainty in the value of q in equation (46), p. 29, probably give rise to a greater error.

The measurement of flow rates was achieved by means of a cathetometer having an internal scale of length 12 mm. The divisions of this scale were 1.2×10^{-2} cm apart. As the liquid level passed successive divisions the times were recorded. This same procedure was followed when flow through Millipore filters was investigated, but because of the filter thickness (150 micron) there was insufficient inertia within the pore to provide measurable oscillations. Thus in order to calculate the flow velocity through the pores use was made of figures for open area and channel diameter supplied by the Millipore Filter Corporation. The open cross-section of the filters was so large that the exposed area of each filter had to be restricted to the smallest hole that could be precision-bored.

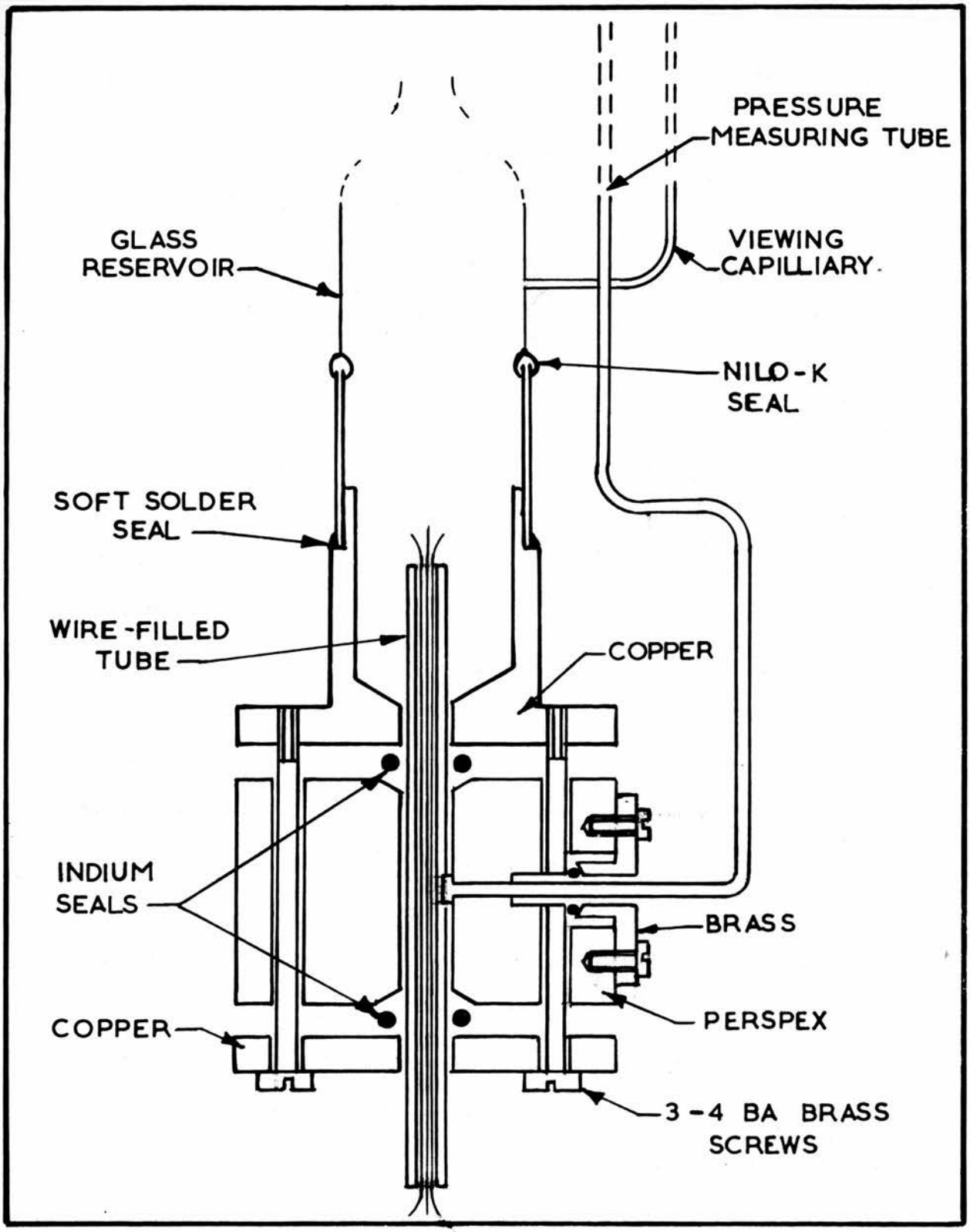
PRESSURE MEASURING TUBE
GLASS RESERVOIR
VIEWING CAPILLIARY
NILO-K SEAL
SOFT SOLDER SEAL
WIRE-FILLED TUBE
COPPER
INDIUM SEALS
BRASS
PERSPEX
COPPER
3-4 BA BRASS SCREWS

Figure 2.

The procedure followed in taking the measurements was to pump down to a temperature just above the lambda point and there to check for flow of helium I. Flow measurements were then made in temperature steps separated by twenty or thirty millidegrees down to 1.2°K where the oscillations were examined. In those cases where damping was heavy many independent observations of the period were made thus enabling an accurate mean value of τ to be calculated.

In the later stages of this research when it had become apparent that flow through the larger channels was pressure dependent and in the smaller channels pressure independent, it became desirable to examine the transition to see if it resulted from a spurious thermal effect or whether it was a fundamental change connected with the condition of the flowing superfluid. The obvious check was to measure the pressure gradients within two superleaks, one where the flow was independent of pressure and the other where the flow depended strongly on it. Figure (23) shows the apparatus used for this investigation. The stand pipe was connected to the wire-filled tubes at an intermediate point and care was taken to make the volume at the point of junction large compared to that of the channel. This lowered the velocity at the point and avoided pressures due to the Bernoulli effect. After a transient behaviour the manometer monitored the pressure at the

point where it was joined to the channels. A discussion of the results obtained using this arrangement is given in Chapter 6.

In the present series of experiments a small filling hole at the top of each reservoir designed to allow thermal contact by means of the vapour phase also permitted film transport. The quantity of liquid transported by the film is approximately 6×10^{-5} $cm^3/sec/cm$ so that for a hole of radius $r \sim 1$ mm the quantity q transported is given by

$$q = \pi.10^{-1}.6.10^{-5}$$

$$\sim 2.10^{-5}\ cm^3\ sec^{-1}\ .$$

Each reservoir also had a viewing capillary whose constricting hole was about 1 mm so the total film transport was about 4×10^{-5} $cm^3\ sec^{-1}$. Since volume flow rates via the channels provided by the wire-filled tubes were about two orders of magnitude greater than those due to the film, the correction was neglected in the calculations of critical velocity.

5.3 Thermal contact between the liquid in the reservoir and that in the bath

If the heat generated by the flow is Q then the thermal contact c is defined by the equation

$$Q = c\Delta T$$

where $T + \Delta T$ is the temperature in the reservoir and T that in the

bath. Perfect contact corresponds to zero temperature difference for a finite heat flow. In the present experiments contact was achieved via the reservoir walls and via the vapour phase. We first evaluate the magnitude of c for copper walls.

Consider a reservoir where the only thermal contact with the bath is by means of a copper wall and in which heat is being generated by the flow. We refer to the accompanying figure:

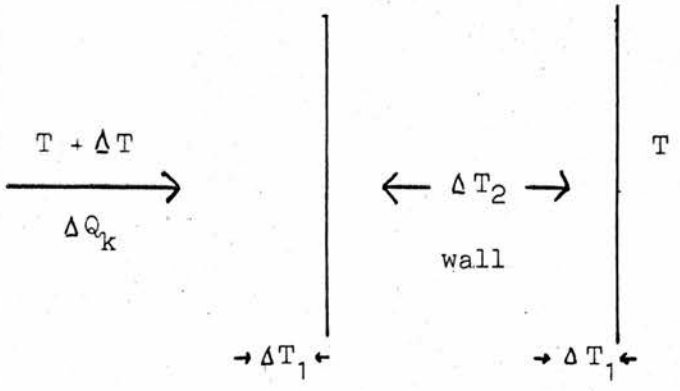

By continuity and referring to a single wall

$$\Delta Q_k = \alpha \Delta T_1 = \frac{k}{l} \Delta T_2$$

where α^{-1} is the Kapitza boundary resistance and where k and l are the thermal conductance and thickness of the wall respectively.

We notice that the total temperature drop ΔT is given by

$$\Delta T = 2\Delta T_1 + \Delta T_2$$

and thus since $\Delta Q_k = \alpha \Delta T_1 = \frac{k}{l} \Delta T_2$

$$\frac{\Delta T_1}{\Delta T_2} = \frac{k}{l\alpha}$$

we find by substitution that

$$\frac{\Delta T}{\Delta T_2} = \frac{2\Delta T_1}{\Delta T_2} + 1 = \frac{2k}{l\alpha} + 1 .$$

Finally we obtain

$$\Delta T = \Delta Q_k \left\{ 2/\alpha + 1/k \right\} .$$

So that the constant defining the degree of contact is, effectively,

$$C = \left[2/\alpha + 1/k \right]^{-1} .$$

According to measurements of Kapitza (1941), α for polished copper is equal to $T^3/10$ and according to Fairbank and Wilks (1955) equal to $T^2/45$.

For copper we take $k = 10^7$ erg cm^{-2} deg K^{-1} and $l = 0.025$ cm. Thus

$$1/k = 2.5 \times 10^{-3}/10^7 = 2.5 \times 10^{-10}$$

At 1.2°K, using Kapitza's form for α[†],

$$\alpha = T^3/10 = 0.17 \times 10^7 = 1.7 \times 10^6 \text{ erg units}$$

hence $$2/\alpha = 1.2 \times 10^{-6} \gg 1/k$$

Thus

$$c_{copper} = \frac{\alpha}{2} = 0.85 \times 10^6 .$$

~~Since the conductivity of copper is unimportant, the contact via~~

[†] a cubic contact relation is generally accepted.

~~the glass will contribute, and taking the total area of glass and copper A = 20 cm^2 the effective contact will be~~

$$c_{wall} \sim 17 \times 10^6 \ .$$

~~In those cases where a narrow glass capillary was used to measure flow the copper wall then provided the major part of the contact area.~~

The contact via the vapour phase can be obtained from an equation derived in connection with the damping of oscillations in Chapter 6, namely

$$c_{vapour} = \frac{\lambda p}{RT} \left(\frac{a^4}{8\eta l}\right) \left(\frac{\partial p}{\partial T}\right)_{svp}$$

$$= \left(\frac{a^4}{8\eta l}\right) \frac{\lambda^2}{R^2} \frac{p^2}{T^{3+n}}$$

where a and l are the dimensions of the constriction at the vapour access point, λ is the latent heat of vaporisation, R the gas constant and p the vapour pressure at temperature T. Taking

$$R = 8.10^7 \text{ erg deg}^{-1} \text{ mole}^{-1}$$

$$\lambda = 83.10^7 \text{ erg mole}^{-1}$$

$$p = 0.625 \text{ mm Hg}$$

$$T = 1.2^\circ K$$

$$\left(\frac{\partial p}{\partial T}\right)_{svp} = 5 \text{ mm Hg deg } K^{-1}$$

$$n = 0.68$$

$$a = 5.10^{-2} \text{ cm}$$

$$l = 10^{-1} \text{ cm}$$

$$\eta = 5.10^{-6} \text{ poise}$$

We find

$$\frac{a^4}{8\eta l} = \frac{25^2 \times 10^{-2}}{4}$$

so that

$$c_{vapour} \sim \frac{25^2.10^{-2}.10^2(6.25 \times 10^{-2}.13.6.981)^2}{4.2}$$

$$\sim 5.10^7 \text{ erg sec}^{-1} \text{ deg K}^{-1}.$$

We thus see that the contact is comparable and is of course additive since both processes occur at the same time. The total contact is about 5.10^7.

We are now able to estimate the extent of thermal effects since as we have already shown that ΔT is given by

$$\Delta T = - \frac{ST}{c} \frac{dv}{dt}$$

where $\frac{dv}{dt}$ is the volume flow rate, and S is the entropy per unit volume.

At 1.2°K, $S \sim 7 \times 10^4$ erg cm^{-3}

$$\frac{dv}{dt} < 10^{-2} \text{ cm}^3 \text{ sec}^{-1}$$

$$c \sim 5 \times 10^7 \text{ erg deg K}^{-1}$$

Thus

$$\Delta T = \frac{7.10^{4}.1.2.10^{-2}}{4.10^{7}} \sim 2.1 \times 10^{-5} \text{ °K}$$

The fountain pressure h is given by

$$h = S/g \,.\, \Delta T$$

$$\sim \frac{7.10^{4}}{10^{3}} \times 2.1 \times 10^{-5}$$

$$\sim 14.10^{-4} \text{ cm}$$

One cathetometer division is 1.2×10^{-2} cm, thus the fountain effect should not have exceeded one tenth of one cathetometer division at 1.2°K. At higher temperatures the thermal contact improves and the flow rates fall but the entropy per unit volume increases exponentially so the net effect is that at higher temperatures the fountain pressure may have become somewhat larger but it is unlikely that it exceeded 2 or 3 cathetometer divisions.

The total pressure π can be written as

$$\pi = \rho gh + \rho s\, T + (\frac{\partial p}{\partial T})\Delta T \,.$$

We have so far neglected to calculate the effect of the term $(\frac{\partial p}{\partial T})\Delta T$.

Now $(\frac{\partial p}{\partial T}) = 5.10^{-1}.981.13.6$

$$\sim 5.10^{3}$$

so that for $\Delta T = 2.1 \times 10^{-5}$ °K, this term gives rise to an excess

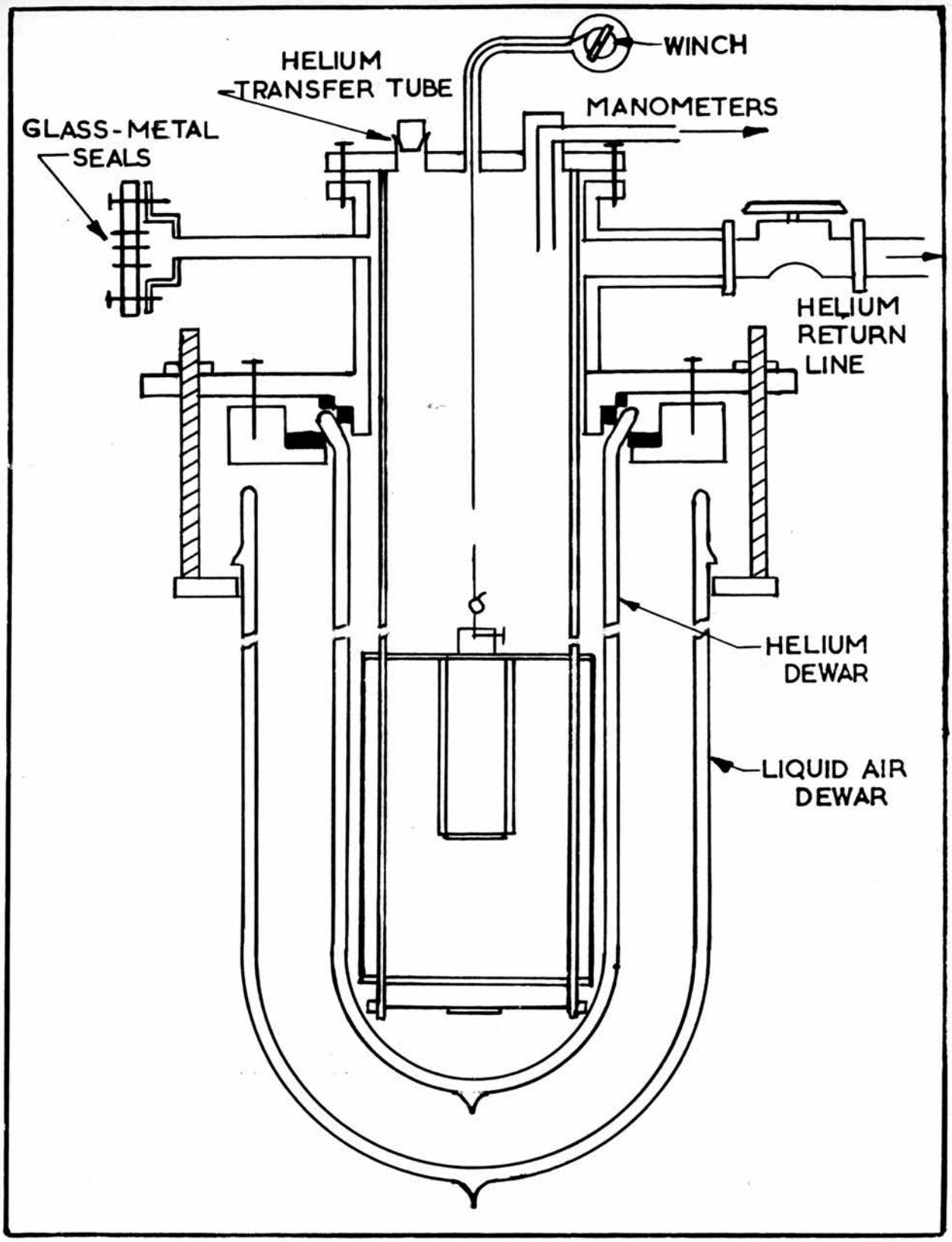
WINCH
HELIUM
TRANSFER TUBE
MANOMETERS
GLASS-METAL
SEALS
HELIUM
RETURN
LINE
HELIUM
DEWAR
LIQUID AIR
DEWAR

Figure 2.

pressure,

$$p \sim 2.1 \cdot 10^{-5} \cdot 5.10^{3}$$

$$\sim 10^{-1} \text{ dynes cm}^{-2} .$$

Thus the excess vapour pressure above the reservoir leads to a negligible correction.

5.4 The helium cryostat

The essential features of the helium cryostat are shown in figure (24). The dewars, made of Monax glass, were completely silvered except for narrow strips left clear for the purpose of observation. The monax glass has the valuable property of being practically impervious to helium gas. The reservoirs (from which flow took place) were mounted inside a copper radiation shield polished on the outside and blackened on the inside. The shield has windows of Chance ON22 heat absorbing glass. It was supported by a terylene thread and constrained to move parallel to the viewing slits by two fixed copper-nickel tubes. The thread was connected internally to a winch situated at the cryostat top which served to raise or lower the entire system relative to the liquid helium level. To minimize effects due to heat entering the cryostat from outside, the reservoirs were illuminated by light from a twelve volt lamp from which heat radiation had been removed by means of a water tank and a Chance (ON22) glass window. The efficacy of this procedure was proved by the fact that varying the

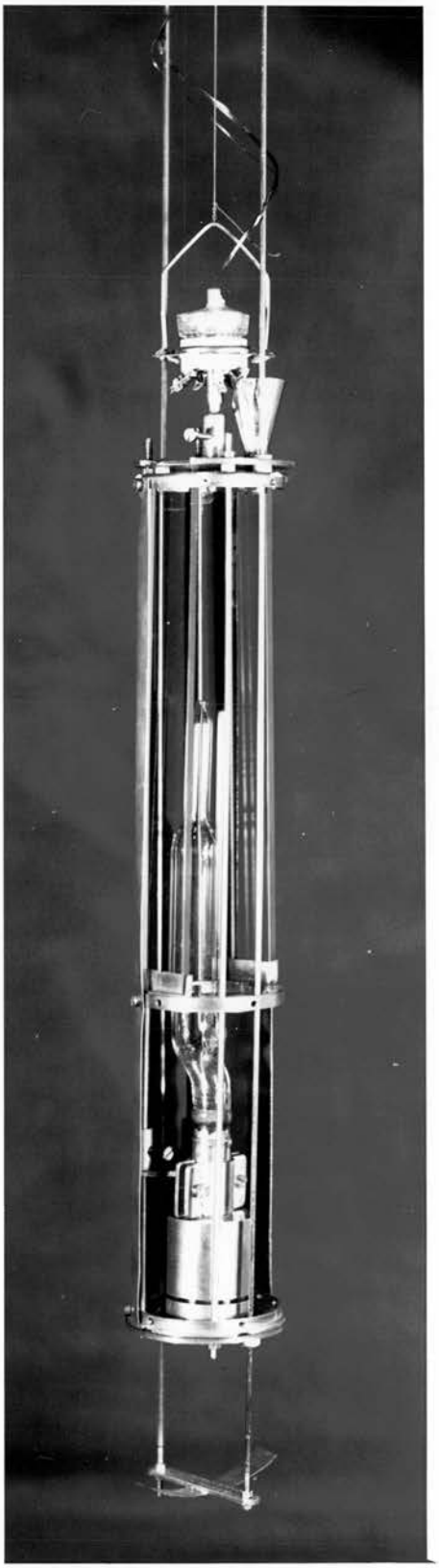

Figure 25

light intensity of the lamp had no effect on the flow rates and produced no observable fountain effect.

The main bath of the cryostat was connected to a large rotary pump used to lower the vapour pressure. The adopted procedure of filling was (1) to evaculate the helium dewar to 10^{-2} mm Hg overnight; (2) to precool the cryostat to liquid nitrogen temperature and then to let in helium gas from the return line thus allowing the dewar to cool so as to obtain an inexpensive helium transfer; (3) the cryostat was uncoupled from the pumping line and from its support, then carried to the liquefier where the transfer took place; (4) the transfer completed, the cryostat was replaced, recoupled and the pump started. The pump, working flat out, enabled temperatures as low as 1.16°K to be reached.

Steady vapour pressures and hence constant temperatures were maintained either by a manually adjusted needle valve and oil manometer or automatically by means of a device suggested to us by J. C. Fineman. This consisted of a very thin high quality rubber tube sealed into the pumping line and surrounded by a closed space which was connected through a valve to the pumping line at a point nearer the pump. Temperature control was obtained in the following way: the needle valve was set to give approximate stability but the temperature drift was arranged to be in the direction of decreasing temperature. Throughout this procedure the valve con-

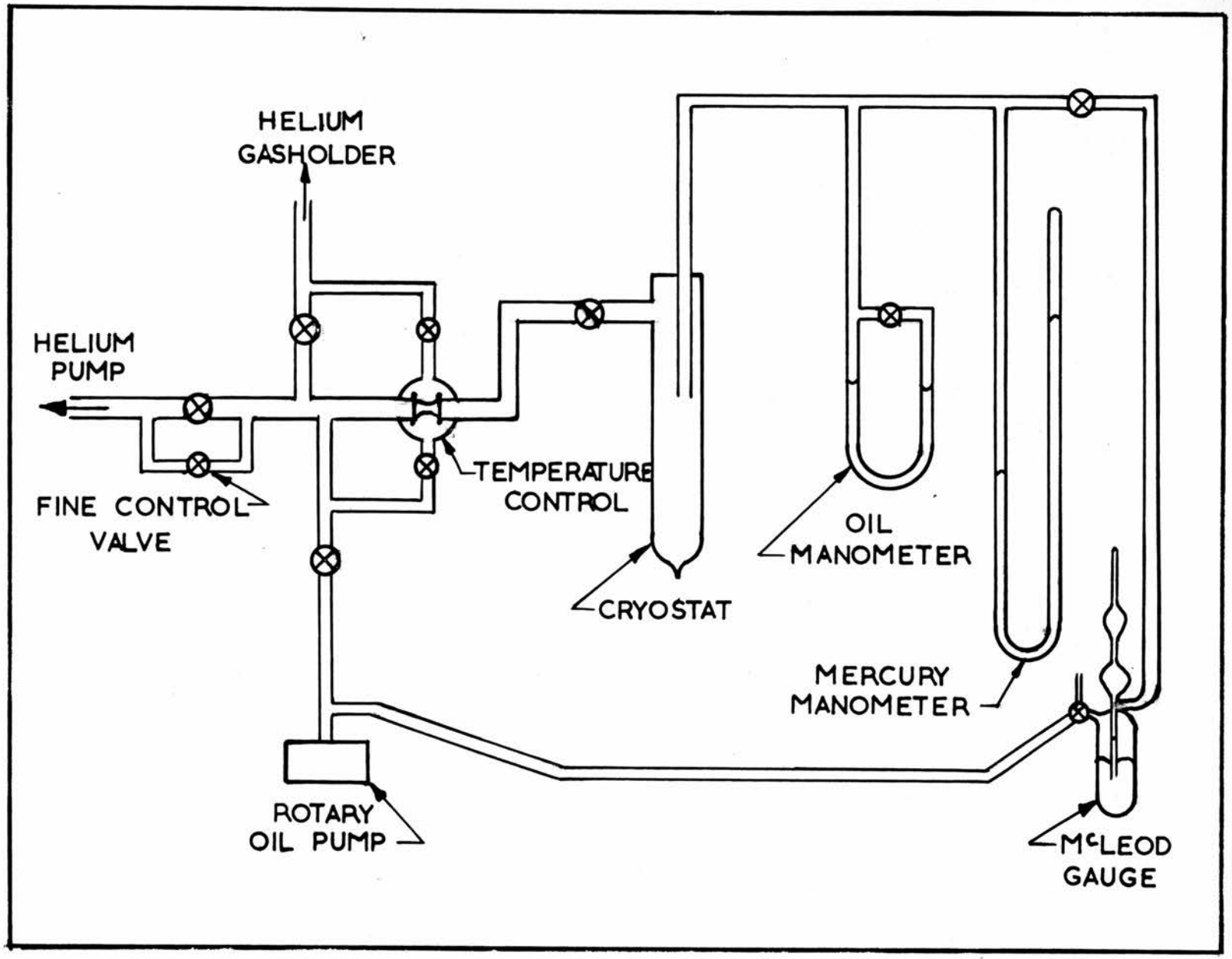
HELIUM
GASHOLDER
HELIUM
PUMP
FINE CONTROL
VALVE
TEMPERATURE
CONTROL
CRYOSTAT
OIL
MANOMETER
MERCURY
MANOMETER
ROTARY
OIL PUMP
McLEOD
GAUGE

necting the pumping line and the rubber sleeve on the external side was open. When it was closed any increase in the pumping rate lowered the pressure thus causing the rubber tube to shrink. The shrinkage reduced the volume pumping rate and any further decrease in temperature was prevented. The device, once started, operated satisfactorily for several minutes, before it lost control and drift began. The measurements of vapour pressure and hence of temperature were made using a McLeod gauge. The '1958 scale' was used for temperature conversion. Figure (26) shows schematically the gas-handling system.

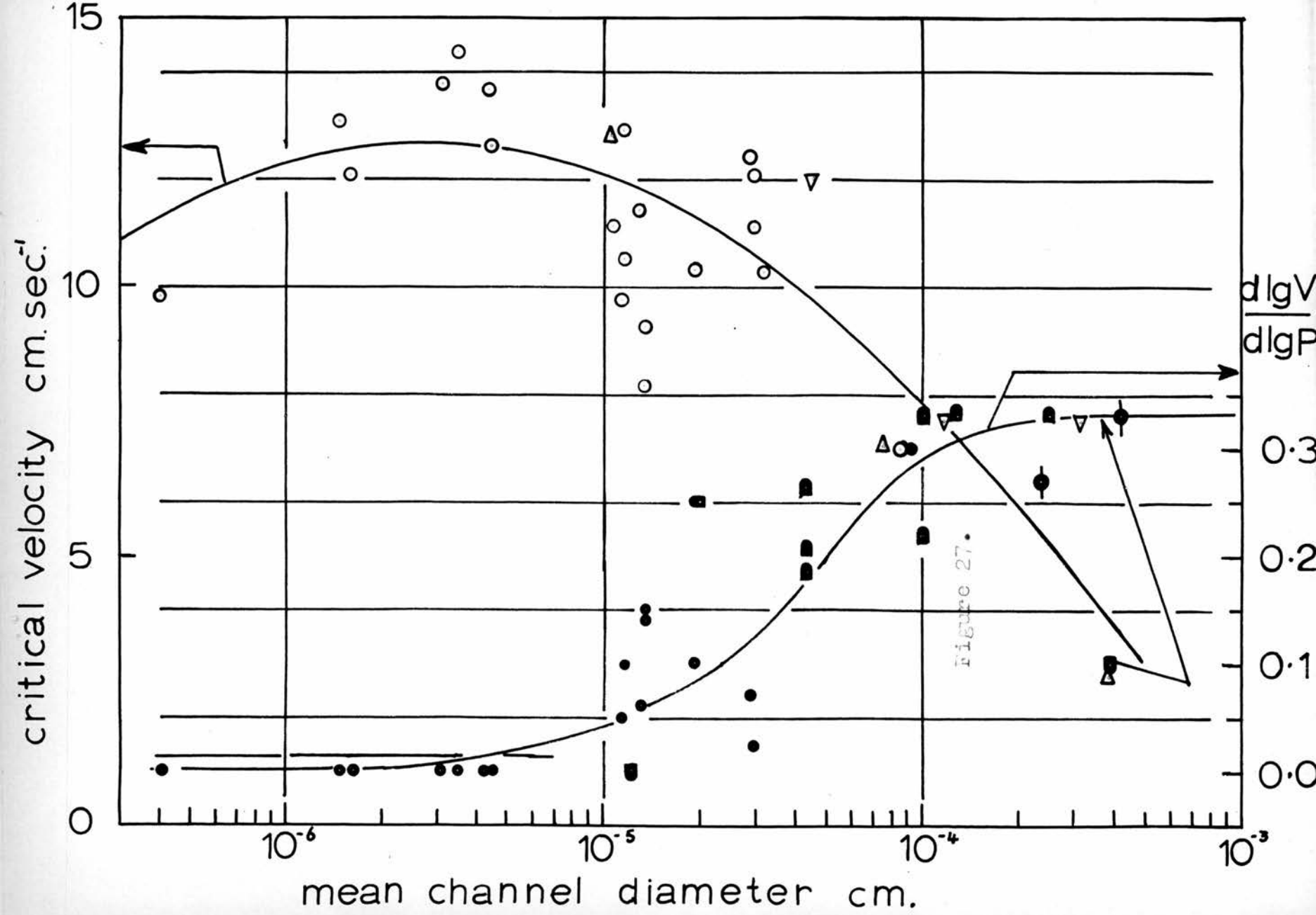
15
10
5
0
critical velocity cm. sec.⁻¹
dlgV / dlgP
0·3
0·2
0·1
0·0
10⁻⁶
10⁻⁵
10⁻⁴
10⁻³
mean channel diameter cm.

Figure 27.

Critical velocity:

△ oscillation method, Allen and Misener, (1939).

▽ Winkel, Delsing and Gorter, (1955).

○ oscillation method, present author.

Pressure dependence of flow .

Hung, Hunt and Winkel (1952) and Winkel,

Delsing and Gorter, (1955).

Wansink, Taconis, Staas and Reuss, (1955).

Allen and Misener (1939).

Swim and Rorschach (1955).

● Present author.

CHAPTER 6

EXPERIMENTAL RESULTS AND DISCUSSION

6.1 Critical velocity and pressure dependence of flow in wire-filled tubes

Using the experimental method described in Chapter 5 the mean superfluid critical velocity v_c has been measured. Values of v_c † at 1.2°K and at zero pressure head, seen in figure (29), show that v_c increases with decreasing channel width d up to a maximum value of about 14 cm sec^{-1} for $d = 3 \times 10^{-6}$ cm and then falls again for still smaller values of d. In channels of width $d < 10^{-5}$ cm, v_c is not only fairly insensitive to d but also over the whole range of d its magnitude is smaller than predicted by the simple Feynman theory. According to Feynman's equation, $v_c = \frac{\hbar}{md} \ln \frac{d}{a}$, the critical velocity when $d = 3 \times 10^{-6}$ cm should be about 250 cm sec^{-1} if the vortex core size a is taken to be 3 Å, and the maximum in the v_c - d curve should occur when d 10^{-7} cm. Atkins theory of critical velocity also predicts values of v_c about two orders of magnitude larger than those observed in very narrow channels.

Figure (29) shows values of v_c obtained by Allen and Misener (1939) who used a similar form of superleak. Winkel, Delsing and

---

†Details of tube length, reservoir area, channel perimeter and period of oscillation are given in table 1 of the appendix.

Poll (1955) studied thermally induced flow with slit type superleaks obtaining values of v_c † which are in good agreement with the present measurements. Hammel and Schuch (1957) investigated flow through a channel of width $d = 10^{-4}$ cm and found v_c to be about 4 cm sec^{-1}. Thus for $d > 10^{-5}$ cm there is generally good agreement between the present measurements and those previously reported. The value of v_c when $d = 3 \times 10^{-6}$ cm is about a factor three lower than values inferred from film transfer rates; the significance of this observation is not understood but may be connected with the fact that the film has one free surface.

It is relevant to enquire how the spread of sizes in each wire-filled tube will affect the value of v_c. The oscillation method will give some averaged value v_{md} which will depend on the distribution function f(d). To examine this question we begin by considering equation (63) of 4.1(b) which gives,

$$S_o = \frac{1}{2} \frac{\left(\int_o^\infty df(d)\, v(d)\, dd\right)^2}{\int_o^\infty df(d)\, v^2(d)\, dd}$$

The volume of liquid flowing via the channels is

$$Q = \frac{1}{2} \int_\varepsilon^{d_o} v(d)\, f(d)\, d\, dd$$

It follows that v_{md} is given by

---

†The values shown in figure 29 are taken from figure 9, p.34; Winkel, Delsing and Poll (1955).

$$v_{md} = \frac{(\int_{\varepsilon}^{d_1} d\, v(d)\, f(d)\, dd)(\int_{o}^{\infty} df(d)\, v^2(d)\, dd)}{(\int_{o}^{\infty} df(d)\, v(d)\, dd)^2} \tag{83}$$

Now let us suppose that in an ideal channel v_c varies as k/d i.e.

$$v_c(d) = \frac{k}{d} \text{ where } k = \hbar/m \tag{84}$$

We can put $v_c(d)$ into (83) and evaluate the integral to find the effect of a spread of channel sizes on the measured velocity v_{md}. Suppose the distribution function of sizes has the simple form

$$f(d) = 1/(d_1 - \varepsilon) \qquad \varepsilon < d < d_1$$

$$= 0 \qquad d > d_1$$

Equation (83) becomes

$$v_{md} = \frac{\int df(d)\, v^2(d)\, dd}{\int df(d)\, v(d)\, dd}$$

$$= \frac{\frac{k^2}{d_1 - \varepsilon} \int_{\varepsilon}^{d_1} \frac{1}{d} \cdot dd}{\frac{k}{d_1 - \varepsilon} \int_{\varepsilon}^{d_1} dd} \tag{85}$$

$$= \frac{k}{d_1} \cdot \frac{\ln d_1/\varepsilon}{(1 - \varepsilon/d_1)} = \frac{k}{d_1} \cdot f \tag{86}$$

Numerical evaluation of (86) shows that the measured critical velocity is always higher than v_c, except when $r_o = \varepsilon$ when they are the same. Since the form $v_c = \frac{k}{d}$ is a special case it is necessary to see what happens when v_c varies as in Feynman's equation,

$$v_c = \frac{k}{d} \ln \frac{d}{a} \quad \text{where } k = \frac{\hbar}{m} . \tag{87}$$

We now put this function into equation (85). The critical velocity will be zero when r = a so the limits of integration are taken as a and d_1.

For v_{md} we find

$$v_{md} = \alpha/\beta$$

where

$$\alpha = \frac{\hbar^2}{m^2(d_1 - a)} \int_a^{d_1} \frac{1}{d} (\ln \frac{d}{a})^2 \, dd$$

and

$$\beta = \frac{h}{m(d_1 - a)} \int_a^{d_1} (\ln d/a) \, dd .$$

After some reduction we finally obtain

$$v_{md} = [\frac{h}{md_1} \ln \frac{d_1}{a}] . \frac{\frac{1}{3}(\ln d_1/a)^2}{\ln(d_1/a - 1) + a/d_1}$$

$$= \frac{hf'}{md_1} \ln \frac{d_1}{a} , \text{ say.} \tag{88}$$

Evaluation of f' shows that a spread of sizes does not lead to values of $v_{md} < v_c$ except when $d < ea$ and in this case d is comparable with the vortex core size and Feynman's theory is inapplicable. It therefore seems that a mechanism other than the creation of

vortex lines at the channel exit is required to explain the magnitude of observed critical velocities.

The pressure dependence of flow, $n = \frac{d \log v}{d \log p}$, where v is the mean velocity and p the pressure, was also measured. Values of n were found by differentiating graphically curves of level difference versus time. It was found that n depended on channel size and as previously reported by Swim and Rorschach, n did not vary significantly with temperature. The index of pressure dependence shown in figure (27) is related to the right hand ordinate scale. In channels where $d > 10^{-5}$ cm the pressure dependence did not maintain its value much below a level difference of 1 mm of liquid helium. In these channels the flow velocity at zero level difference was plotted as critical velocity.

Values of n seen in figure (27) suggest that there are two regimes of critical flow. In order to test this hypothesis an experiment already described in Chapter 5 was devised. The essence of the method was to attach a glass manometer pipe at a point part way along a wire-filled tube where a v-shaped slit allowed liquid access. The height of the liquid level in this tube was observed during the flow process together with the levels of reservoir and bath and thus it was possible to measure the pressure gradient within the superleak itself.

The experiments showed that in a channel where $d = 8 \times 10^{-5}$ cm

there was an almost uniform pressure gradient along the tube, but when $d = 4 \times 10^{-6}$ cm the manometer indicated that the liquid was flowing under zero pressure gradient*. It was inferred that the pressure drop occurred in this case in the narrowest section of the channels. Such subcritical frictionless transfer is similar to that observed by Daunt and Mendelssohn (1946) in the case of film flow from a double beaker. This behaviour, taken together with the insensitivity of v_c to d when $d < 10^{-5}$ cm and the decrease of n to zero, strongly support the hypothesis that there are two flow regimes.

Although the pressure index n shows considerable scatter in going from $n = 0.3$ when $d = 8.5 \times 10^{-5}$ cm to a value $n = 0$ when $d < 10^{-5}$ cm these measurements compare favourably with comparable data from previous investigations. Exceptions are the values $n = 0.3$ and $n = 0.5$ found by Seki (1962). The value $n = 0.3$ has been examined by Allen and Watmough (1965) and is discussed in section 6.2. Recently, van Alphen et al (1965) have found that when thermal effects are minimised values of $n = 0$ are also found for flow through Vycor glass $d = 60$ Å and jewellers rouge $d \sim 10^{-5}$ cm. These authors reduced thermal effects by attaching a copper bellows to their reservoir system. It would thus appear that thermal effects can be very important. The analysis given in

---

*Typical results are shown in figure (37) to (41).

Chapter 5 shows that in the limiting case when thermal contact is extremely poor, values of n = 1 are to be expected. Only with large reservoirs and low flow rates is it possible to achieve sufficiently good thermal contact to completely avoid thermal effects. Measurements of level difference plotted against time for a number of different superleaks are shown in figures (28) to (36). The fact that pressure independent flow is observed over a wide range of d suggests that the spread of channel sizes in a given tube is unlikely to be greater than a factor ten.

The hydrodynamic equation (23) which describes isothermal gravitational superflow reduces to

$$\frac{\rho_s}{\rho} \text{ grad } p = A \rho_s \rho_n |v_s - v_n|^2 . (v_s - v_n)$$

In a channel of width $d = 8 \times 10^{-5}$ cm it was found that the flow could be described by this equation but that the constant A was less than unity. When the quantity $|v_s - v_n|^2$ was replaced by $|(v_s - v_n) - v_c|^2$ then A was found to have a value of 21 at 1.2°K. This value compared favourably with the value of 25 at 1.3°K found by Vinen (1957). With this tube, values of v_c at temperatures above 1.2°K could not be measured because the oscillatory motion was too heavily damped. For this reason the temperature dependence of A was not determined.

The transition from the regime governed by the mutual friction

force to one where v does not depend on p is fairly rapid. The transition suggests that when $d < 10^{-5}$ cm the flow is no longer turbulent. It is therefore relevant to enquire how turbulence can be suppressed and hence how values of $n < 0.3$ might arise. First we recall the evidence obtained by Critchlow (1960) which showed that turbulence propagates from the ends of a channel but not from the walls. If vortex lines are unable to enter the channels it is not unreasonable to assume that the turbulent regime will be unable to develop.

According to Vinen (1957) the image force on a vortex line causes it to move downstream parallel to the wall. The Magnus force on this line then causes it to move towards the wall with velocity v_c given by,

$$v_c = \frac{B}{2} \frac{\rho_n}{\rho} \frac{\hbar}{2mx} \tag{89}$$

It is suggested that at the wall vortex lines are annihilated in a single quantum process. The time $\tau(d)$ taken by a line to reach the wall when initially at distance d/2 from it is found by integrating equation (89) and is

$$\tau(d) = \rho m d^2/2 B \rho_n \hbar \tag{90}$$

With the following values $\rho_n/\rho \sim 10^{-2}$, B = 1 and $m/\hbar = 6 \times 10^3$ this decay time is 0.3 sec when d = 10μ but decreases to 30 microseconds when d = 0.1μ. We therefore see that in 10^{-5} cm channels

the decay rate for vortex lines is 10^4 times faster than for $d = 10^{-3}$ cm. If the build up of turbulence requires a length of line to enter the channels from the reservoir, then the above argument suggests that in sufficiently small channels this mechanism will be suppressed by the rapid decay of incoming lines.

It has been pointed out by Feynman (1955) and Vinen (1961) that the mechanism of critical velocity can be associated with the build up of turbulence. The experiments of Vinen (1957) and Critchlow (1960) are consistent with this hypothesis. In those small channels where turbulent flow is not observed then some other mechanism of critical velocity must operate. Kuper (1958) proposed the existence of low energy rotons. When created sufficiently close to a wall these might have the required low ratio of ε/p to explain the values of v_c which have been observed.

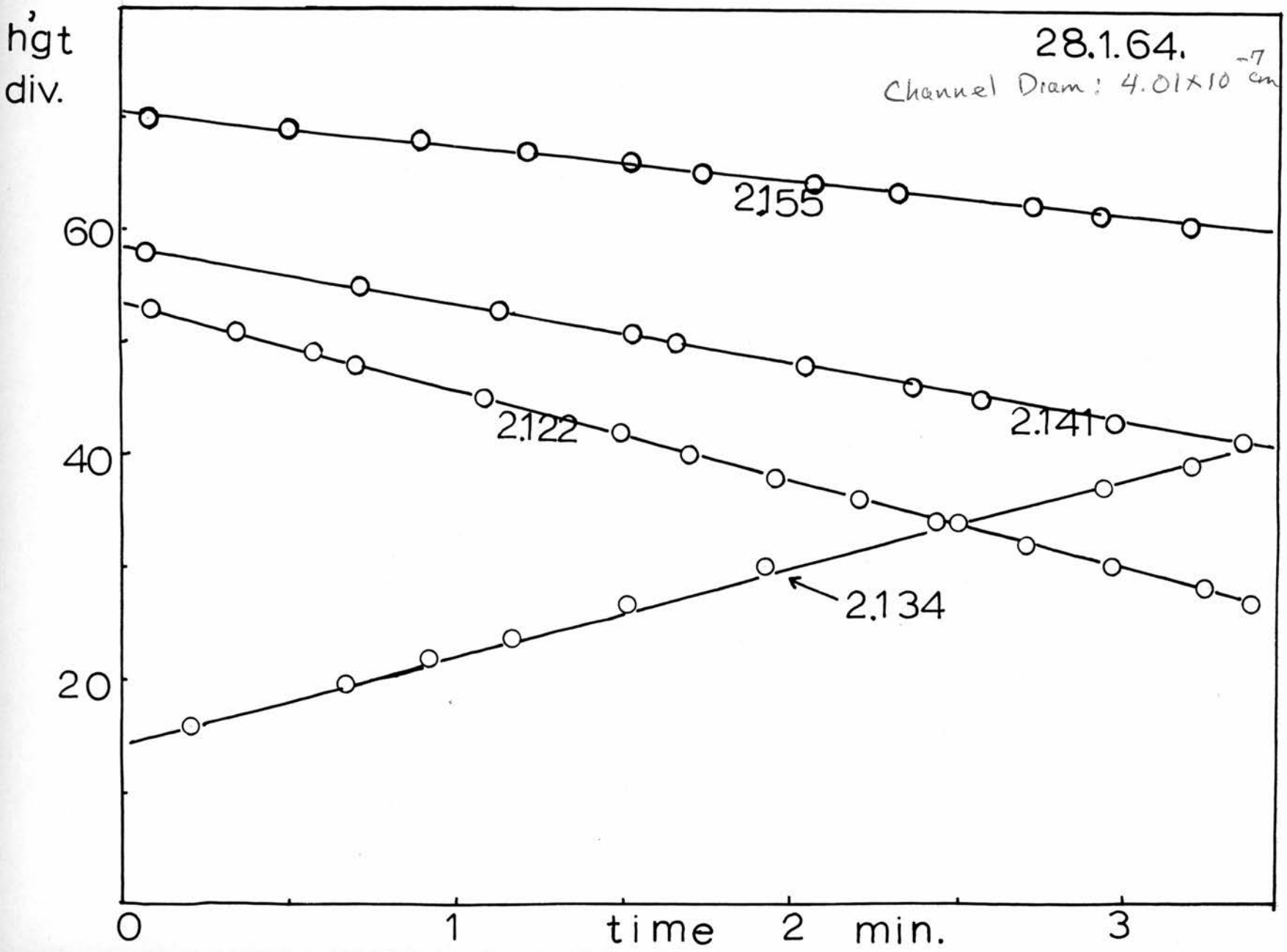
h'gt
div.
28.1.64.
Channel Diam: 4.01×10⁻⁷ cm
2.155
2.141
2.122
2.134
60
40
20
0
1
time
2
min.
3

Figure 28.

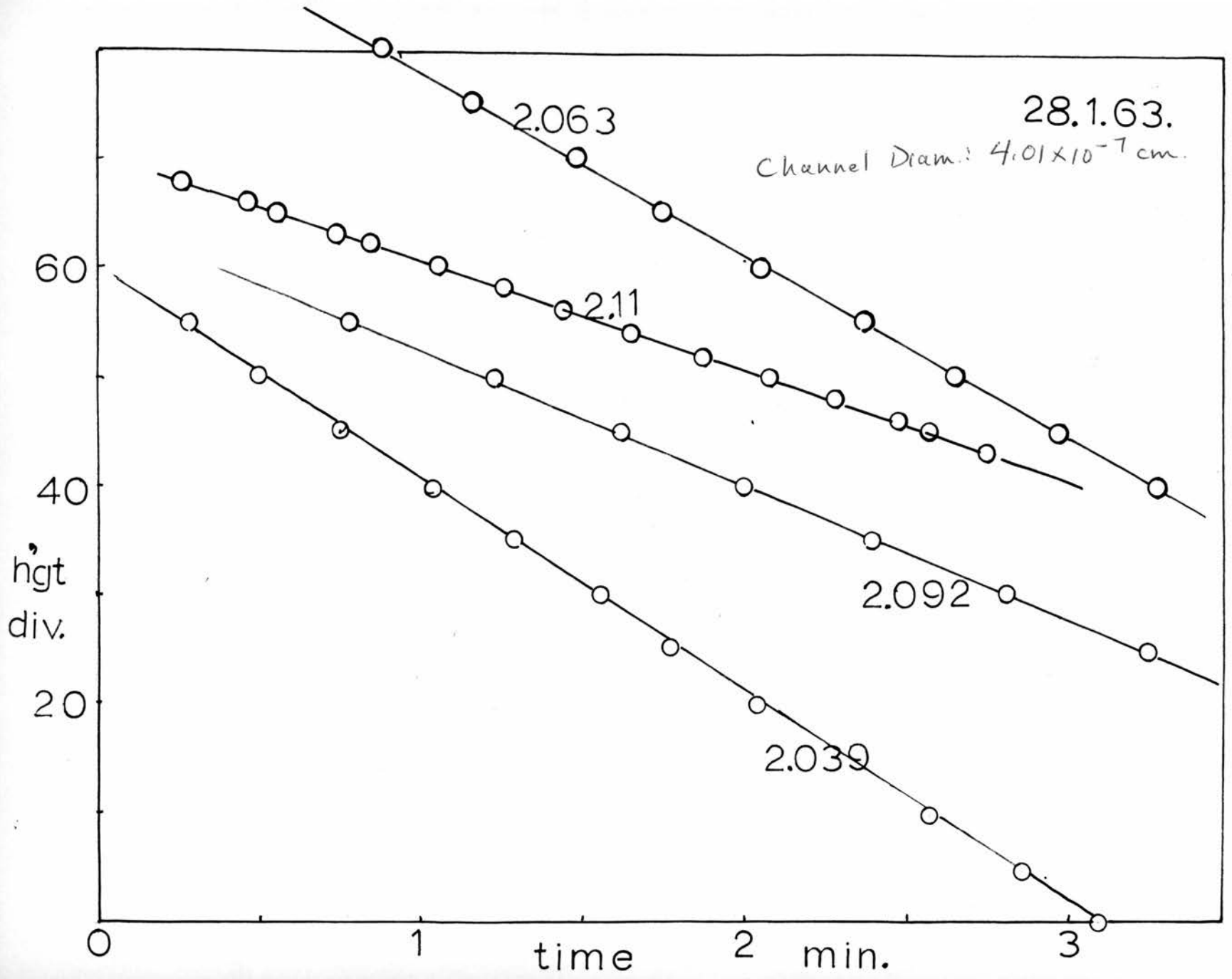
28.1.63.
Channel Diam.: 4.01×10⁻⁷ cm.
2.063
2.11
2.092
2.039
60
40
20
hgt
div.
0
1
2
3
time
min.

Figure 29.

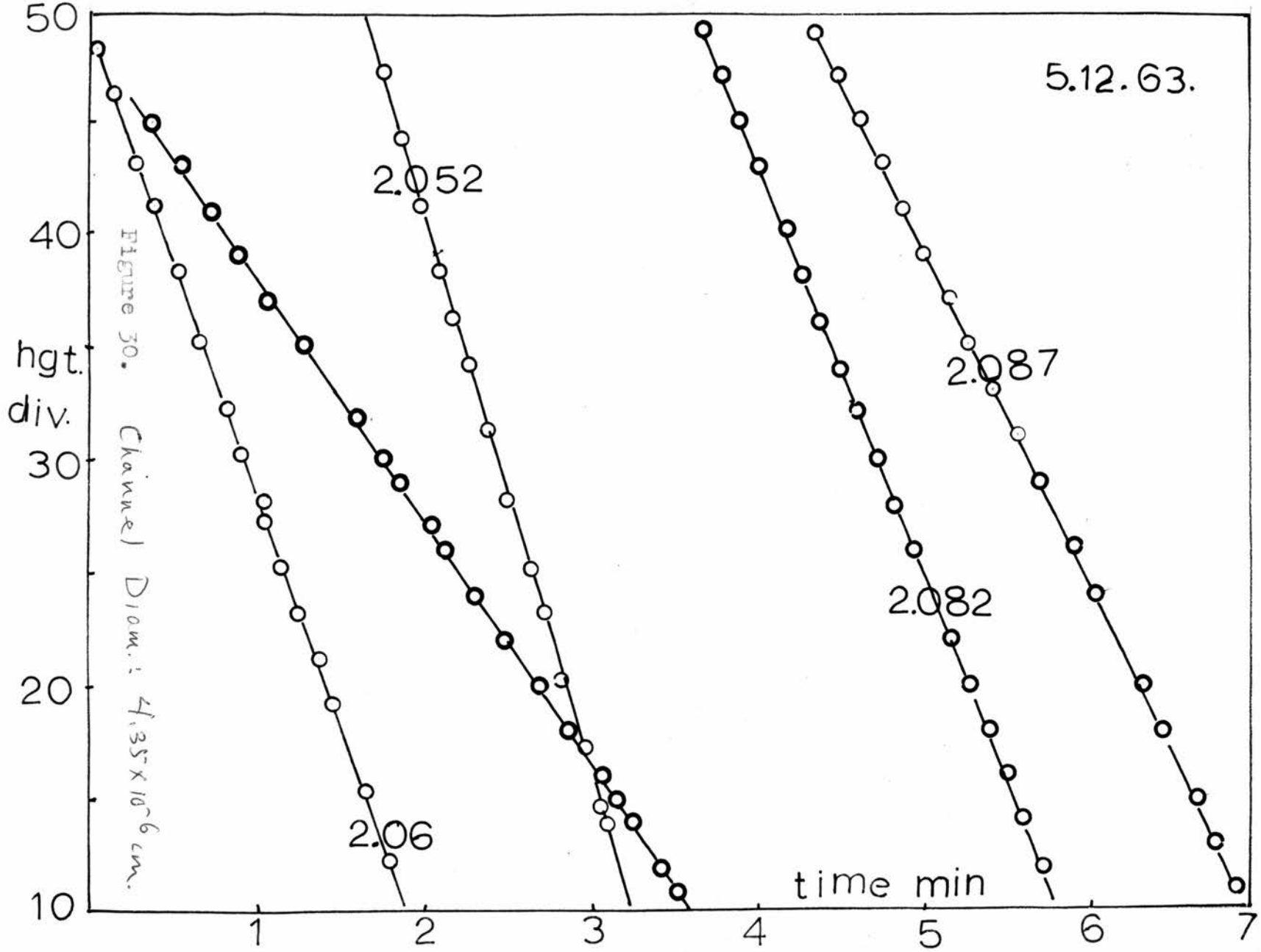
50
40
hgt.
div.
30
20
10
1
2
3
4
5
6
7
time min
5.12.63.
2.052
2.087
2.082
2.06
Figure 30. Channel Diam.: 4,35 x 10^6 cm.

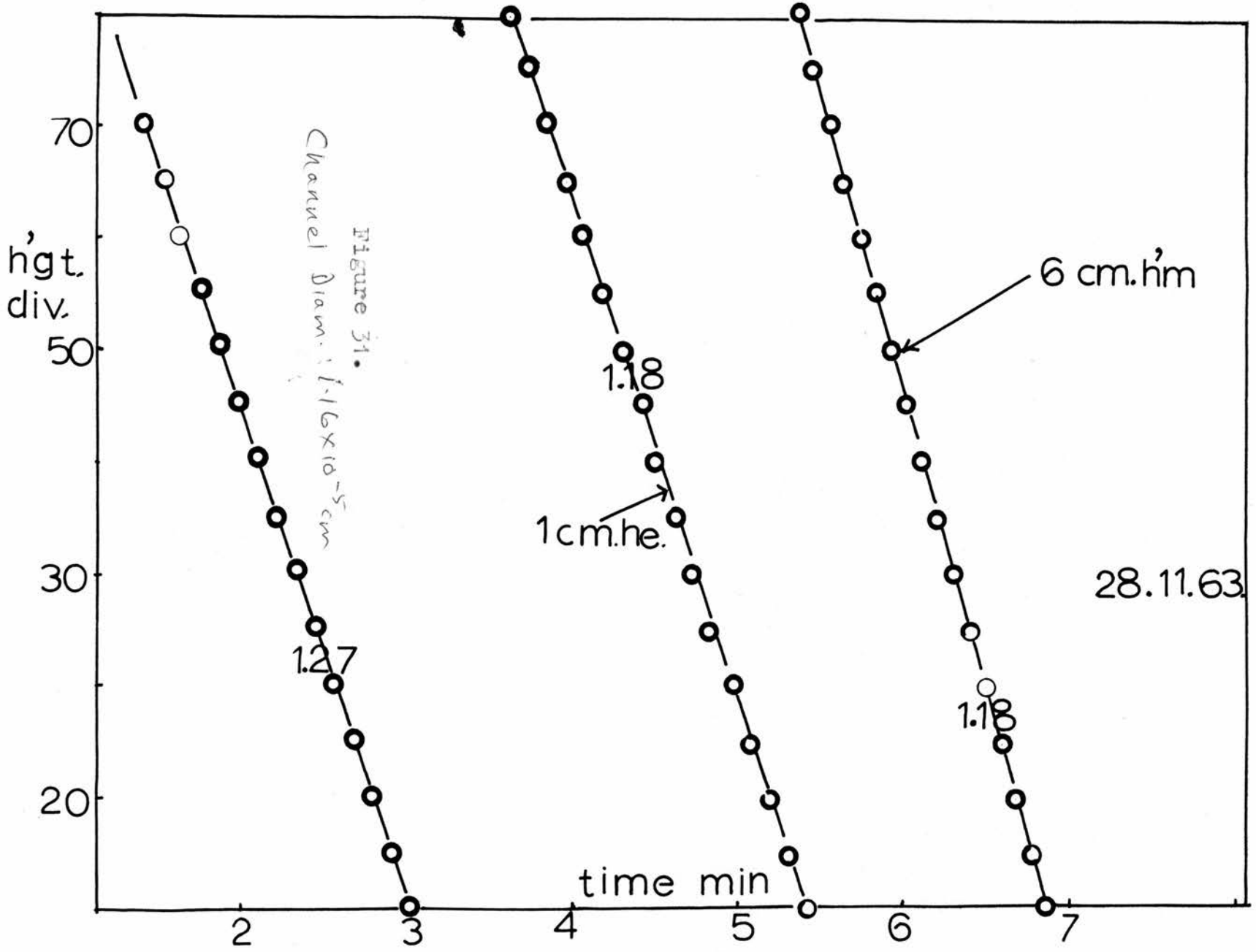

Figure 31.
Channel Diam. 1.16 x 10⁻⁵ cm

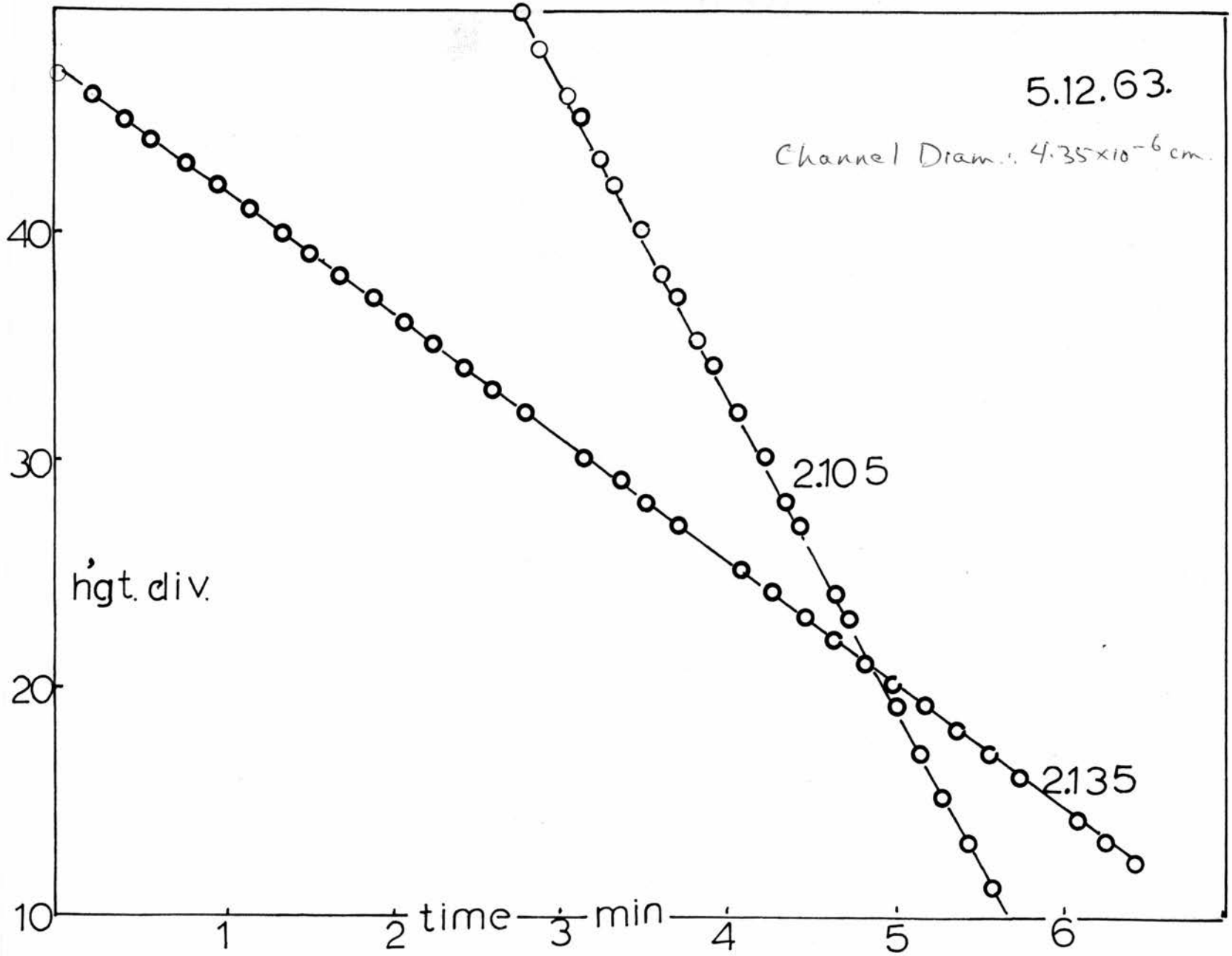
5.12.63.
Channel Diam.: 4.35×10⁻⁶ cm.
40
30
20
10
hgt. div.
2.105
2.135
1
2
time — min
3
4
5
6

Figure 32.

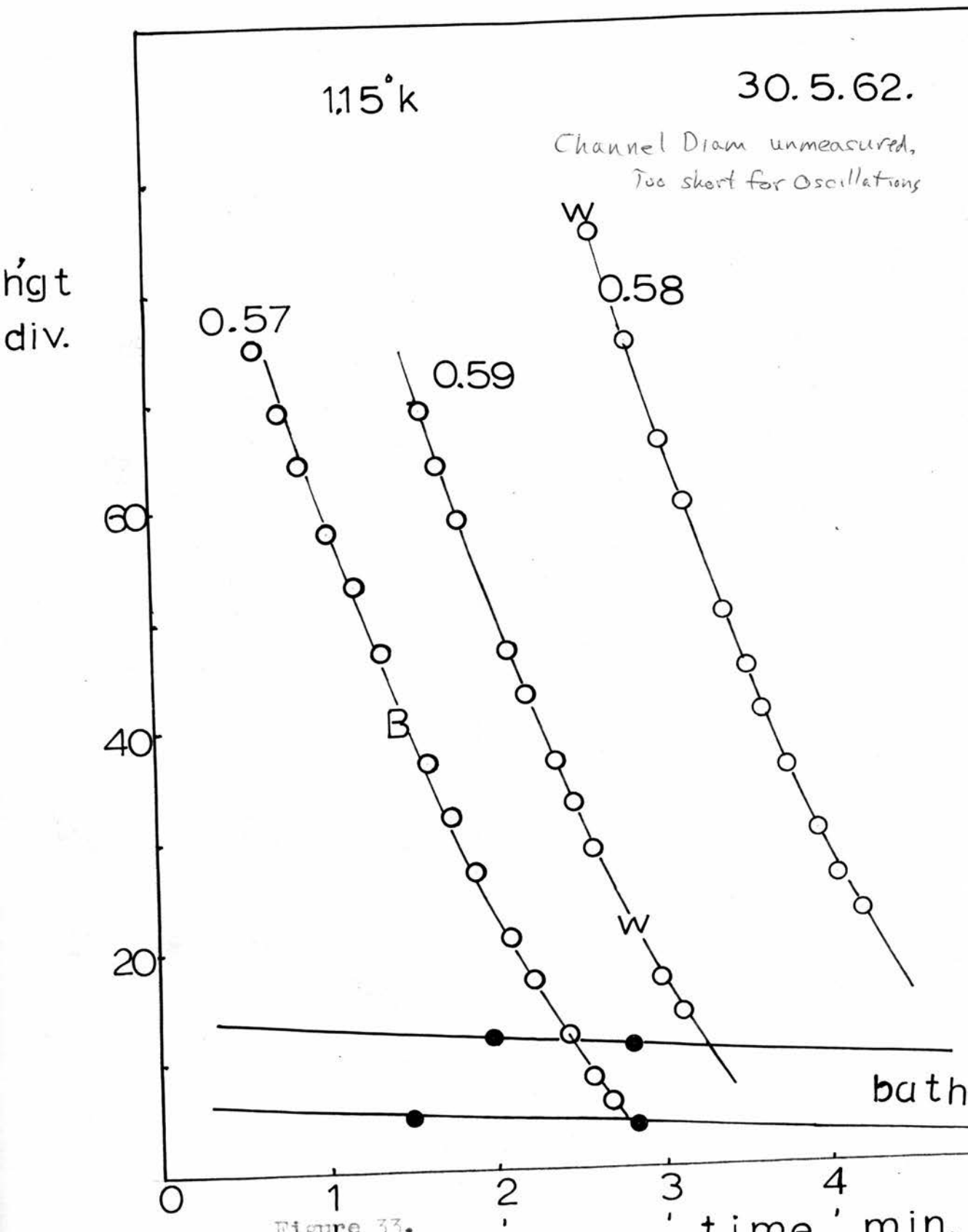
1.15°k
30.5.62.
Channel Diam unmeasured,
Too short for Oscillations
W
0.58
0.57
0.59
B
W
bath
60
40
20
0
1
2
3
4
' time ' min.

Figure 33.

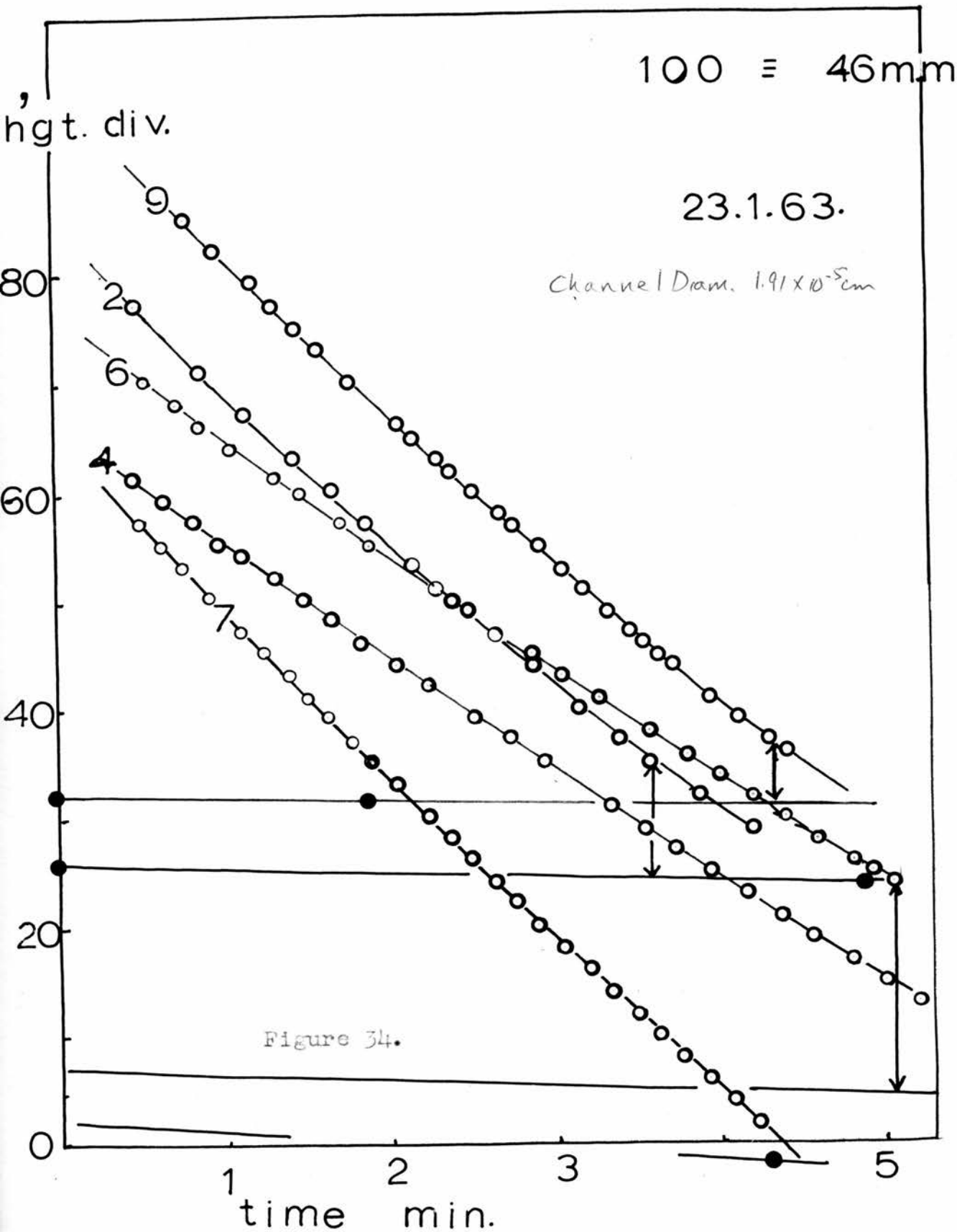
100 ≡ 46m.m.
hgt. div.
23.1.63.
Channel Diam. 1.91 x 10⁻⁵cm
9
2
6
4
7
80
60
40
20
0
1
2
3
5
time min.

Figure 34.

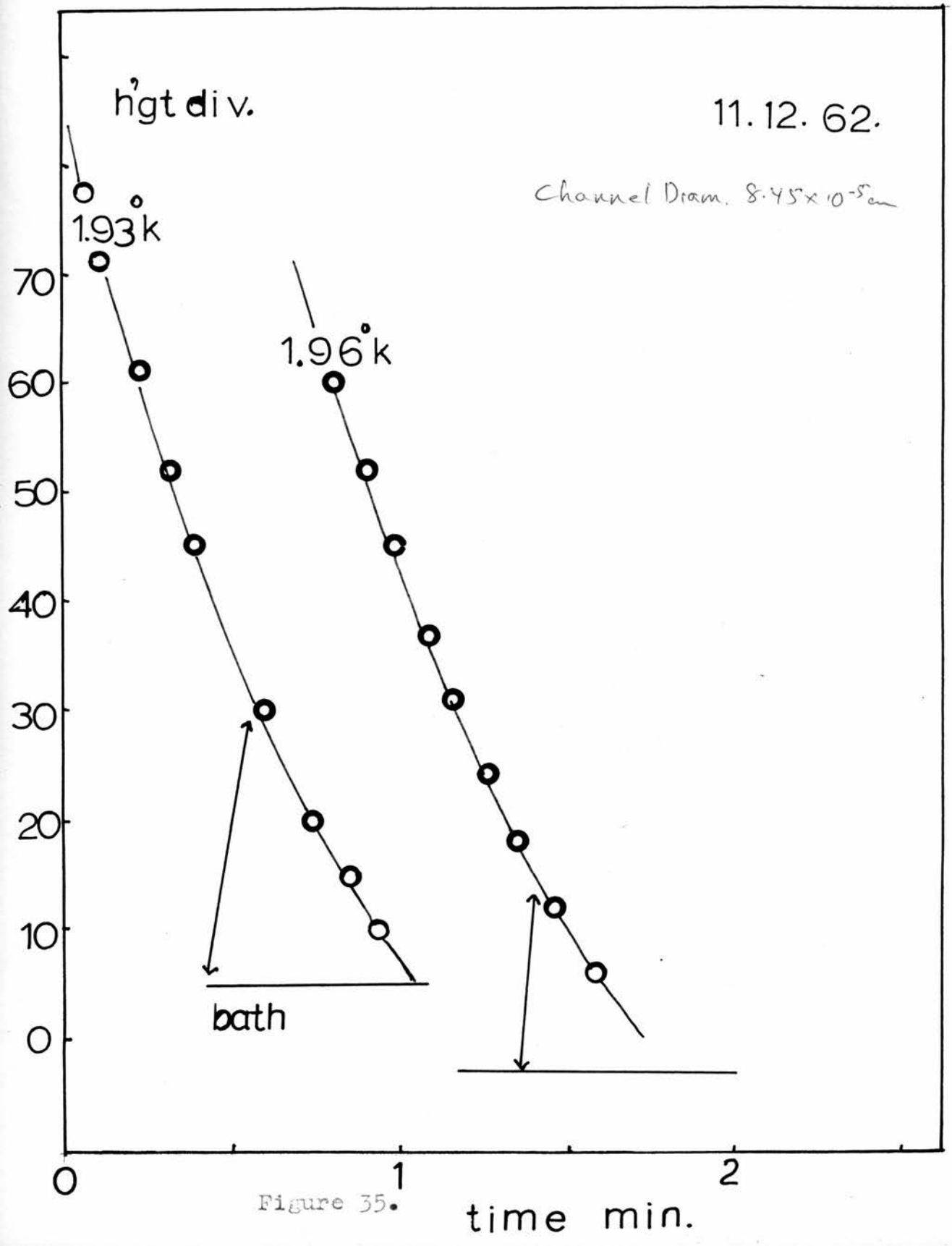
h'gt div.
11.12.62.
Channel Diam. 8.45 x 10⁻⁵ cm
1.93°k
1.96°k
70
60
50
40
30
20
10
0
bath
0
1
2
time min.

Figure 35.

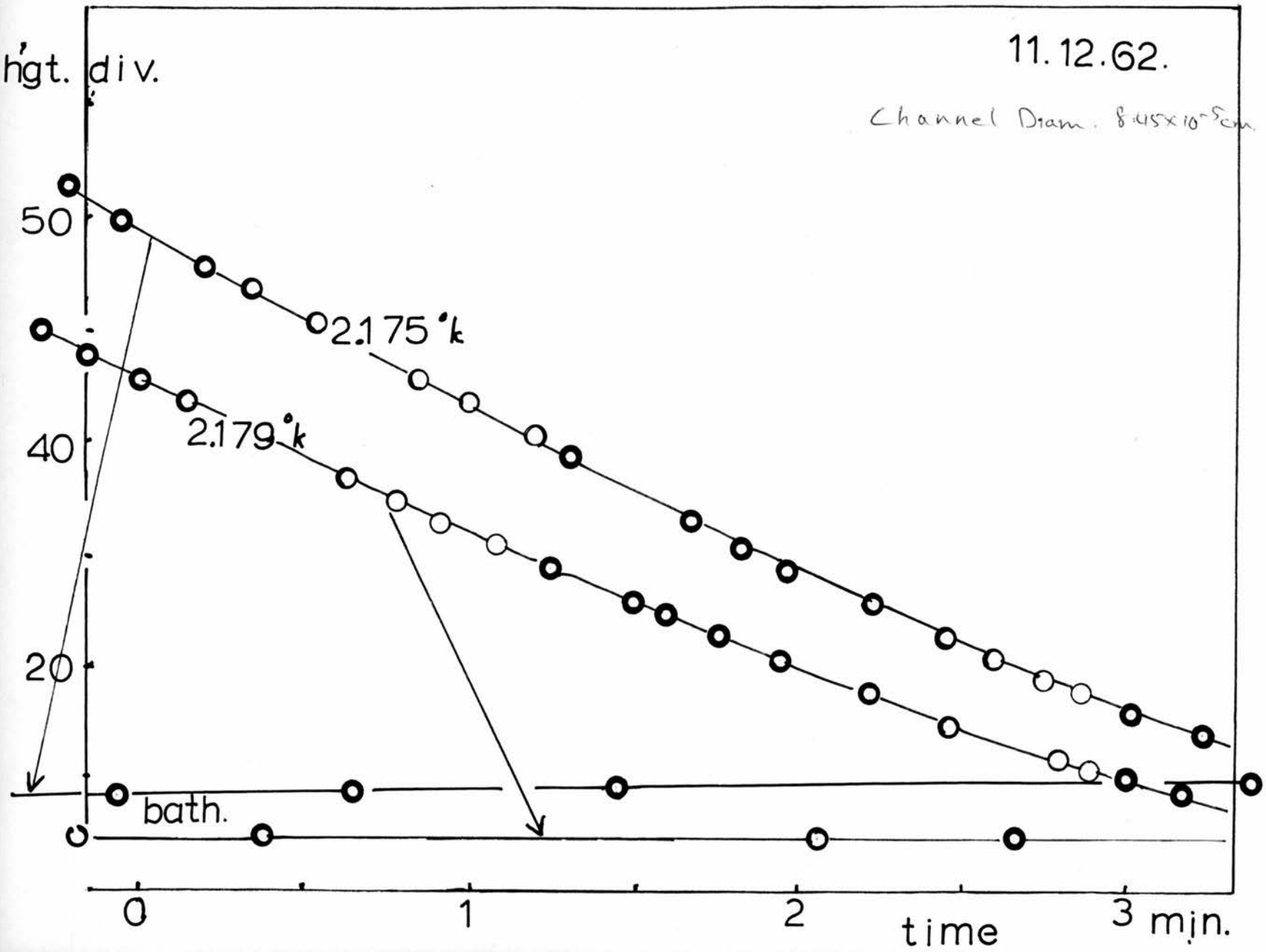
hgt. div.
11.12.62.
Channel Diam. 8.45x10⁻⁵cm.
50
40
20
2.175°k
2.179°k
bath.
0
1
2
3 min.
time

Figure 36.

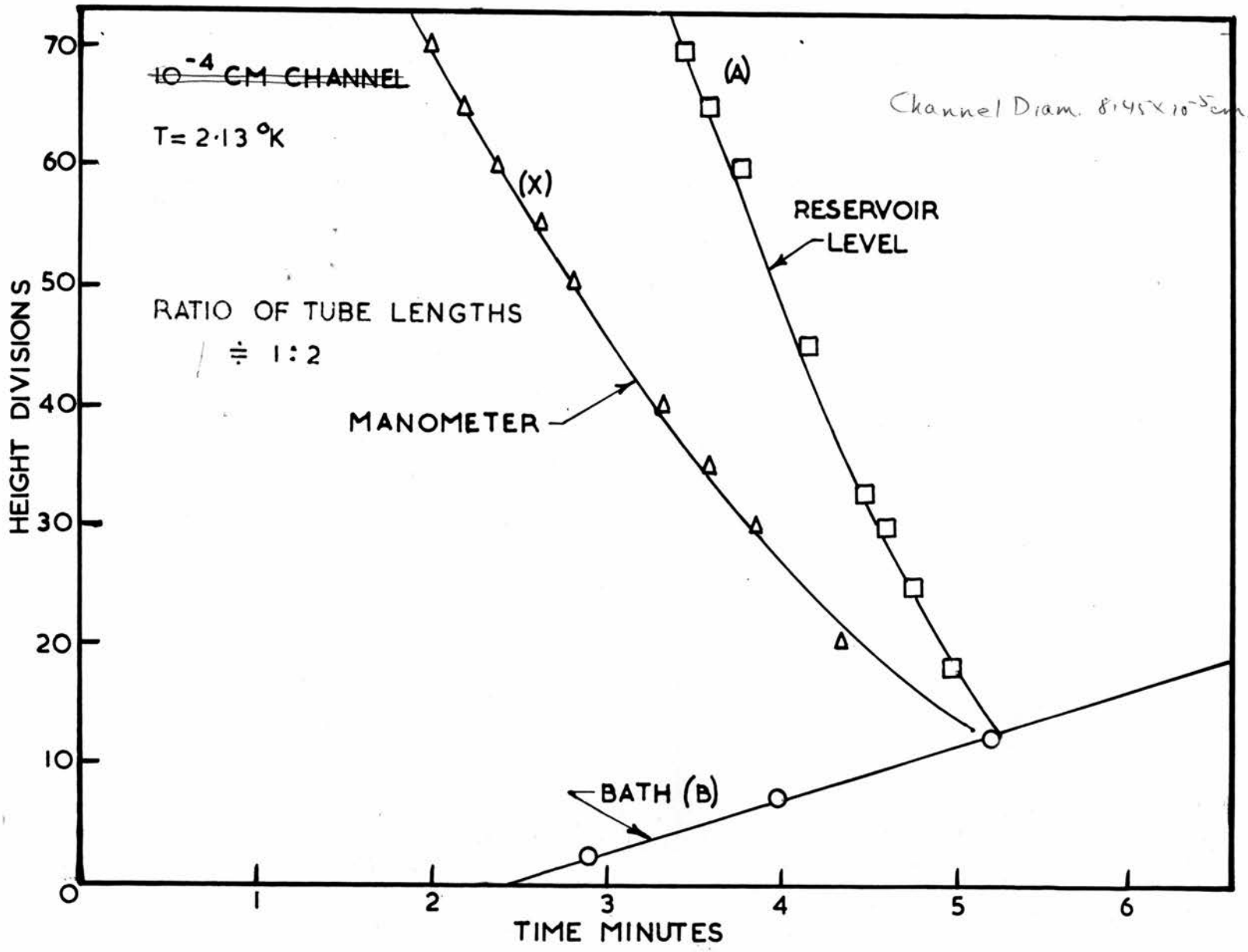
~~10^{-4} CM CHANNEL~~
T= 2·13 °K
Channel Diam. 8.45×10^{-5} cm.
(A)
(X)
RESERVOIR LEVEL
RATIO OF TUBE LENGTHS
≒ 1:2
MANOMETER
BATH (B)
HEIGHT DIVISIONS
TIME MINUTES
0
10
20
30
40
50
60
70
1
2
3
4
5
6

Figure 37.

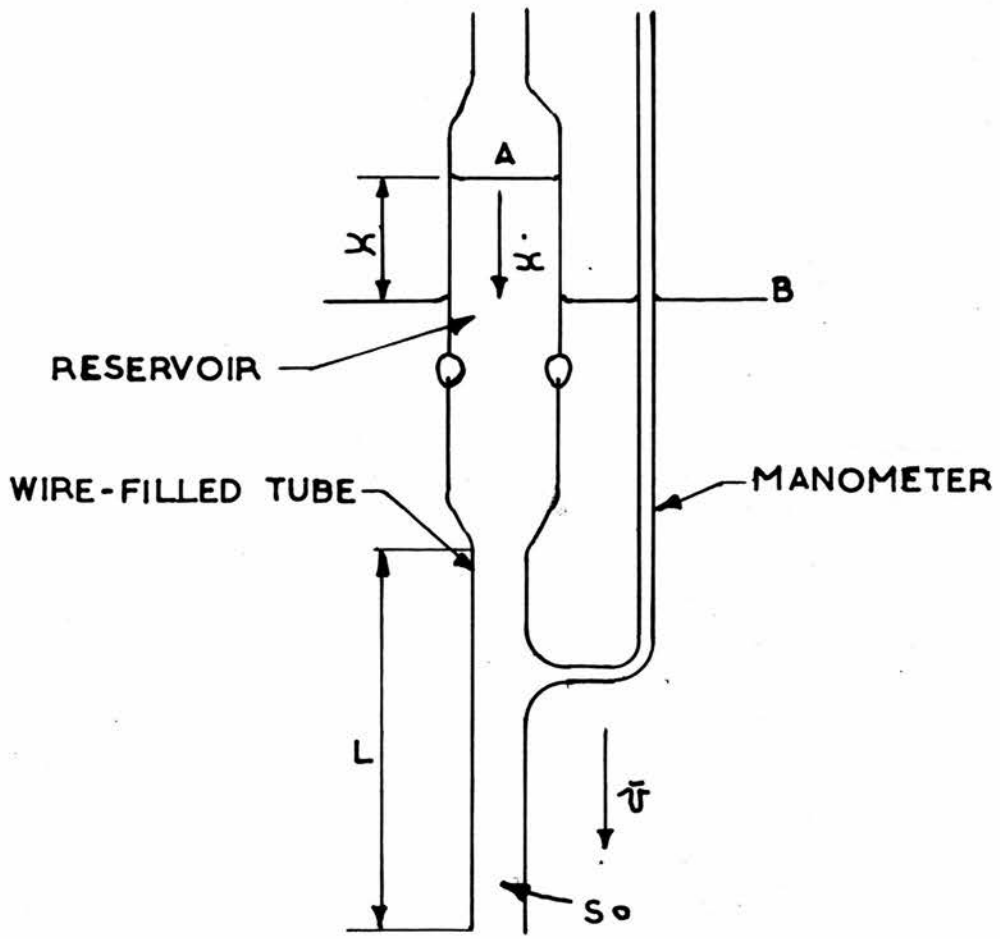

APPARATUS FOR INVESTIGATION
OF PRESSURE GRADIENT
WITHIN A SUPERLEAK

Figure 38.

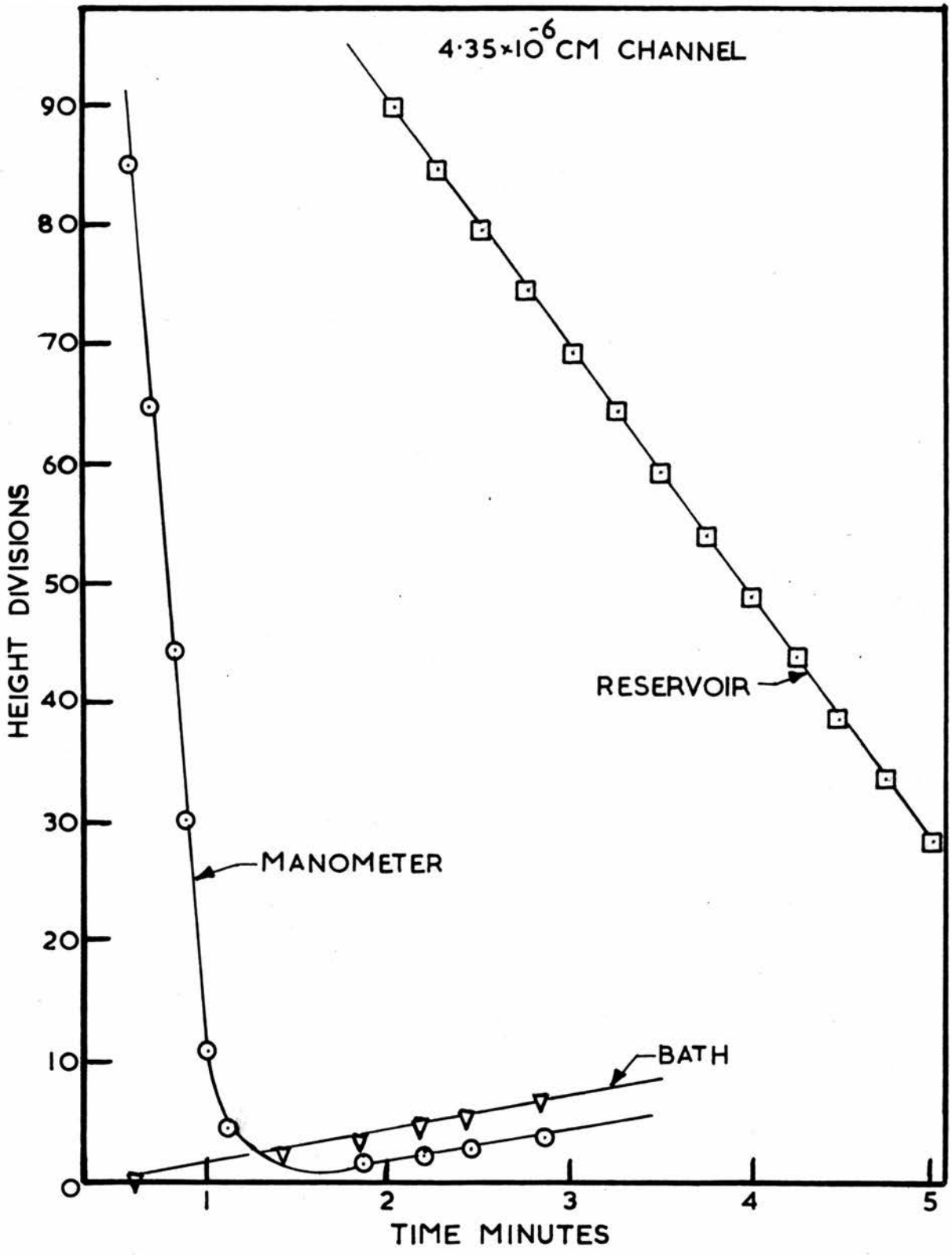
4·35×10⁻⁶ CM CHANNEL
RESERVOIR
MANOMETER
BATH
HEIGHT DIVISIONS
TIME MINUTES
0
10
20
30
40
50
60
70
80
90
1
2
3
4
5

Figure 39.

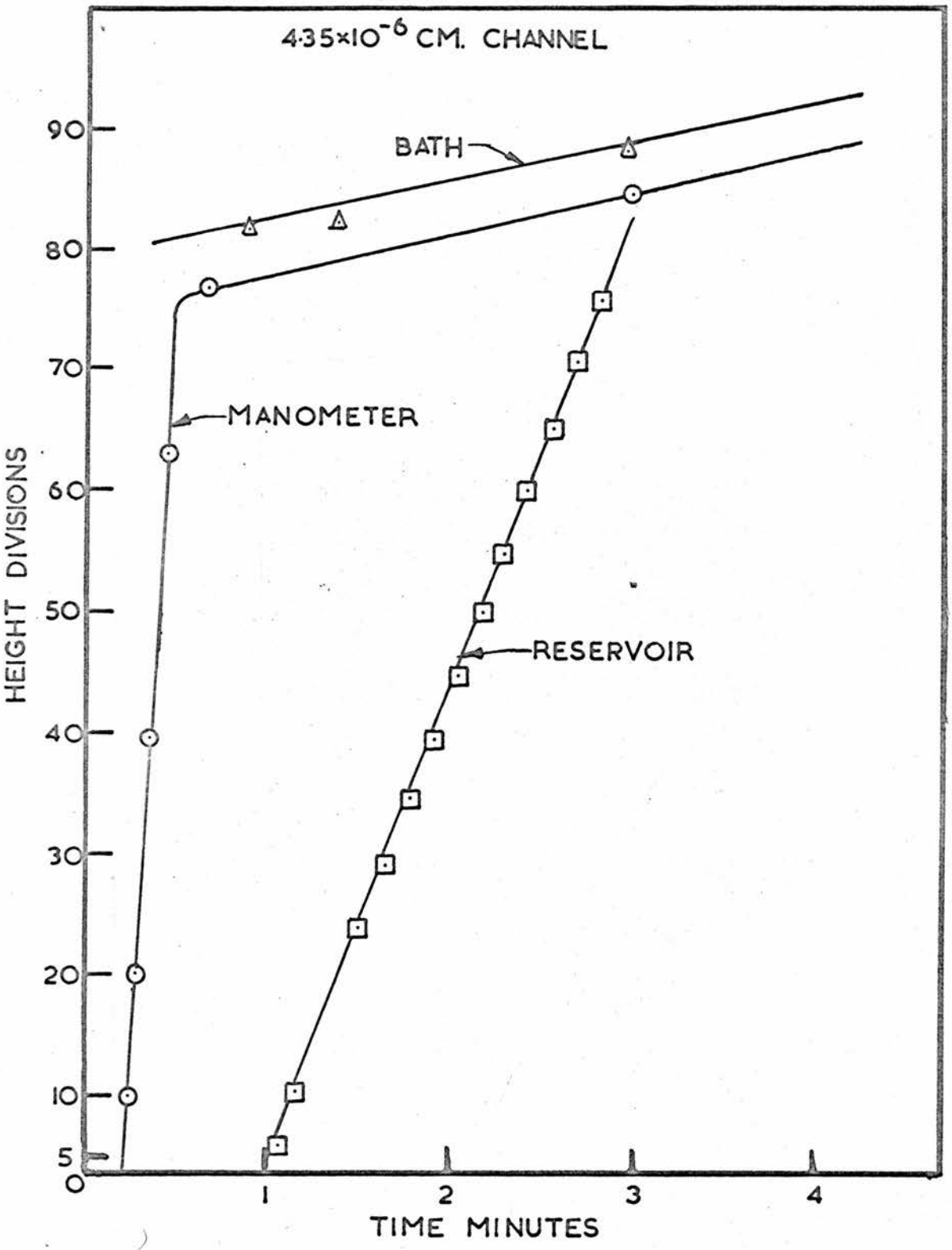
4·35×10⁻⁶ CM. CHANNEL
BATH
MANOMETER
RESERVOIR
HEIGHT DIVISIONS
TIME MINUTES
0
5
10
20
30
40
50
60
70
80
90
1
2
3
4

Figure 40.

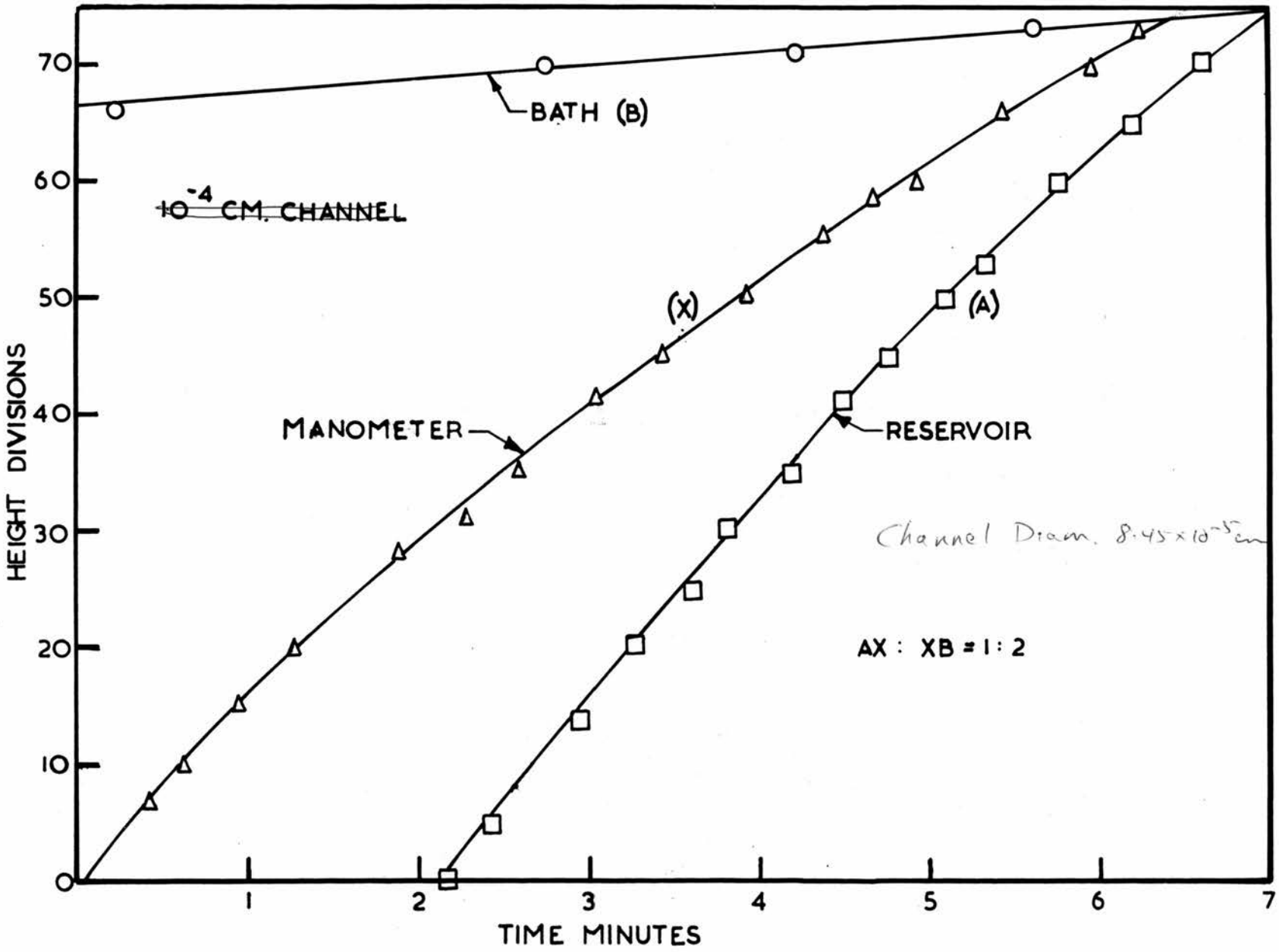
BATH (B)
10⁻⁴ CM. CHANNEL
(X)
(A)
MANOMETER
RESERVOIR
Channel Diam. 8.45×10⁻⁵cm
AX : XB = 1 : 2
HEIGHT DIVISIONS
TIME MINUTES
0
10
20
30
40
50
60
70
1
2
3
4
5
6
7

Figure 11.

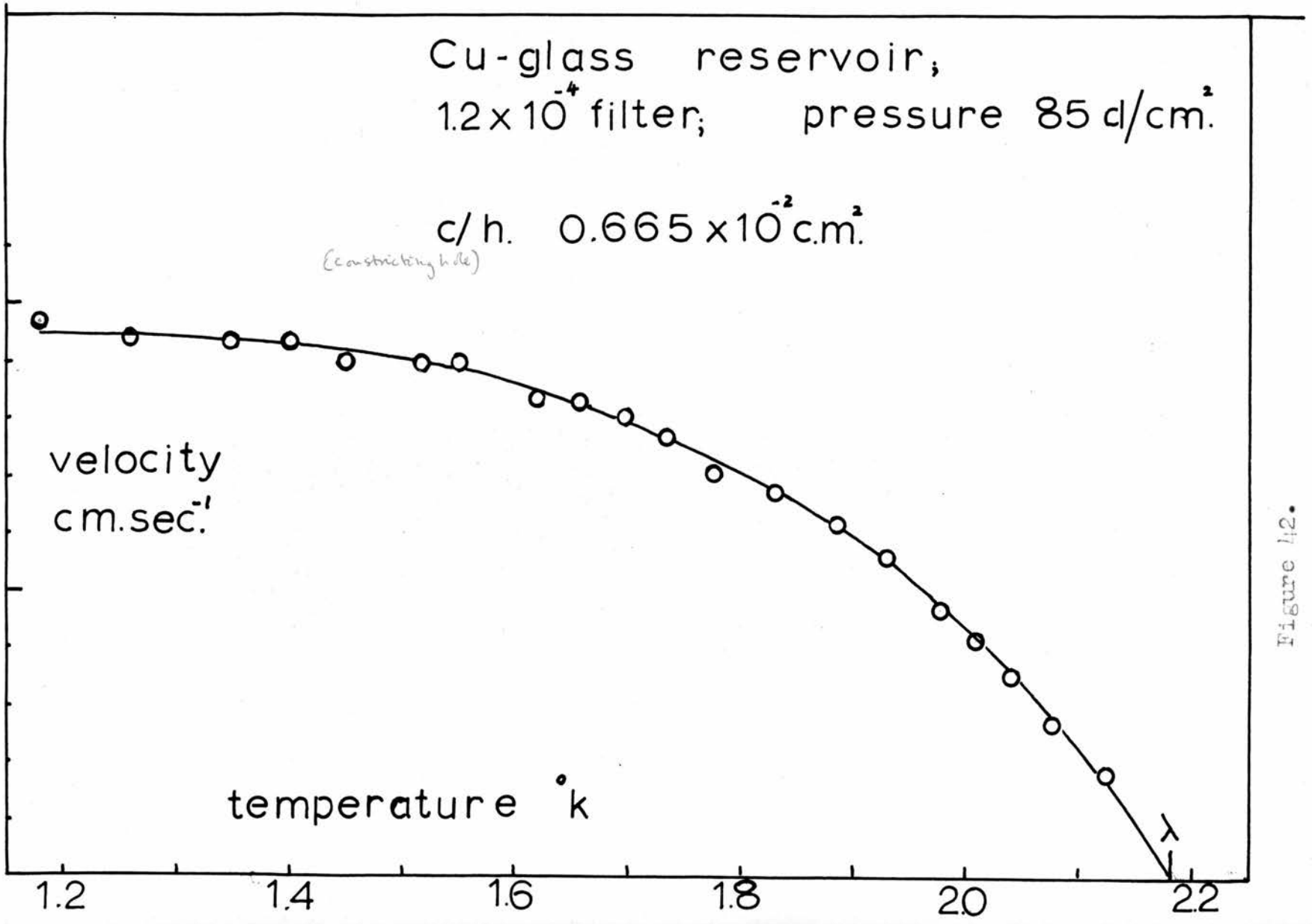
Cu-glass reservoir;
1.2 x 10⁻⁴ filter; pressure 85 d/cm².
c/h. 0.665 x 10⁻² c.m².
(constricting hole)
velocity
cm.sec⁻¹
temperature °k
λ
10
5
0
1.2
1.4
1.6
1.8
2.0
2.2

Figure 42.

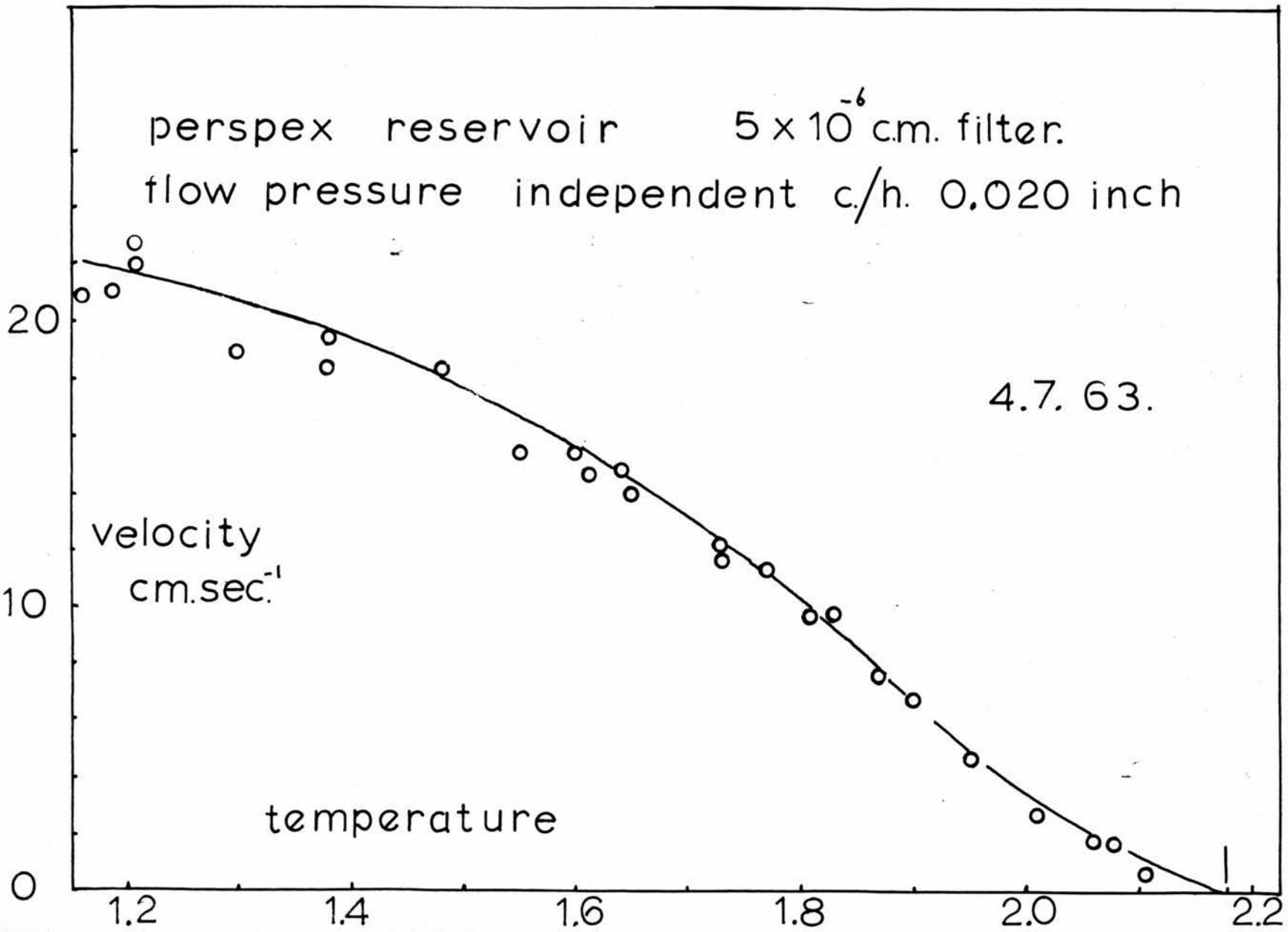
perspex reservoir 5 x 10⁻⁶ c.m. filter.
flow pressure independent c./h. 0.020 inch
4.7.63.
velocity
cm.sec.⁻¹
temperature
0
10
20
1.2
1.4
1.6
1.8
2.0
2.2

Figure 43.

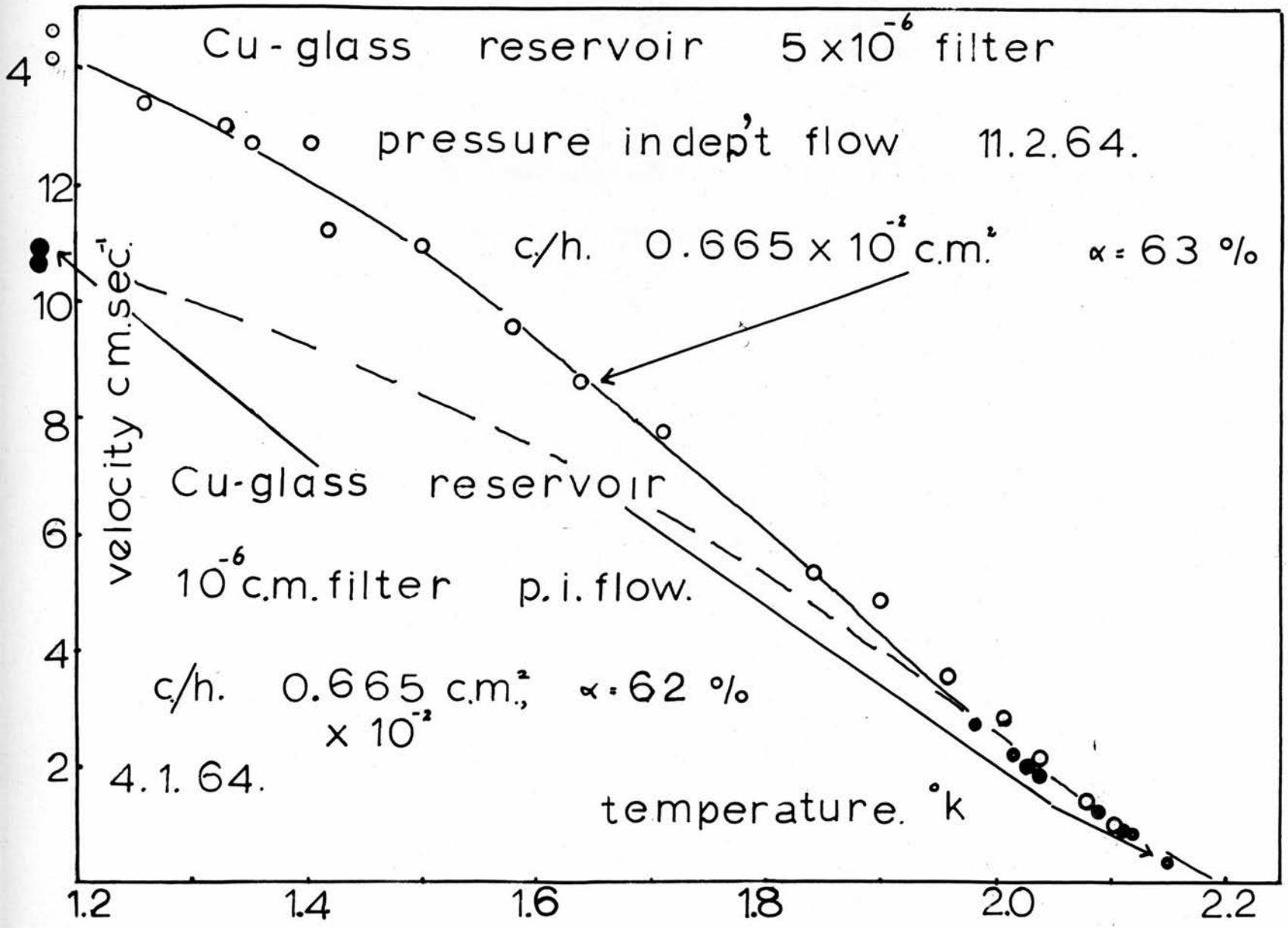
Cu-glass reservoir 5 x 10⁻⁶ filter
pressure indep't flow 11.2.64.
c/h. 0.665 x 10⁻² c.m.² α = 63 %
Cu-glass reservoir
10⁻⁶ c.m. filter p.i. flow.
c/h. 0.665 c.m.² x 10⁻² α = 62 %
4.1.64.
velocity cm.sec⁻¹
temperature. °k
4
12
10
8
6
4
2
1.2
1.4
1.6
1.8
2.0
2.2

Figure 44.

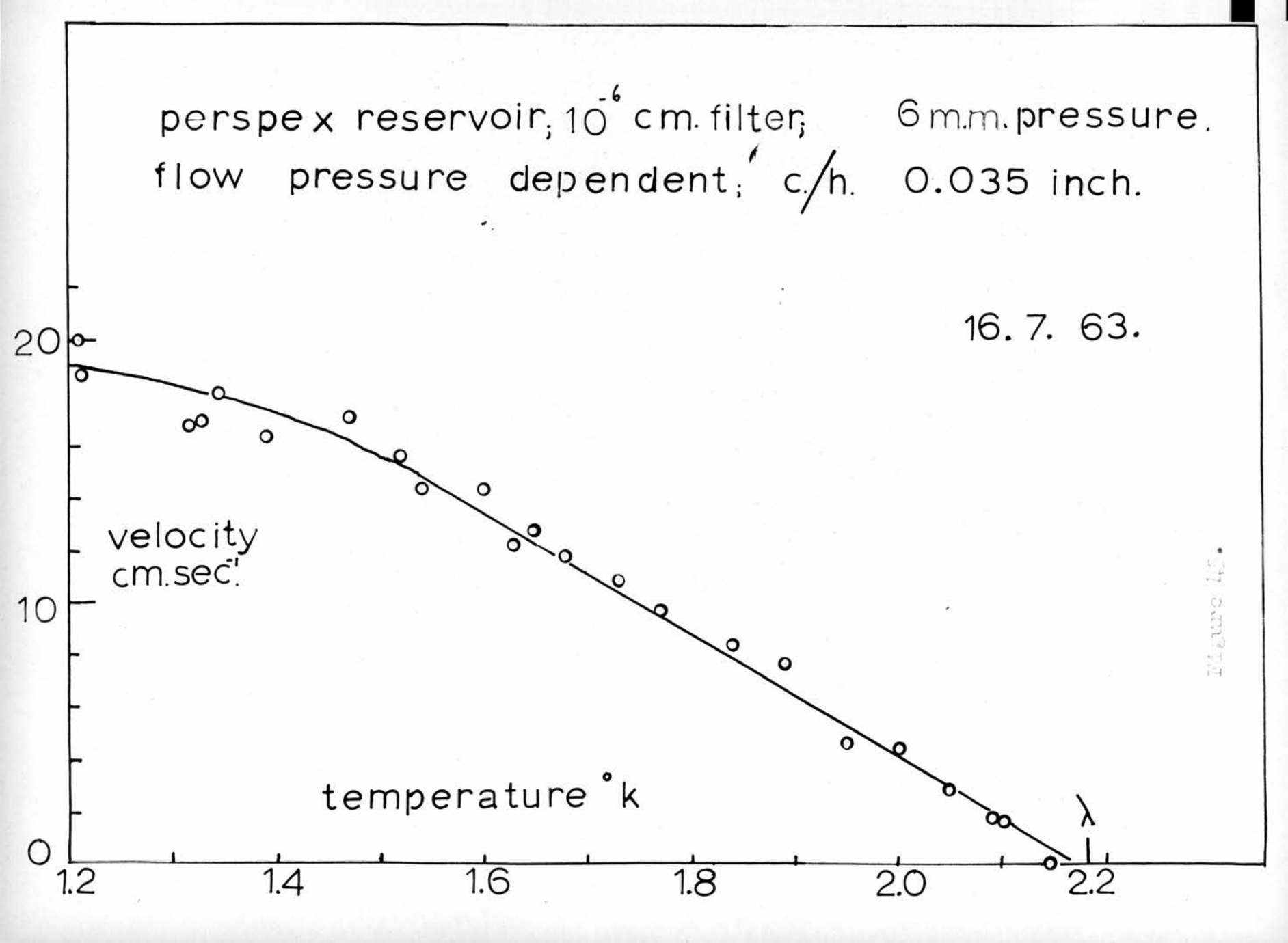
perspex reservoir; 10^{-6} cm. filter; 6 m.m. pressure.
flow pressure dependent; c./h. 0.035 inch.
16. 7. 63.
20
10
0
velocity
cm.sec.$^{-1}$
temperature °k
λ
1.2
1.4
1.6
1.8
2.0
2.2

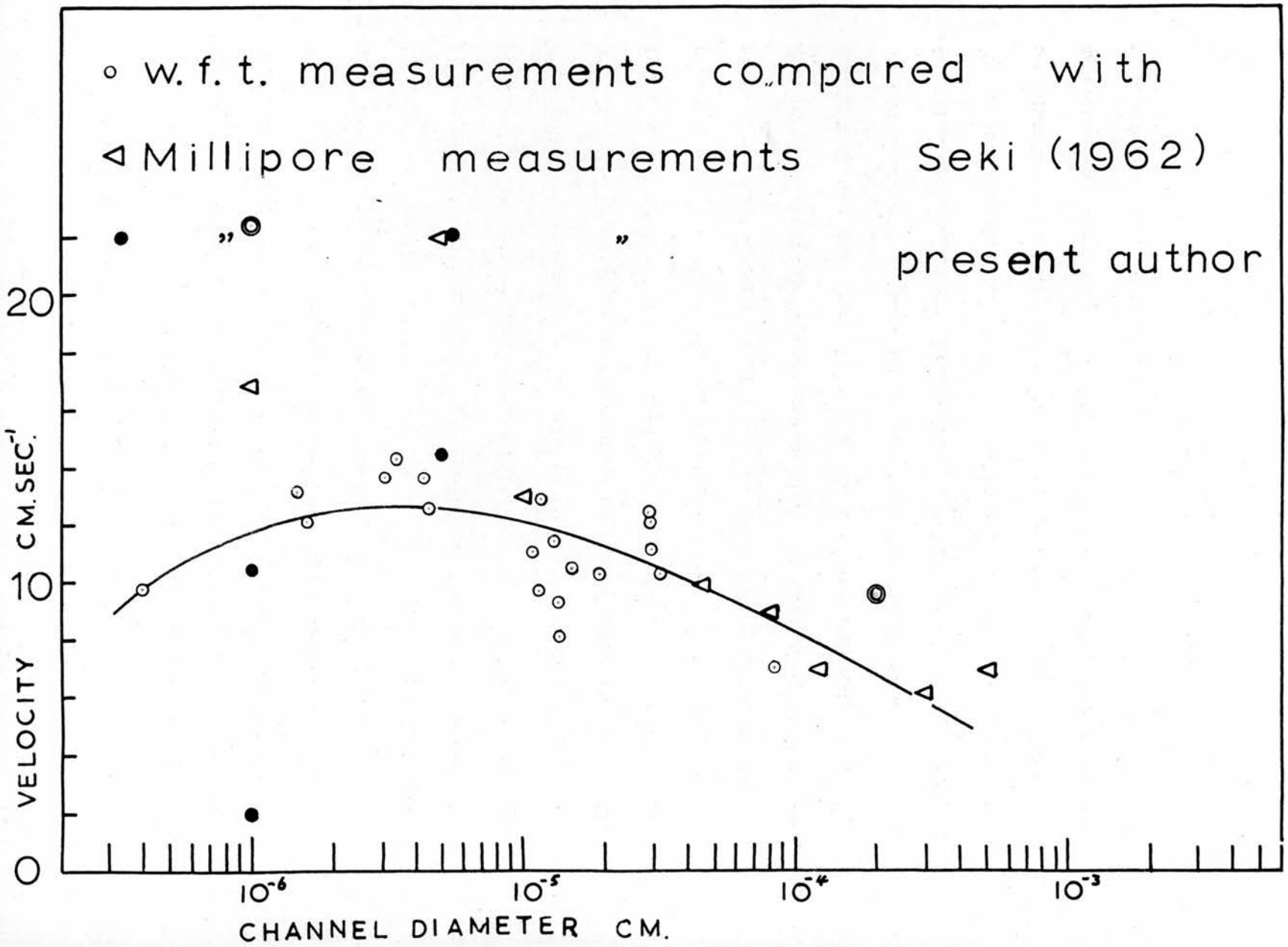
o w.f.t. measurements compared with
◁ Millipore measurements Seki (1962)
" "
present author
20
10
0
VELOCITY CM.SEC.⁻¹
10⁻⁶
10⁻⁵
10⁻⁴
10⁻³
CHANNEL DIAMETER CM.

Figure 16.

6.2 Flow results obtained using Millipore filters

As a check on the critical velocities measured by the wire-filled tube method it was decided to investigate the flow through Millipore filters. Three sizes, 10^{-6} cm, 5×10^{-6} cm and 1.2×10^{-6} cm were used. Preliminary measurements with the 10^{-6} cm size using a reservoir machined from perspex indicated that up to level differences of 1 cm or so the velocity was proportional to the cube root of the pressure and above 1 cm head the velocity became independent of pressure. This behaviour which has already been reported by Seki (1962) was, in the present investigation, at first believed to be connected with thermal effects due to the low thermal conductivity of perspex. When the measurements were repeated using a reservoir made partly of glass and partly of copper, v was independent of p except at very small level differences. Calculations have shown that the effect of poor thermal contact should give rise to a dependence $v \propto p$ and not $v \propto p^{1/3}$, so the above explanation would appear to be ruled out.

Another mechanism giving rise to cubic dependence was sought. The complex variation of index n with channel size can probably be understood in terms of flow partly governed by the filter mounting and partly by the filter itself. We now refer to the accompanying schematic diagram.

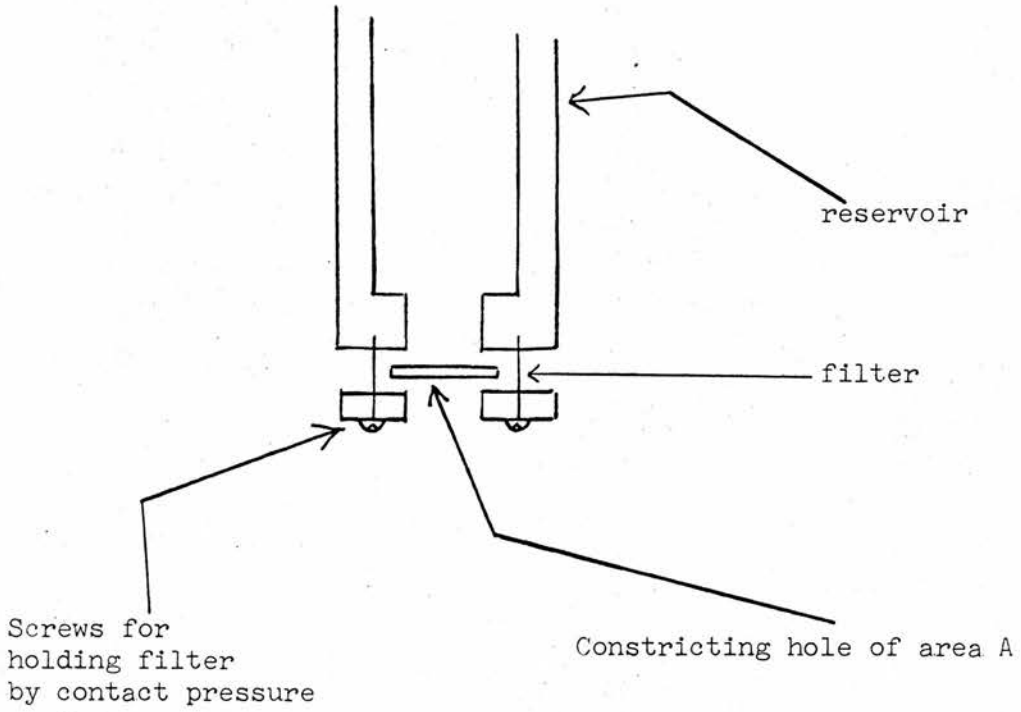

Suppose that the velocity through the filter is v and the exposed area of the filter is αA. If the velocity in the constricting hole is v' then by continuity

$$\rho A v' = A\alpha\, v \rho_s$$

so that

$$v' = \alpha v \rho_s / \rho$$

If the flow through the constricting hole of length l is governed by the mutual friction force, then the pressure p_c below which the flow is cubic is given by

$$\frac{\rho_s}{\rho} \text{ grad } p = \frac{\rho_s}{\rho} \cdot \frac{p_c}{l} = A \rho_s \rho_n \left\{ \alpha\, v_c \frac{\rho_s}{\rho} \right\}^3 \qquad (91)$$

where $v = v_c$ is the critical velocity in the filter. At velocity

v_c the flow does not increase because of the restriction n = 0. Whether or not a cubic regime is observed will depend on l, α, A, v_c and temperature.

Values of v_c obtained in the present investigation can be seen in figure (46). The scatter is very large in the smallest size of filter and this can be attributed to variations in α from sample to sample. Critical velocities measured by the wire-filled tube method are also included in figure (46) together with values of v, at 1 cm head of helium, as measured by Seki (1962). There is fair agreement as to order of magnitude between values obtained by the two methods.

The flow in the 1.2μ filter was pressure-dependent and the velocity at zero level difference was about 5 cm sec^{-1}, this being taken as the critical velocity, while the index $\frac{d \log v}{d \log p}$ was 0.2 at 1.2°K but increased with increasing temperature reaching a value 0.4 at 1.8°K. The reason for this behaviour could also be connected in some way with the geometry of the filter. The dependence of v on T seen in figure (42) can be expressed as $v \propto \left\{1 - (T/T_\lambda)^{\alpha}\right\}$ with $\alpha = 7$. In smaller channels (43), (44) and (45) a different dependence is observed. The flow through the 5×10^{-6} cm filter, figure (44), can best be fitted to a curve with $\alpha = 1.5$.

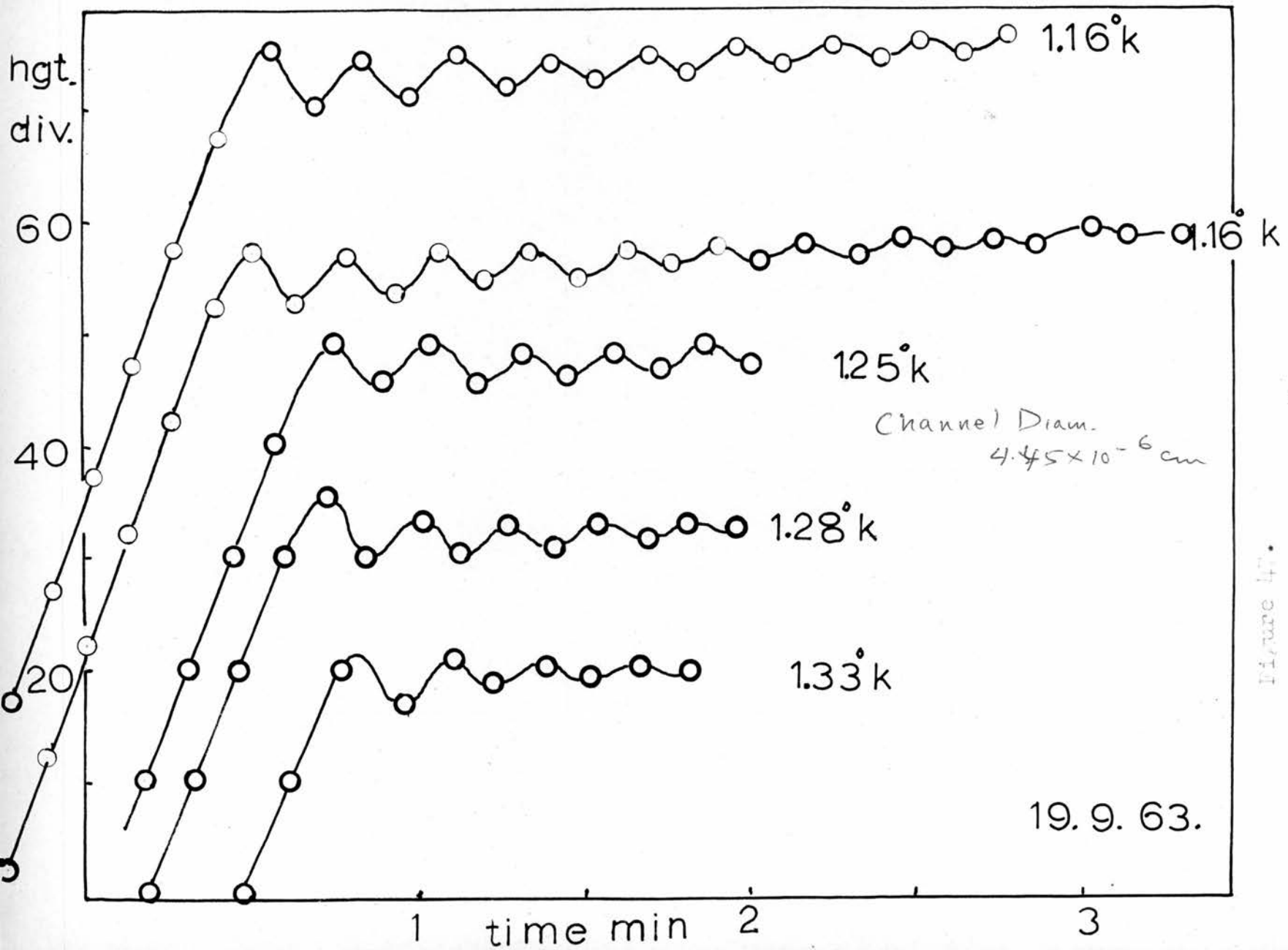
hgt.
div.
60
40
20
1.16°k
1.16° k
1.25°k
Channel Diam.
4.45×10⁻⁶ cm
1.28°k
1.33°k
19. 9. 63.
1
time min
2
3

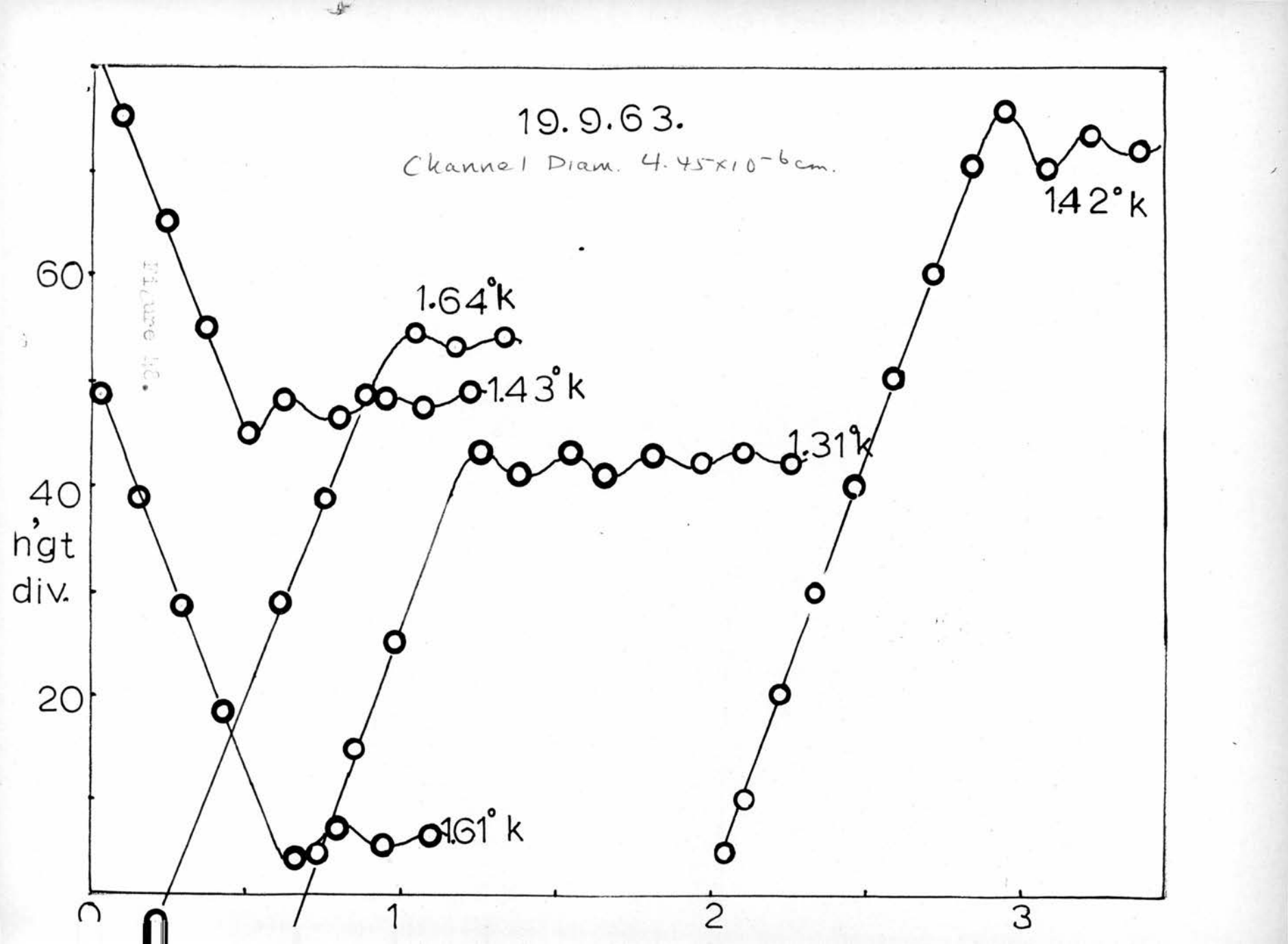
19.9.63.
Channel Diam. 4.45×10⁻⁶cm.
1.64°k
1.43°k
1.31°k
1.42°k
1.61°k
60
40
20
h'gt
div.
0
1
2
3

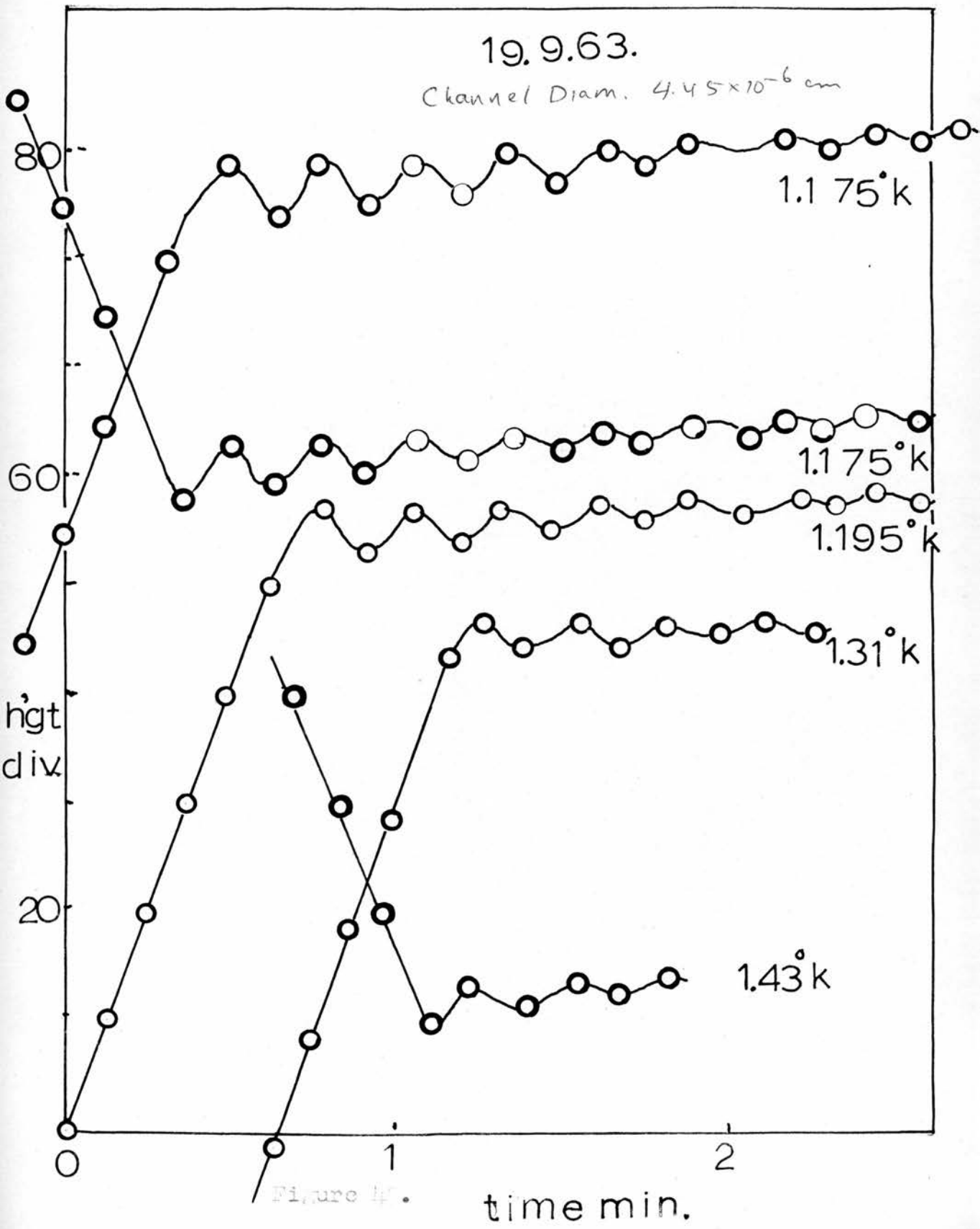
19.9.63.
Channel Diam. 4.45×10⁻⁶ cm
80
60
20
hgt
div.
1.1 75°k
1.1 75°k
1.195°k
1.31°k
1.43°k
0
1
2
time min.

Figure 4.

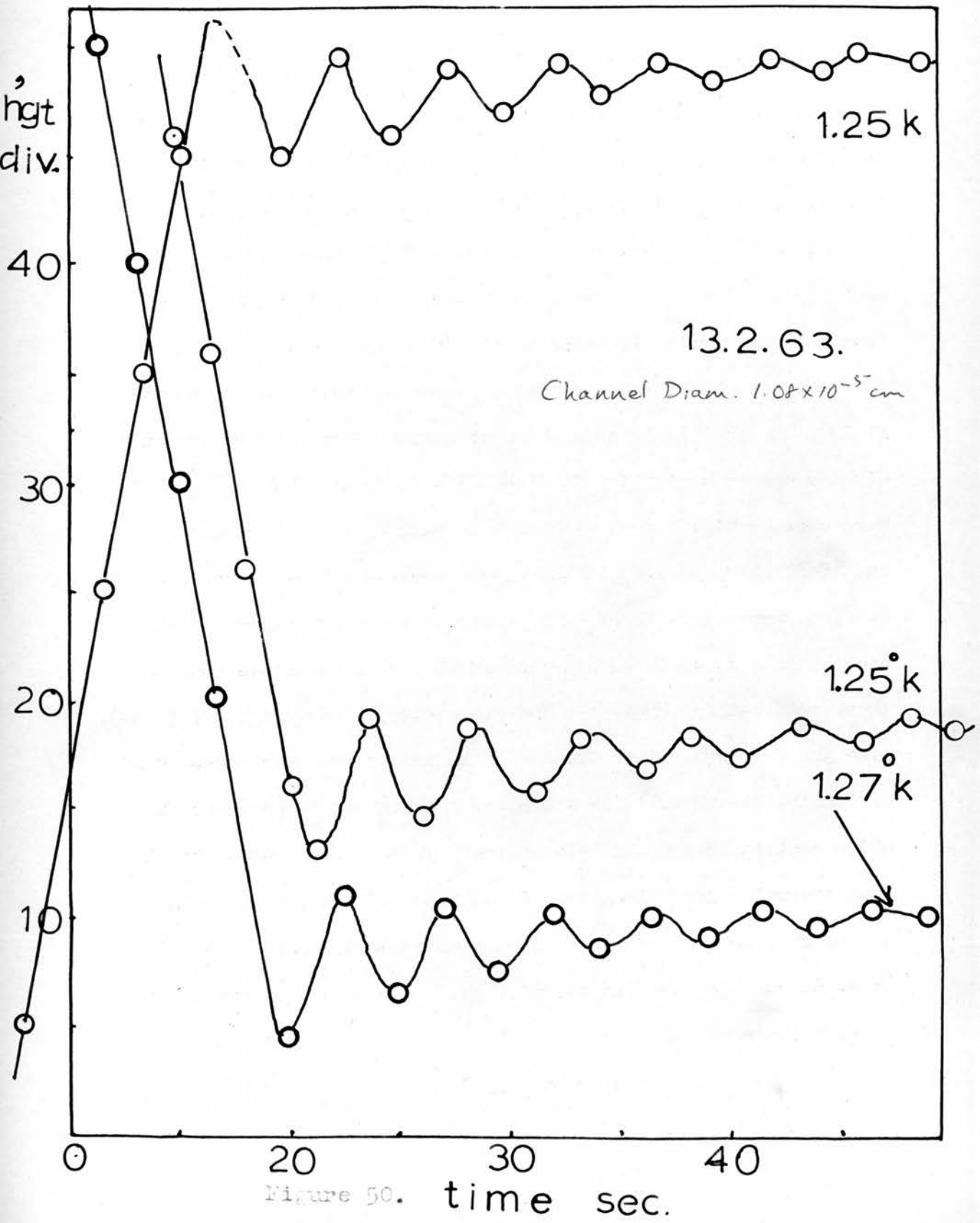
hgt
div.
40
30
20
10
1.25 k
13.2.63.
Channel Diam. 1.08 x 10⁻⁵ cm
1.25°k
1.27°k
0
20
30
40
time sec.

Figure 50.

6.3 The inertial oscillations (wire-filled tubes)

Atkins (1950) has measured the film thickness at 1.2°K as a function of height by means of inertial oscillations. At this temperature the oscillatory motion was only lightly damped. Allen (1963) has shown, however, that at higher temperatures such oscillations become increasingly damped and has suggested that the exponential increase he observed might be due to the interaction of vortex lines in the film with rotons of the normal fluid. The oscillations in the present experiments were also only lightly damped at 1.2°K in the channels for which $d < 10^{-5}$ cm but were more heavily damped at higher temperatures in these channels and at all temperatures in the wider channels. There were, however, no measurable level differences at the commencement of the oscillations as would be expected if they were adiabatic such as those observed by Manchester and Brown (1957), (see figs. 47 to 50). Also the frequency of oscillation that we observed was independent of temperature up to 1.6°K which was the highest temperature at which oscillations could be observed. We have seen in Chapter 5 that thermal contact is not perfect, (indeed it probably could not be so), so the angular frequency of observed oscillations (ω) is always smaller that in the ideal case (ω_o) and ω is related to ω_o by the expression

$$\omega^2 = \omega_o^2 - 1/\tau^2 \qquad (92)$$

where τ is the decay constant.

We shall now attempt to explain the damping by reference to the mechano-caloric effect.

First however we require the solution of an equation of the form

$$A\ddot{x} + B\dot{x} + Cx = 0.$$

Assume a solution of the form

$$x = e^{j(\omega + j\omega')t}$$

which is valid provided that the oscillations do occur.

The substitution yields

$$\left\{-A(\omega + j\omega')^2 + Bj(\omega + \omega' j) + C\right\} x = 0.$$

Taking the real part, we obtain

$$A(\omega^2 - \omega'^2) + B\omega' - C = 0$$

and then the imaginary part which gives,

$$-2j\,\omega\omega' A + Bj\omega = 0.$$

Thus we find $\omega' = B/2A$ and

$$\omega^2 - \omega'^2 = \frac{C}{A} - \frac{B}{A}\omega' = \frac{C}{A} - \frac{B^2}{2A^2} \quad . \tag{93}$$

Therefore

$$\omega^2 = \frac{C}{A} - \frac{B^2}{4A^2} = \omega_o^2 - 1/\tau^2 \tag{94}$$

where $$\tau = \frac{2A}{B} . \qquad (95)$$

During an oscillation, superfluid flows into and out of the reservoir. This causes a heat flow into and out of the reservoir. Assume the heat flow to be given by

$$Q = C\Delta T + VC_p \frac{d(\Delta T)}{dt} \qquad (96)$$

where C_p is the specific heat and C the total thermal contact via the walls and the vapour phase. The problem can be simplified by ignoring the second term in equation (96). (It has magnitude of order $VC_p \omega \Delta T$ being comparable with that of the first term since $VC_p \omega \Delta T \sim 40.10^6.10^{-5} \sim 400$ erg sec^{-1} and $C\Delta T \sim 5 \times 10^7.10^{-5} \sim 500$ erg sec^{-1}.) At equilibrium the entropy per unit volume of the liquid is constant, due to heat flowing away as fast as the entropy is increased. The entropy flowing down the channels is zero since $v_n = 0$ and therefore the entropy per unit volume generated at a rate ds/dt is,

$$\frac{ds}{dt} = - \frac{s}{v} \frac{dV}{dt}$$

i.e. the fractional change in entropy per unit volume is due to the fractional change in volume. The heat flow Q is

$$Q = TV \frac{ds}{dt} = C\Delta T$$

thus

$$C\Delta T = - \frac{TVs}{V} \frac{dV}{dt}$$

$$= -Ts \frac{dV}{dt}$$

or $$\Delta T = - \frac{TS}{C} \cdot \frac{dV}{dt} .$$

This difference in temperature gives rise to a fountain pressure Δp, where,

$$\Delta p_T = -S\Delta T$$

$$= - \frac{S^2 T}{C} \frac{dV}{dt} ,$$

and a vapour pressure difference of

$$\Delta p_v = (\frac{\partial p}{\partial T})\Delta T = - \frac{ST}{C}(\frac{\partial p}{\partial T}) \cdot \frac{dV}{dt}$$

but $\Delta p_v \ll \Delta p_T$ and can be ignored without much error. (We refer only to our own experimental arrangement - see Chapter 5.) The total force on the fluid in the channels is, approximately,

$$(\rho g x + \frac{S^2 T}{C} \frac{dV}{dt}) A_o \rho_s / \rho$$

and the mass being accelerated is $V_o \rho_s$, where the subscript "O" refers to flow in the channel.

The equation of motion becomes

$$(\rho g x + \frac{S^2 T}{C} \frac{dV}{dt}) A_o \rho_s / \rho = -V_o \rho_s \ddot{x}_{o,s}$$

where $x_{o,s}$ indicates that only superfluid flows within the channel.

From continuity of mass flow we obtain

$$A\dot{x} = \rho_s / \rho \; A_o \; \dot{x}_{os} .$$

Thus the volume acceleration in the reservoir volume $\ddot{V}$ is given by

$$\ddot{V} = \rho_s/\rho \, A_o \, \ddot{x}_{os}$$

It follows that,

$$\rho_s g x + \rho_s/\rho \frac{s^2 T}{C} \dot{V} = -l_o \rho_s \, \ddot{x}_{o,s}$$

$$= -l_o \rho_s \, (\rho \ddot{V}/\rho_s A_o)$$

$$= - \frac{l_o \rho \ddot{V}}{A_o} \, .$$

This can be expressed in terms of $\ddot{V}$, $\dot{V}$ and V by putting $V = A(x + l)$ where l is the depth of liquid in the reservoir below the bath level, as seen in the adjoining figure.

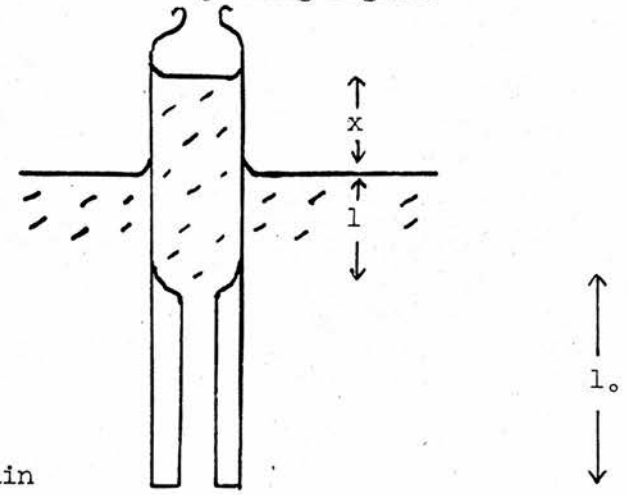

We then obtain

$$\frac{l_o \ddot{V}}{A_o} + \frac{\rho_s}{\rho} \frac{s^2 T}{C} \dot{V} + \rho_s g \frac{V}{A} = \rho_s g l \, .$$

Substituting,

$$\frac{V \rho_s g}{A} - \rho_s g l = Y$$

we finally obtain for the equation of motion,

$$\frac{l_o \rho A}{A_o \rho_s g} \ddot{Y} + \frac{\rho_s}{\rho} \frac{s^2 T}{C} \frac{A}{\rho_s} \dot{Y} + Y = 0 .$$

Now by comparison with equation (93) we see at once that

$$\omega_o = (C/A)^{\frac{1}{2}}$$

$$= \left\{ \frac{l_o A}{g A_o} \cdot \frac{\rho}{\rho_s} \right\}^{\frac{1}{2}}$$

which is the relation obtained by Robinson (1951) for the case of strictly isothermal oscillations. The decay constant τ is given by

$$\tau = \frac{2A}{B} = 2 \left\{ \frac{l_o \rho A}{g \rho_s A_o} \right\} \Big/ \left\{ \frac{s^2 T A}{\rho C g} \right\}$$

$$= \frac{2 l_o \rho^2 C}{A_o \rho_s s^2 T} .$$

We can see at once that the time τ is made longer by increasing the channel length and improving the thermal contact. Also increasing the temperature increases the entropy per unit volume and thus the damping. We find ω is given by

$$\omega^2 = \omega_o^2 \left\{ 1 - \left(\frac{A_o s \rho_s}{l_o C \rho} \right)^3 \frac{s T^2 C}{4A} \right\} = \omega_o^2 \left(1 - \delta \right).$$

This result clearly shows that as $C \to \infty$, $\delta \to 0$.

The dependence of C on temperature

Next we examine the temperature dependence of C in order to see how far this theory can account for the temperature dependence of the damping.

(a) due to thermal contact via the reservoir walls

$$C = \frac{T^3}{10} .10^7 \text{ A.}$$

$$= 2.10^7 T^3 \quad \text{erg/sec-deg.}$$

{Kapitza (1941), with A = 20 cm^2; see p67};

(b) due to evaporation from the reservoir

$$Q = \lambda \frac{dm}{dt}$$

where λ is the latent heat and $\frac{dm}{dt}$ the mass evaporating per second. It follows that

$$Q = \frac{\lambda P}{RT} \frac{dV}{dt} .$$

The volume flow causes a pressure drop ΔP across the constricting hole at the top of the reservoir, so

$$Q = \frac{\lambda P}{RT} \left(\frac{a^4}{8\eta l}\right) \Delta P$$

$$= \frac{\lambda P}{RT} \left(\frac{a^4}{8\eta l}\right) \left(\frac{\partial P}{\partial T}\right)_{svp} \Delta T$$

$$= \frac{\lambda P}{RT} \left(\frac{a^4}{8\eta l}\right) \frac{\lambda}{TV} . \Delta T$$

$$= \left(\frac{a^4}{8\eta_o l}\right) \frac{\lambda^2}{R^2T^2} \frac{p^2}{T^{1+n}} \cdot \Delta T$$

where we have put

$$\eta = \eta_o T^n$$

nø being about 0.68 for helium gas and $\eta_o = 5 \times 10^{-6}$ poise.

Also λ, the latent heat, can be written as

$$\lambda \sim 20T + 60 .$$

Furthermore the saturated vapour pressure p is given approximately by

$p \sim AT^{5/2} e^{-3/T}$, where A is a constant, (see for example van Dijk and Durieux, 1955).

Thus in this case the temperature dependence of C is

$$C \sim T^2 . T^5 . (e^{-3/T})^2 / T^{n+3}$$

$$T^3 (e^{-3/T})^2 .$$

The temperature dependence of τ

For contact via the copper

$$\tau \propto T^3 / S^2 T = e^{2\Delta/kT}$$

since $S \propto T/\Delta\ e^{-\Delta/kT}$, where Δ is the roton energy gap.

For contact via the vapour

$$\tau \propto (T^3 (e^{-3/T})^2 e^{2\Delta/kT}) / T^3$$

$$\sim e^{(24/k - 6)/T}$$

We thus see that τ decreases exponentially with increasing temperature. This does not give exactly the dependence observed by Allen (1963) but the damping would be a very rapidly increasing function of temperature. Figure 51 shows the logarithmic decrement of oscillations plotted as a function of inverse temperature; the data was derived from figures 47 and 48. The plot suggests that the damping is indeed an exponential function of temperature. We must now calculate the magnitude of this effect, in other words, show that τ is of order of 60 sec.

Taking values from table 1

$l_o \sim 10$ cm

$\rho_s/\rho \sim 1$

$A_o \sim 1.9 \times 10^{-4}$ cm^2

$S = 5 \times 10^{-3} T^{5.6}$ cal gm^{-1} deg K^{-1}

$C \sim 5 \times 10^{7}$ erg units (from section 5.3)

$A \sim 14.8 \times 10^{-2}$ cm^2

$T \sim 1.2°K$

$S \sim 5 \times 10^{4}$ erg cm^{-3} deg K^{-1}

$d = 4.5 \times 10^{-6}$ cm

Thus

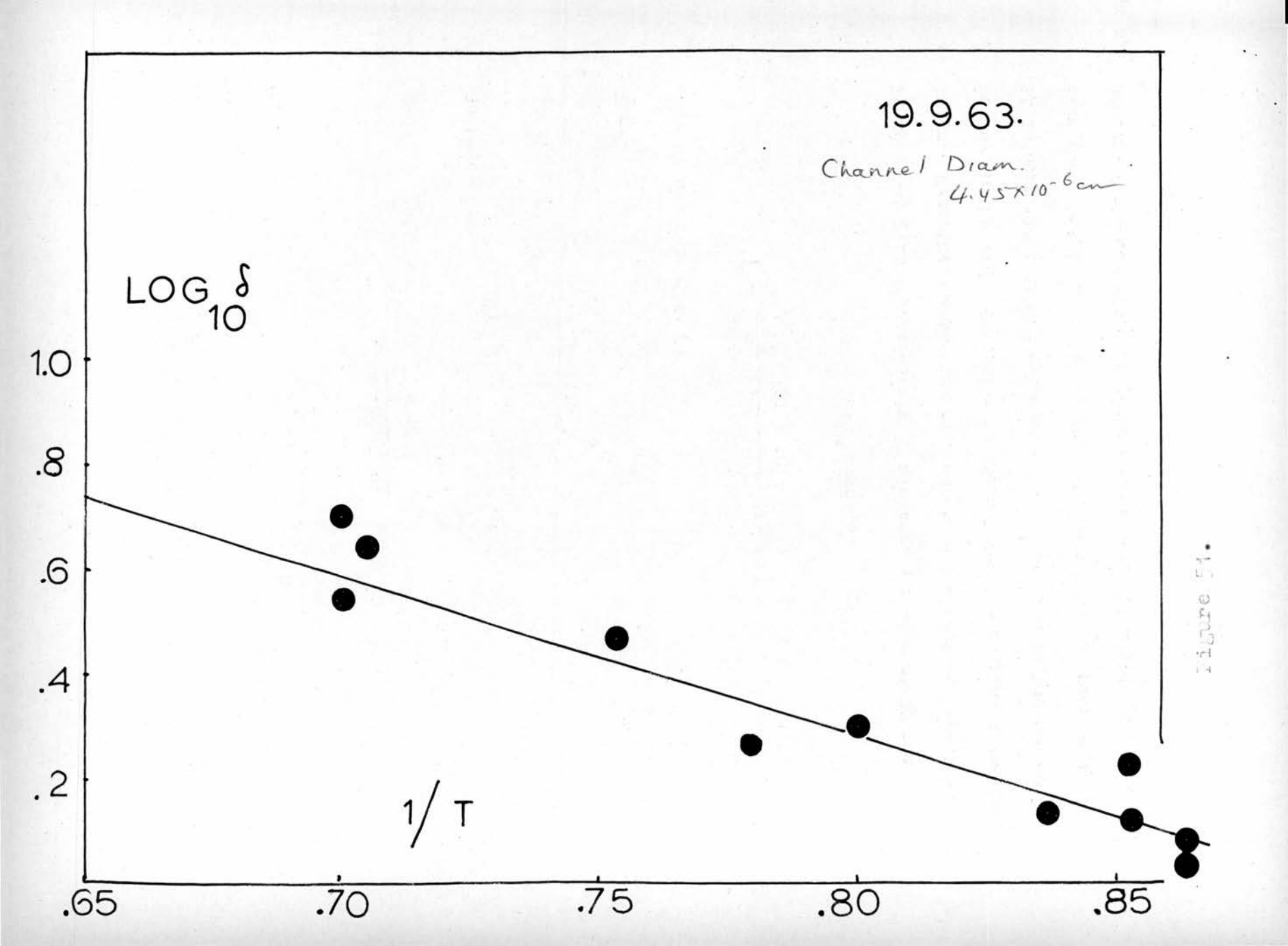

Figure 51.

$$\frac{A_o S \rho_s}{l_o C \rho} \sim \frac{2.10^{-4}.5 \times 10^4}{10.5.10^7}$$

$$\sim 10^{-7}/5 = 2 \times 10^{-8}$$

$$\frac{ST^2C}{4A} \sim \frac{5.10^4.5.10^7}{4.10^{-7}} \sim 5.10^{12}$$

So that

$$\delta \sim 8.10^{-24}.5.10^{12}$$

$$\sim 4.10^{-11}$$

Thus $$\omega = \omega_o .$$

We now calculate $\hat{\tau}$:

$$\hat{\tau} \approx \frac{2l_o C}{A_o S^2} = \frac{20.5.10^7}{21 \times 10^{-4}} .25.10^8$$

$$= 2.10^3 \text{ seconds} .$$

We see that $\hat{\tau}$ is approximately 30 minutes, a factor of 30 too large. Nevertheless the theory predicts a temperature dependence acting in the right direction to account for the increased damping. It is possible that our estimate of C is out by a factor two or even three but it is unlikely that the contact is so poor as to account for decay times of order one minute. It would seem that

something as drastic as vortex line-roton interactions even at subcritical velocities will be required if we are to explain satisfactorily the damping which at temperatures above about 1.6°K prevents the occurrence of oscillatory motion. It appears that a more detailed experimental investigation is required. For example it would be interesting to vary the area of contact between reservoir and bath (for a particular wire-filled tube) and then to compare the damping. Similar experiments varying the diameter of the constricting hole would show whether viscous effects in the vapour phase affect the damping. Clearly there is much scope for an investigation which would distinguish between damping due to vortex lines and that due to thermal effects.

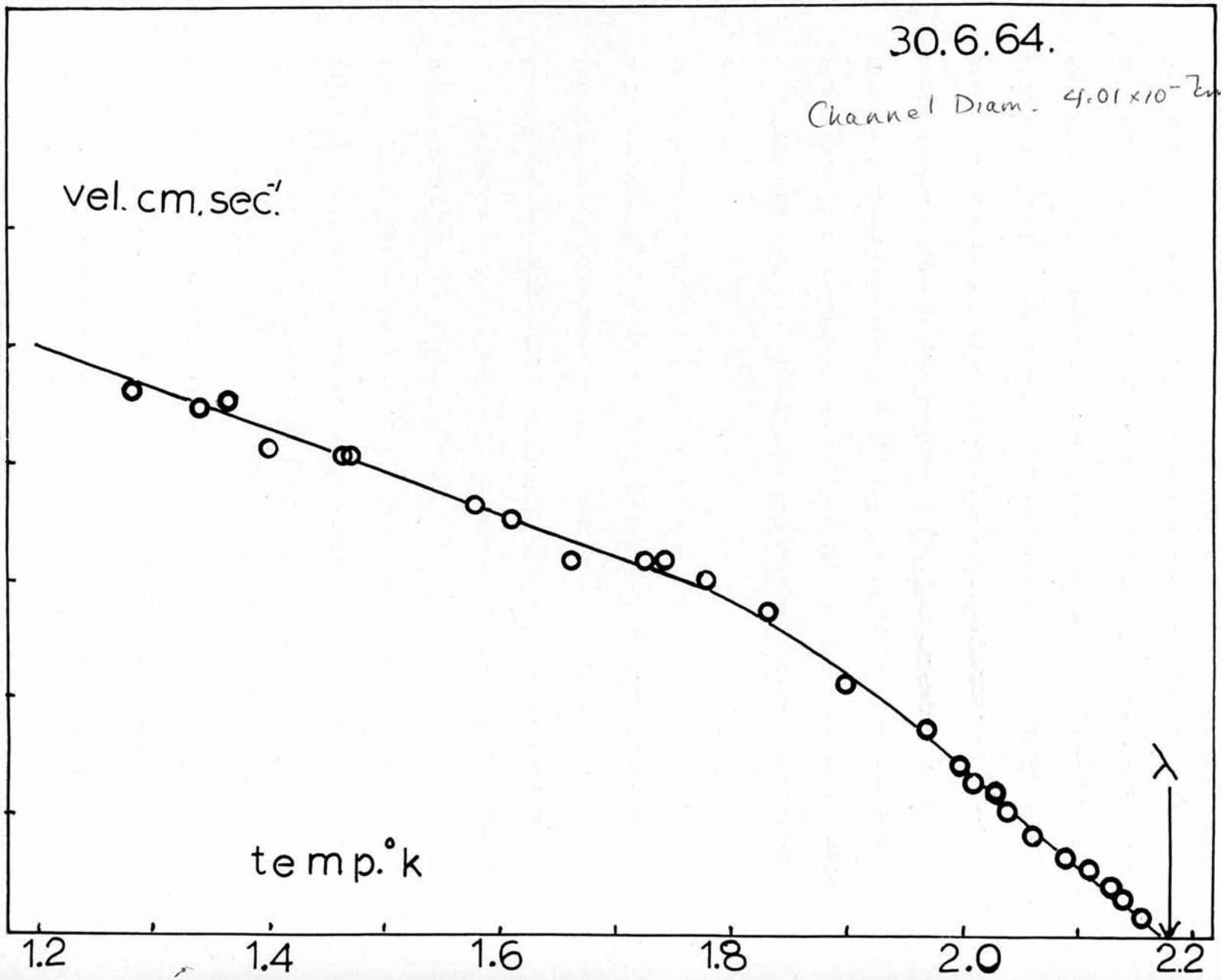
30.6.64.
Channel Diam. 4.01 x 10⁻⁷m.
vel. cm. sec⁻¹
12
10
8
6
4
2
temp.°k
1.2
1.4
1.6
1.8
2.0
2.2
λ

Figure 52.

6.4 Onset depressions and the velocity-temperature relation

Measurements of mean velocity, v, and in those cases where n = 0, of v_c, have been made in the temperature region 1.2°K to the λ-point. These results are shown in figures (52) to (62). Whereas several of these curves fitted the relation $v \propto \{1 - (T/T_\lambda)^\alpha\}$, with $\alpha = 7$, the 4×10^{-7} cm wire-filled tube, figure (52), fitted better to a value $\alpha = 3$, and the 5×10^{-6} cm Millipore, figure (57), a value $\alpha = 1.5$.

Evidence such as that found by Bowers, Brewer and Mendelssohn (1951), Champeney (1957), Seki (1962) strongly favours the existence of onset depressions. The onset effect means that only at a temperature $T_o < T_\lambda$ does superflow set in. The magnitude of the depression, $|T_\lambda - T_o|$, is governed by the channel or film size.

Assuming that the wire-filled tubes each contain a spread of sizes then it is reasonable to suppose that in the largest channels flow will occur even when $T = T_\lambda$, but the other small channels will begin to contribute at temperatures $T_o(d)$ appropriate to their size. In Chapter 4.3 it was shown how suitable choice of $f(d)$, $v(d)$ and $(\rho_s/\rho)_{d,T}$ could lead to a dependence v on T different from that in wide channels. Comparison of figures (52) and (57) with figure (62) $d = 1.33 \times 10^{-5}$ cm, or with figure (59) $d = 2.9 \times 10^{-5}$ cm, suggests that the predicted effect has been observed.

It must be pointed out that Long and Meyer[†] (1951) investigated onset phenomena in the unsaturated film. In one method where a superleak was initially connected at one end to a high vacuum and at the other to a chamber containing helium gas at pressure p, they observed the onset effect. In a second method where the first chamber also contained helium gas at a small but finite pressure no effect was observed. The discrepancy between these two methods appears never to have been resolved. Near the λ-point the fountain pressure is approximately 6 cm He per millidegree temperature difference. It is also noteworthy that even at temperature $T_\lambda > T_o$ there is a finite volume flow rate; this is seen in figure (3) of the paper by Long and Meyer (1951). Recent work by Edwards et al (1965) on flow of helium II through saran charcoal revealed no evidence of onset depressions greater than 10 millidegrees but this result can be explained as the charcoal contains a few large pores. While it is possible to interpret the present data as supporting the onset effect it might be that the present observations in fact show similarity to the second method of Long and Meyer, and that the v - T dependence changes for some other reason.

[†]For details of their experiment see Long, E. and Meyer, L. (1951) Phys. Rev. 85, 1030.

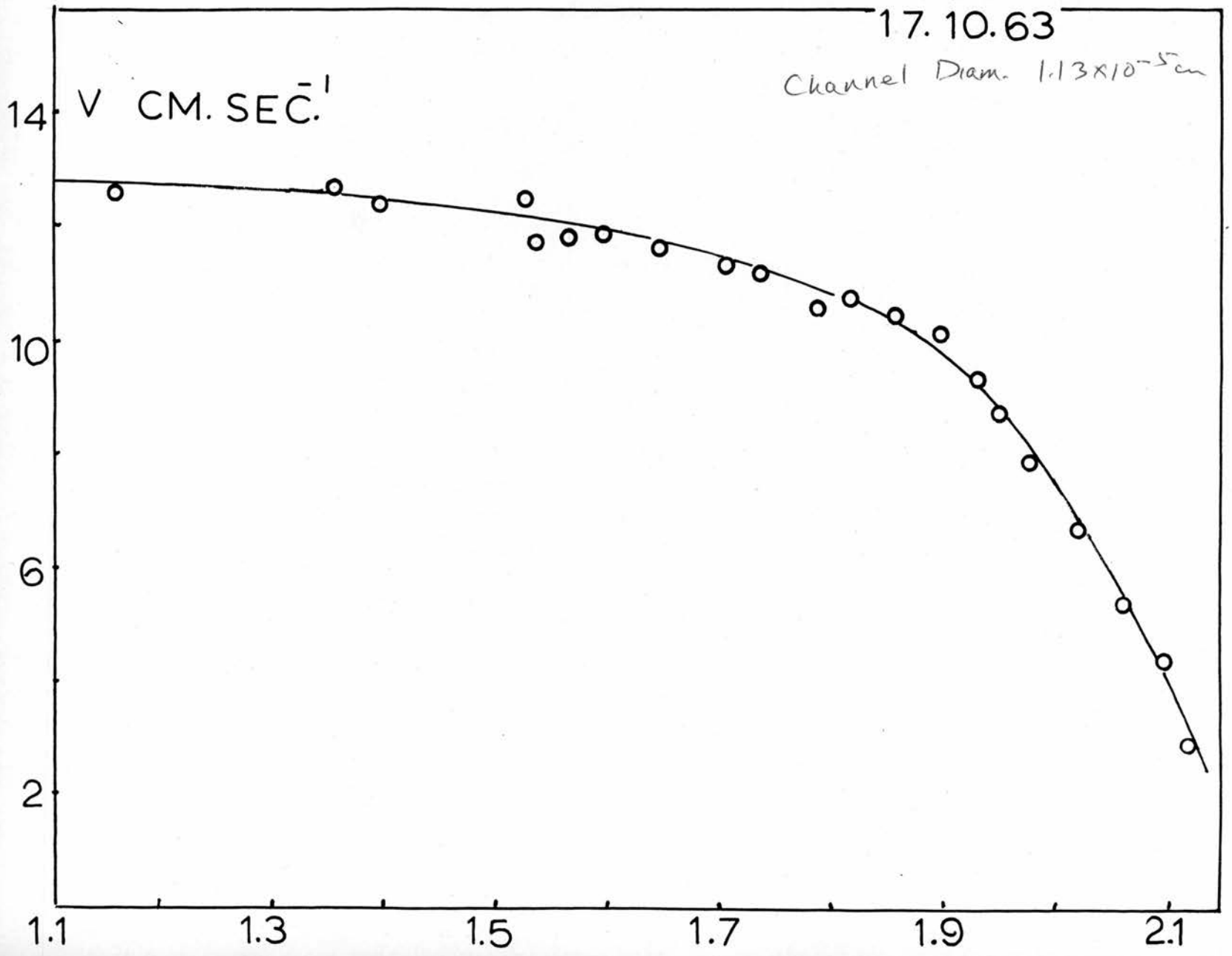
17. 10. 63
Channel Diam. 1.13×10⁻⁵cm
V CM. SEC.⁻¹
14
10
6
2
1.1
1.3
1.5
1.7
1.9
2.1

Figure 53.

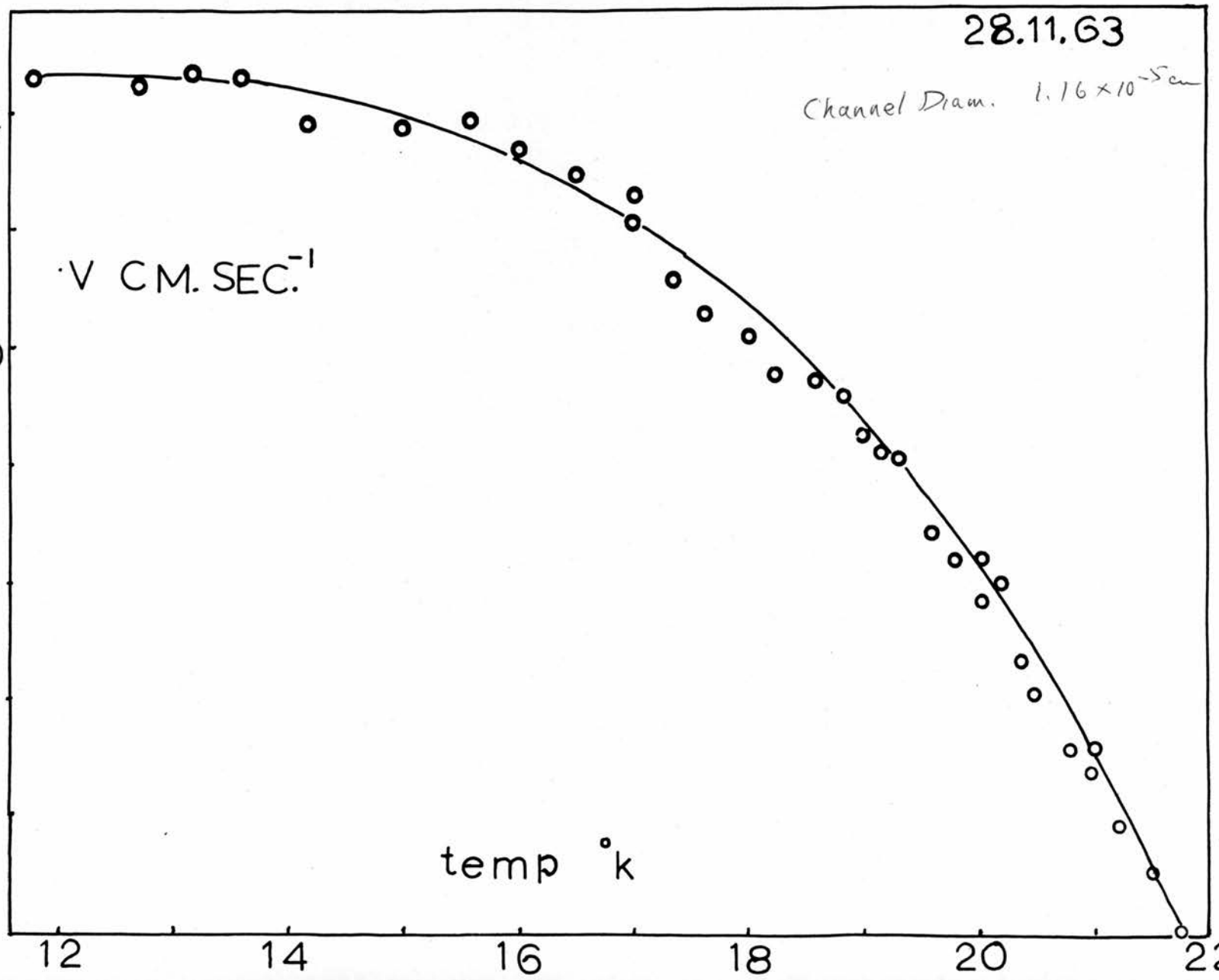
28.11.63
Channel Diam. 1.16 × 10⁻⁵ cm
V CM. SEC.⁻¹
14
10
6
2
temp °k
12
14
16
18
20
22

Figure 54.

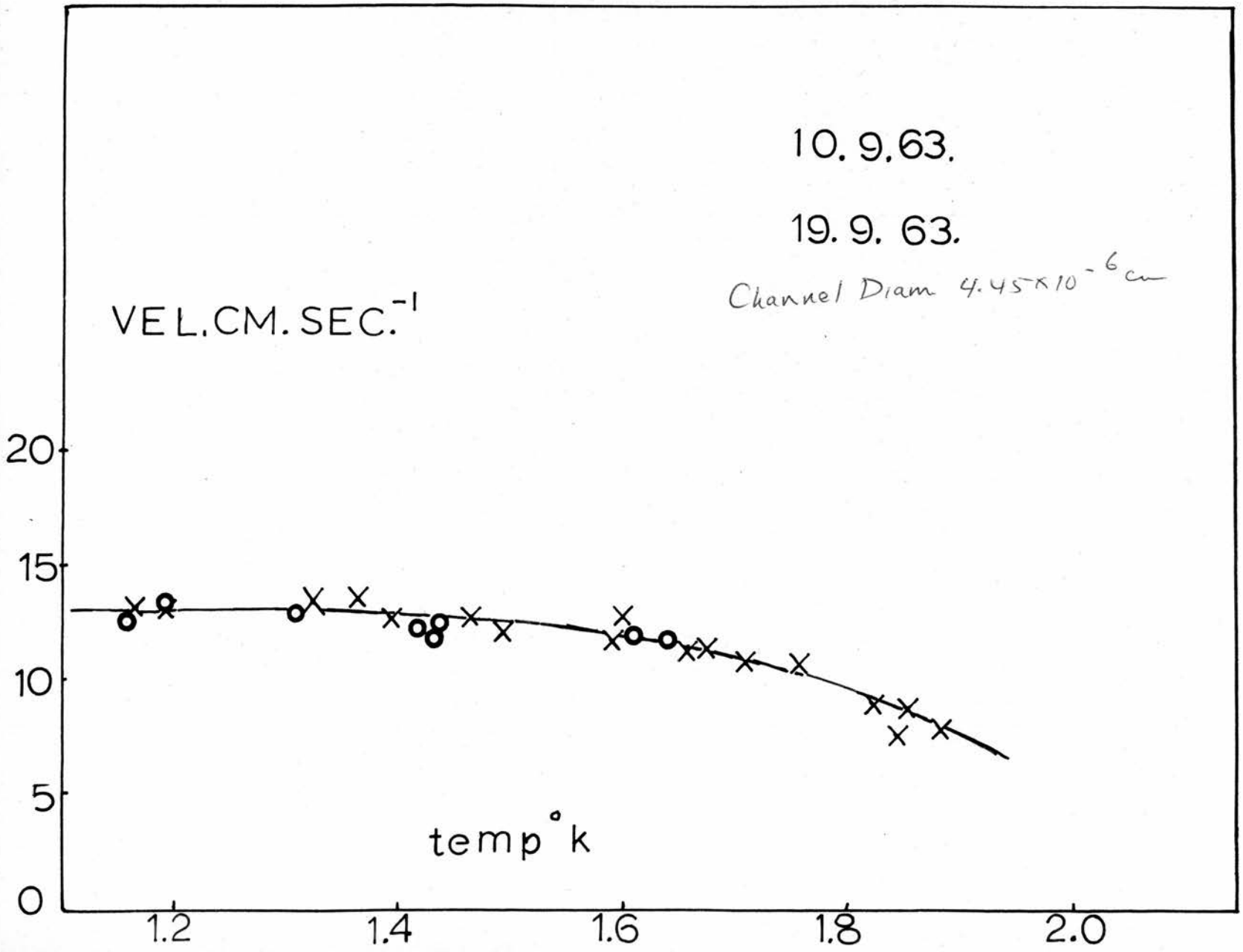
10. 9. 63.
19. 9. 63.
Channel Diam 4.45 x 10 - 6 cm
VEL. CM. SEC.-1
20
15
10
5
0
temp °k
1.2
1.4
1.6
1.8
2.0

Figure 55.

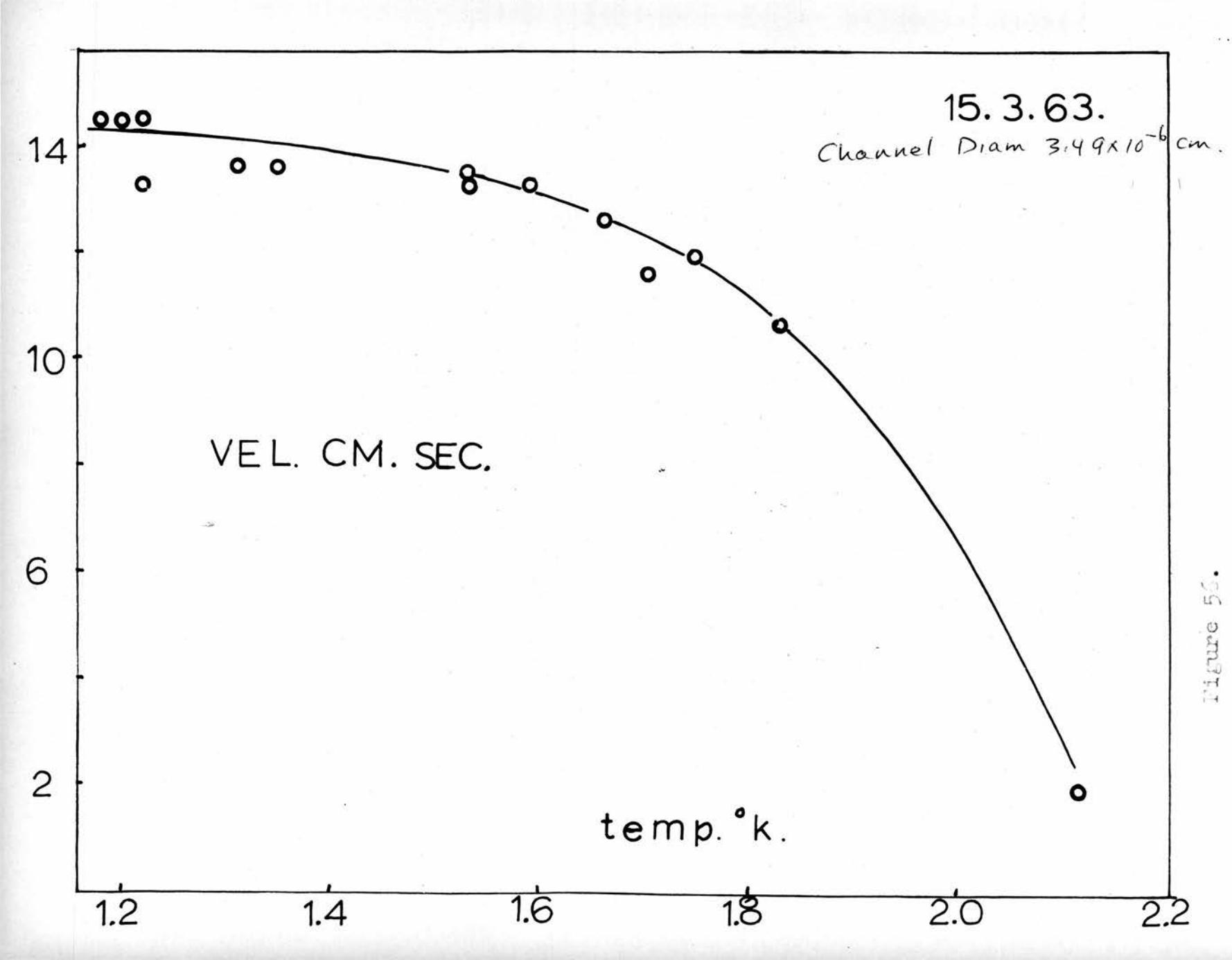
15.3.63.
Channel Diam 3.49x10⁻⁶ cm.
14
10
6
2
VEL. CM. SEC.
temp. °k.
1.2
1.4
1.6
1.8
2.0
2.2

Figure 56.

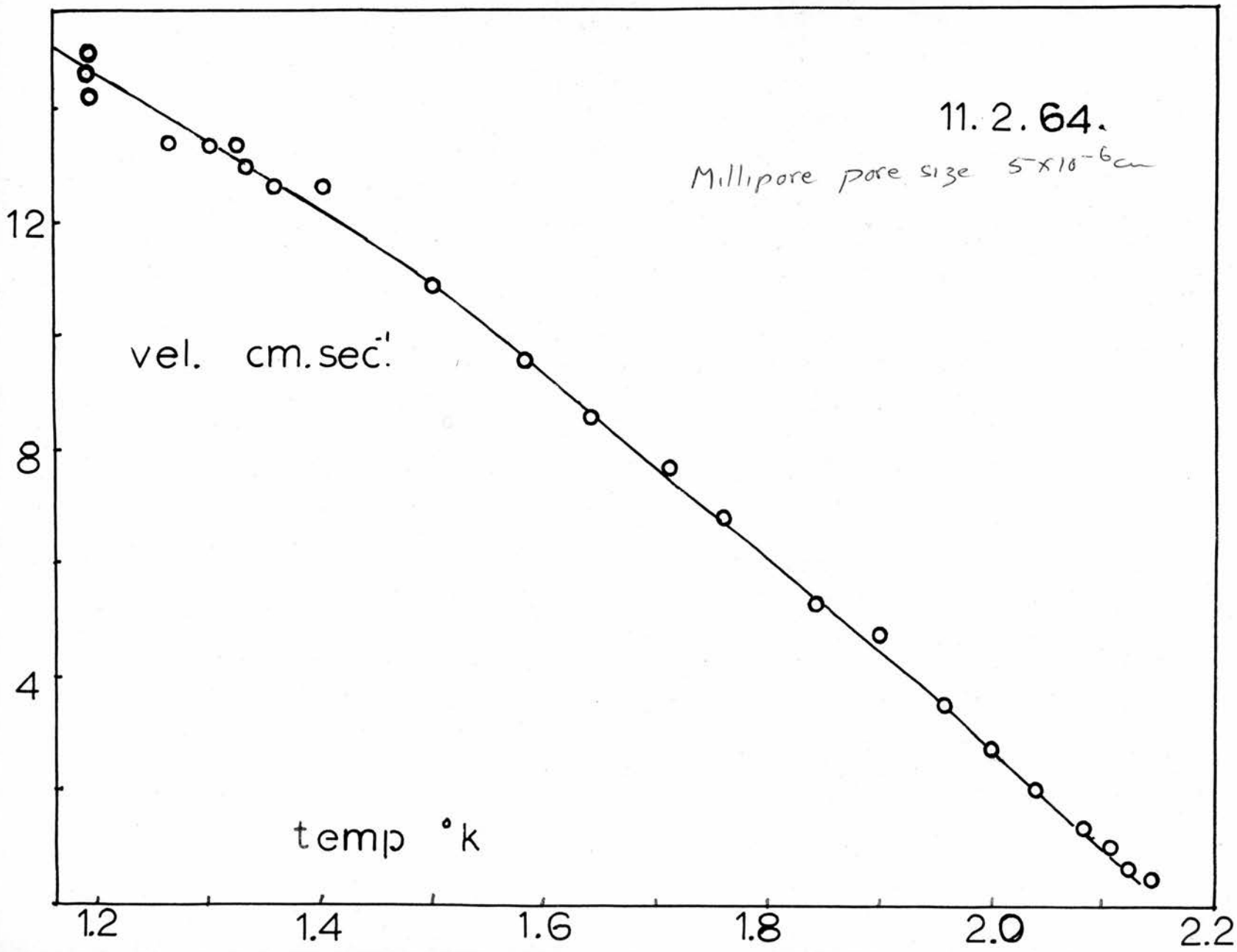
11.2.64.
Millipore pore size 5×10^{-6} cm
vel. cm.sec^{-1}
12
8
4
temp °k
1.2
1.4
1.6
1.8
2.0
2.2

Figure 57.

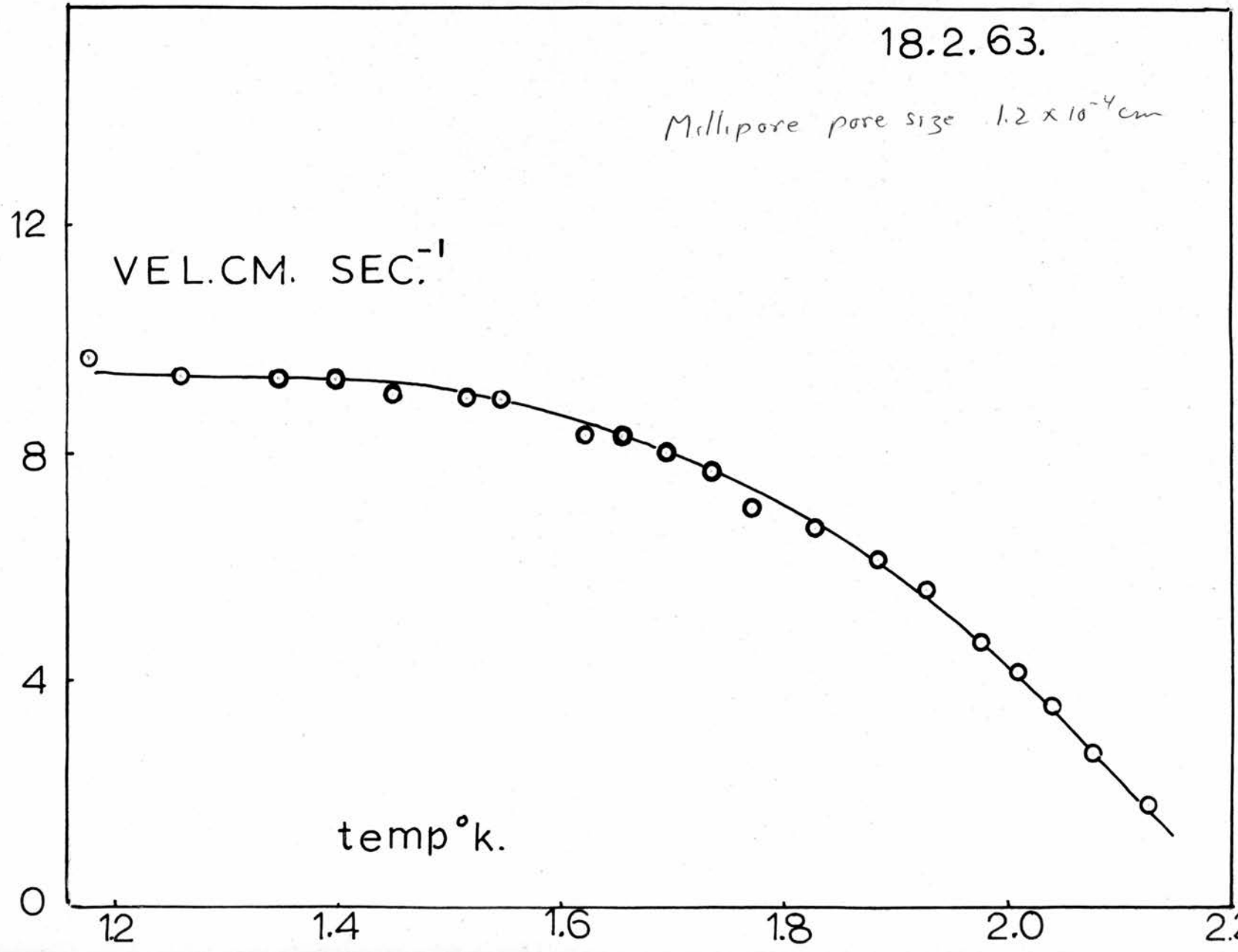
18.2.63.
Millipore pore size 1.2 x 10⁻⁴ cm
VEL.CM. SEC.⁻¹
12
8
4
0
temp°k.
1.2
1.4
1.6
1.8
2.0
2.2

Figure 58.

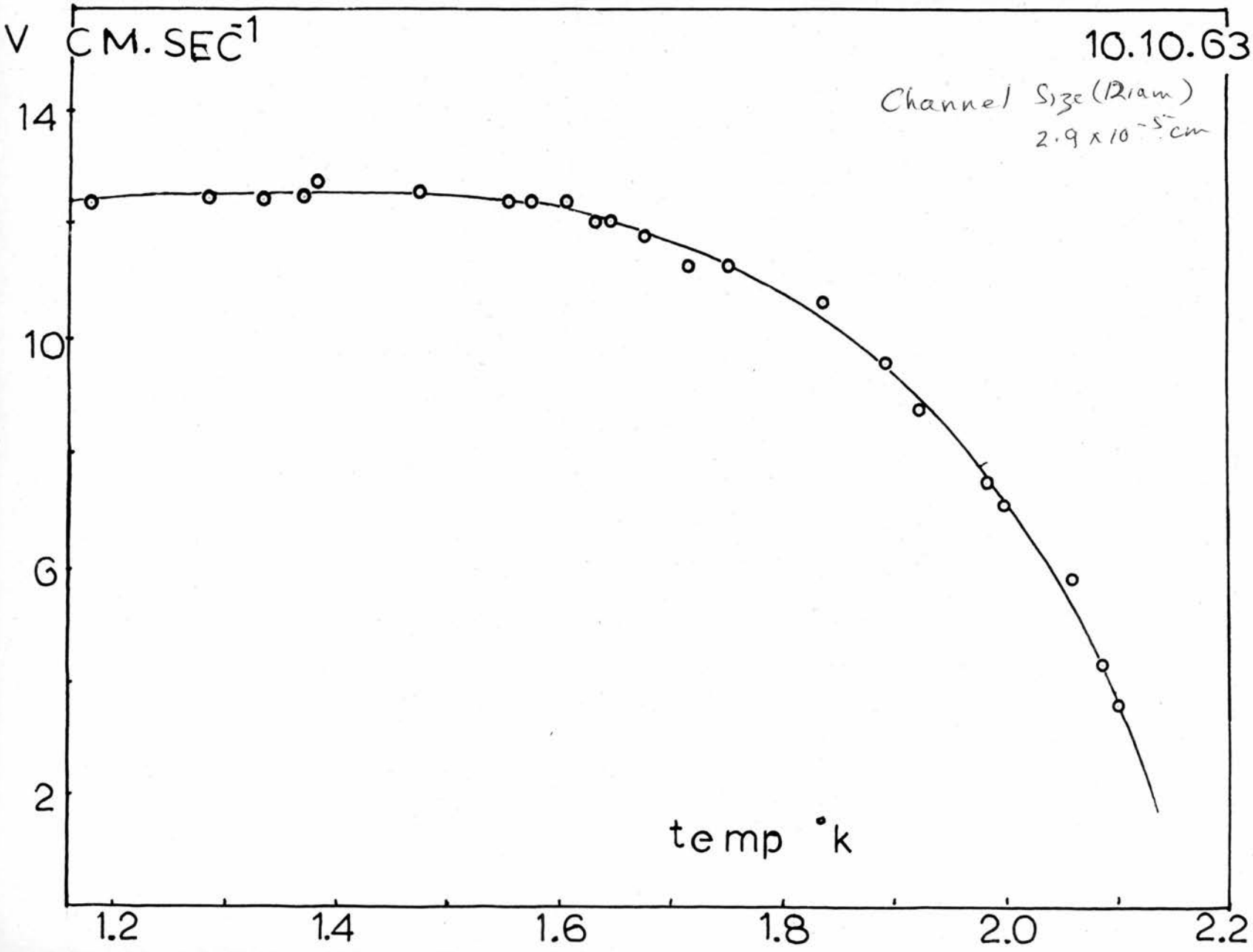
V CM. SEC⁻¹
10.10.63
Channel Size (Diam)
2.9 x 10⁻⁵ cm
14
10
6
2
temp °k
1.2
1.4
1.6
1.8
2.0
2.2

Figure 59.

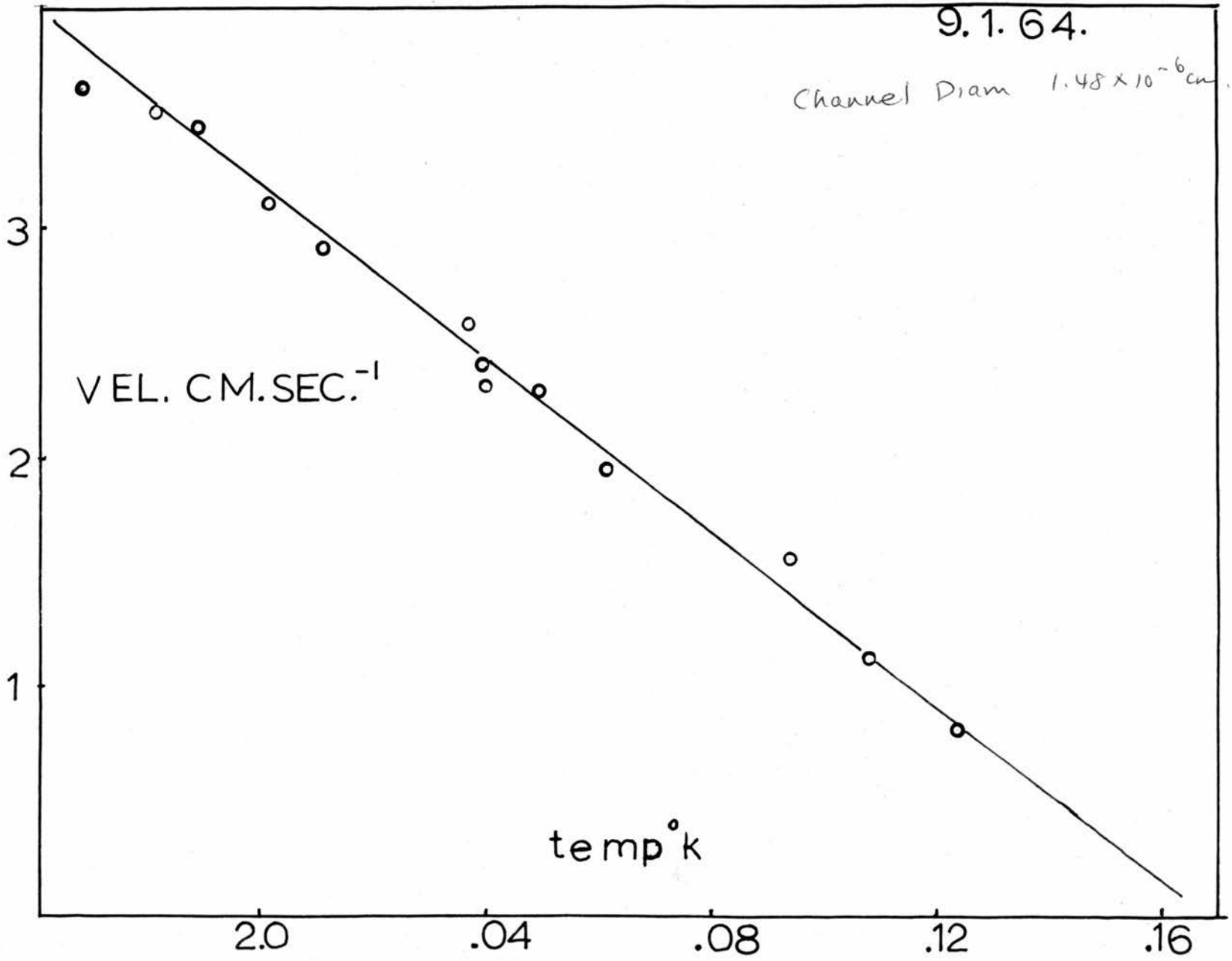
9.1.64.
Channel Diam 1.48 x 10⁻⁶ cm.
VEL. CM. SEC.⁻¹
3
2
1
temp°k
2.0
.04
.08
.12
.16

Figure 60.

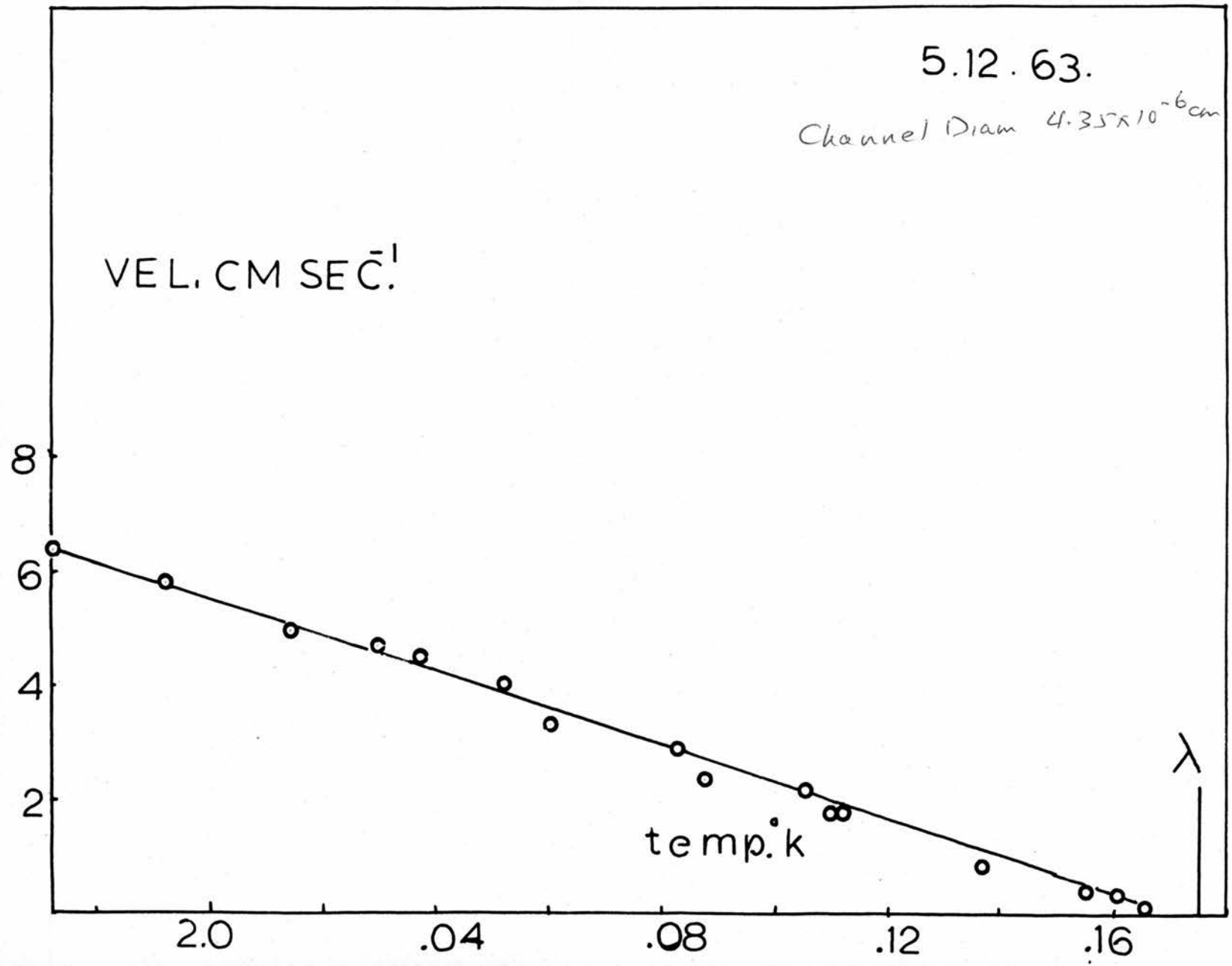
5.12.63.
Channel Diam 4.35×10⁻⁶cm
VEL. CM SEC⁻¹
8
6
4
2
λ
temp.°k
2.0
.04
.08
.12
.16

Figure 61.

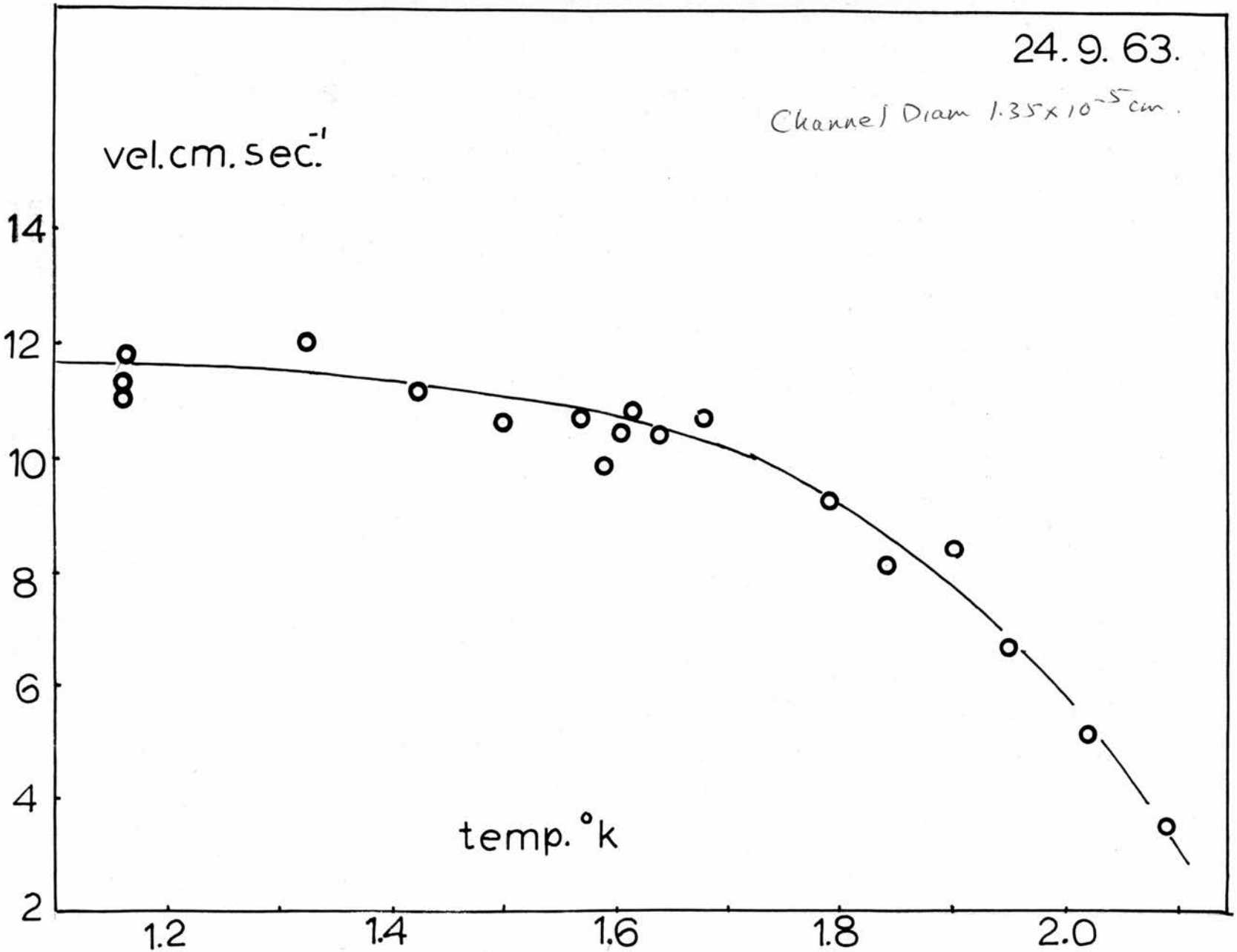
24.9.63.
Channel Diam 1.35x10⁻⁵cm.
vel.cm.sec.⁻¹
14
12
10
8
6
4
2
8
temp.°k
1.2
1.4
1.6
1.8
2.0

Figure 62.

Figure 63.

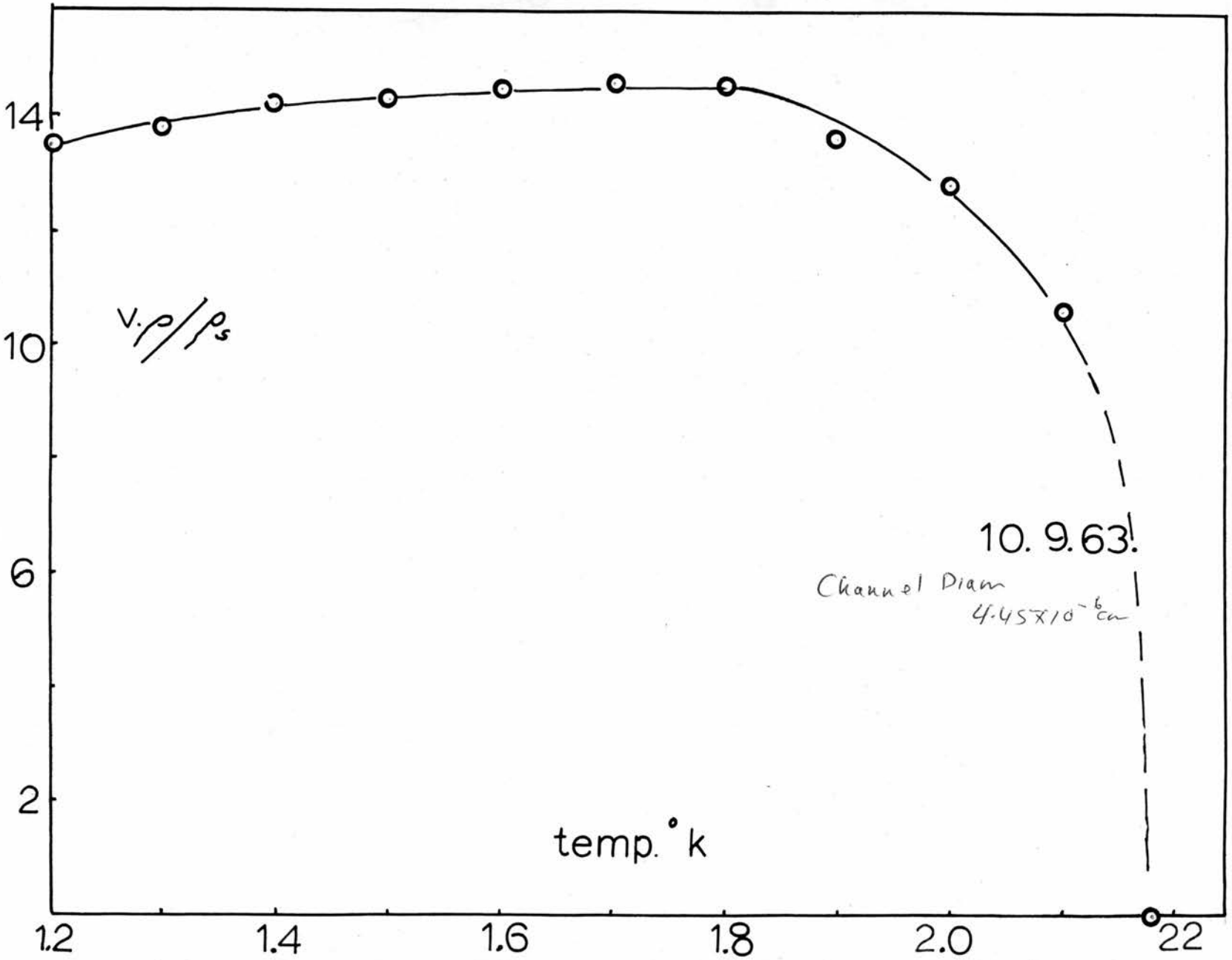
14
10
6
2
V.ρ/ρs
10.9.63!
Channel Diam
4.45×10⁻⁶cm
temp.°k
1.2
1.4
1.6
1.8
2.0
22

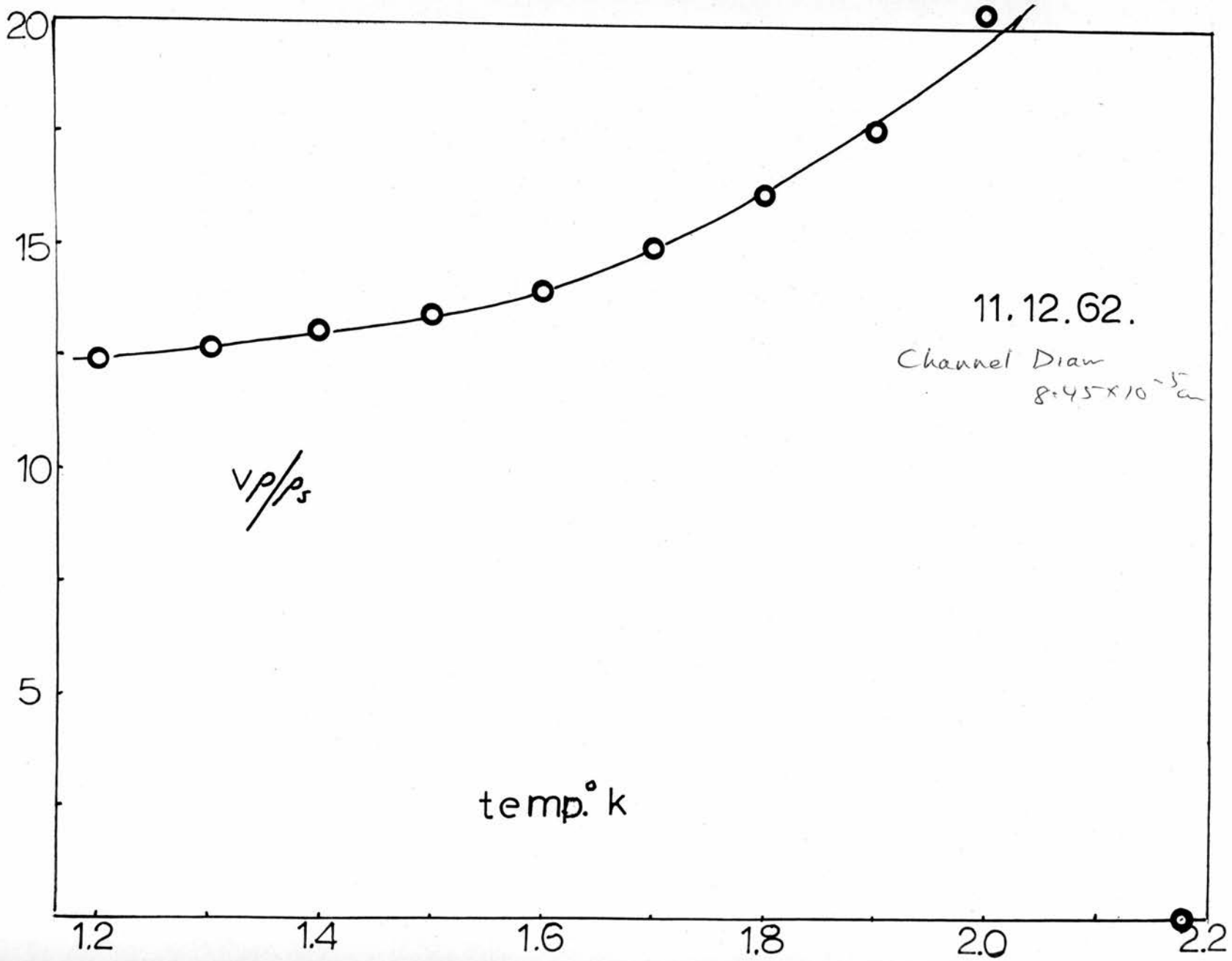
20
15
10
5
11.12.62.
Channel Diam
8·45×10⁻⁵ cm
Vρ/ρs
temp.° k
1.2
1.4
1.6
1.8
2.0
2.2

Figure 65.

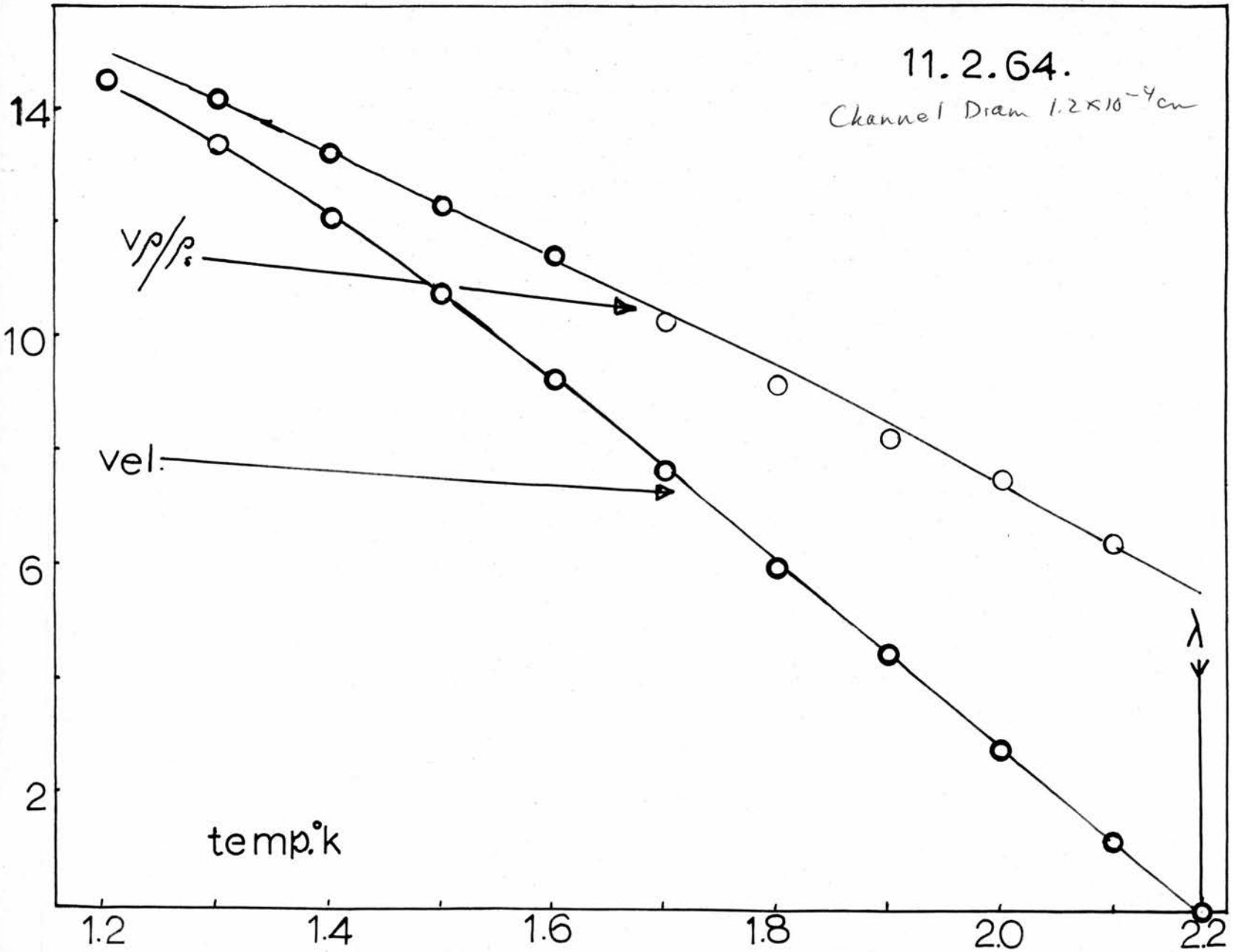
11.2.64.
Channel Diam 1.2×10⁻⁴cm
14
10
6
2
vel:
λ
temp.°k
1.2
1.4
1.6
1.8
2.0
2.2

Figure 65.

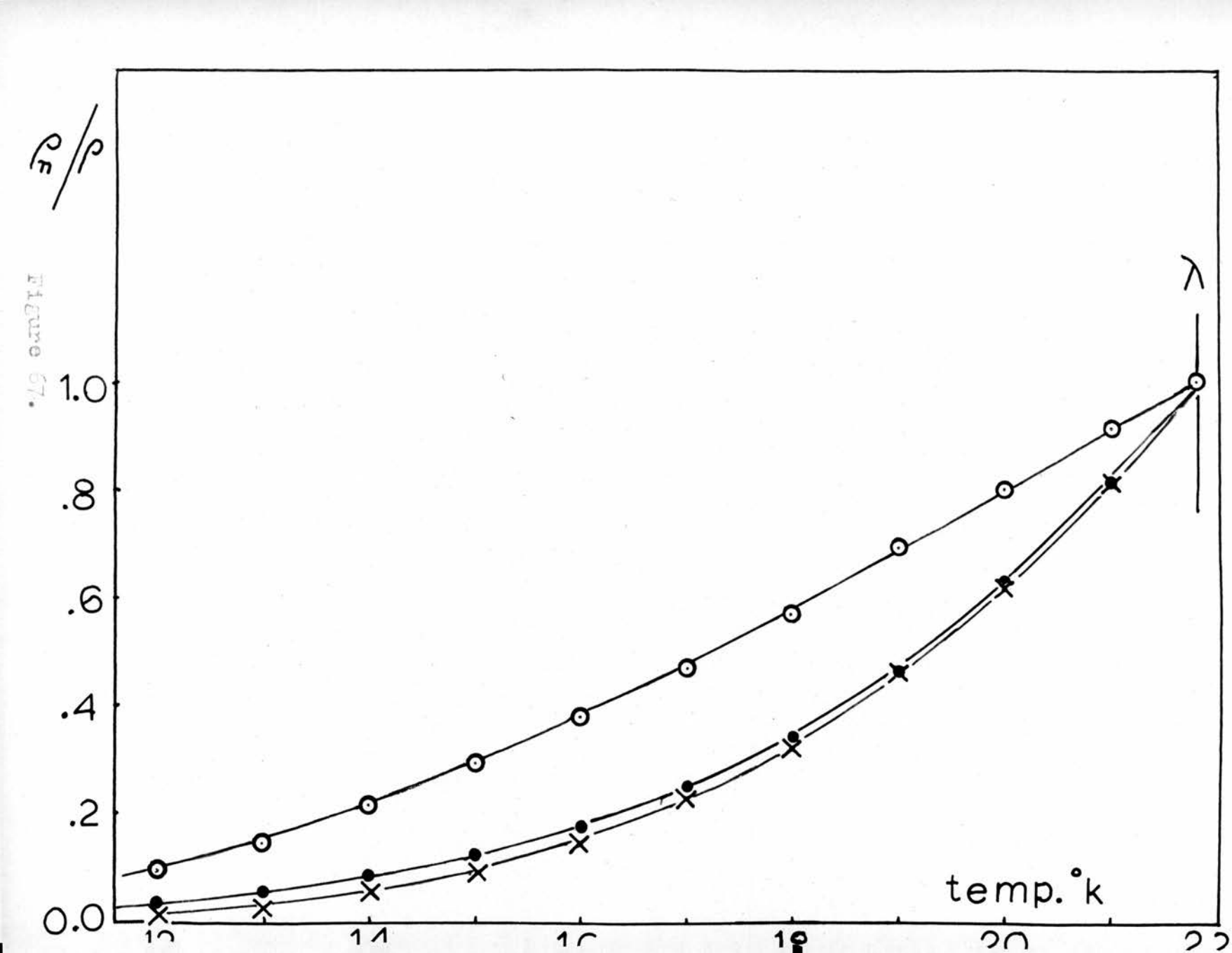
ρ_F/ρ
1.0
.8
.6
.4
.2
0.0
λ
temp. °k
12
14
16
18
20
22

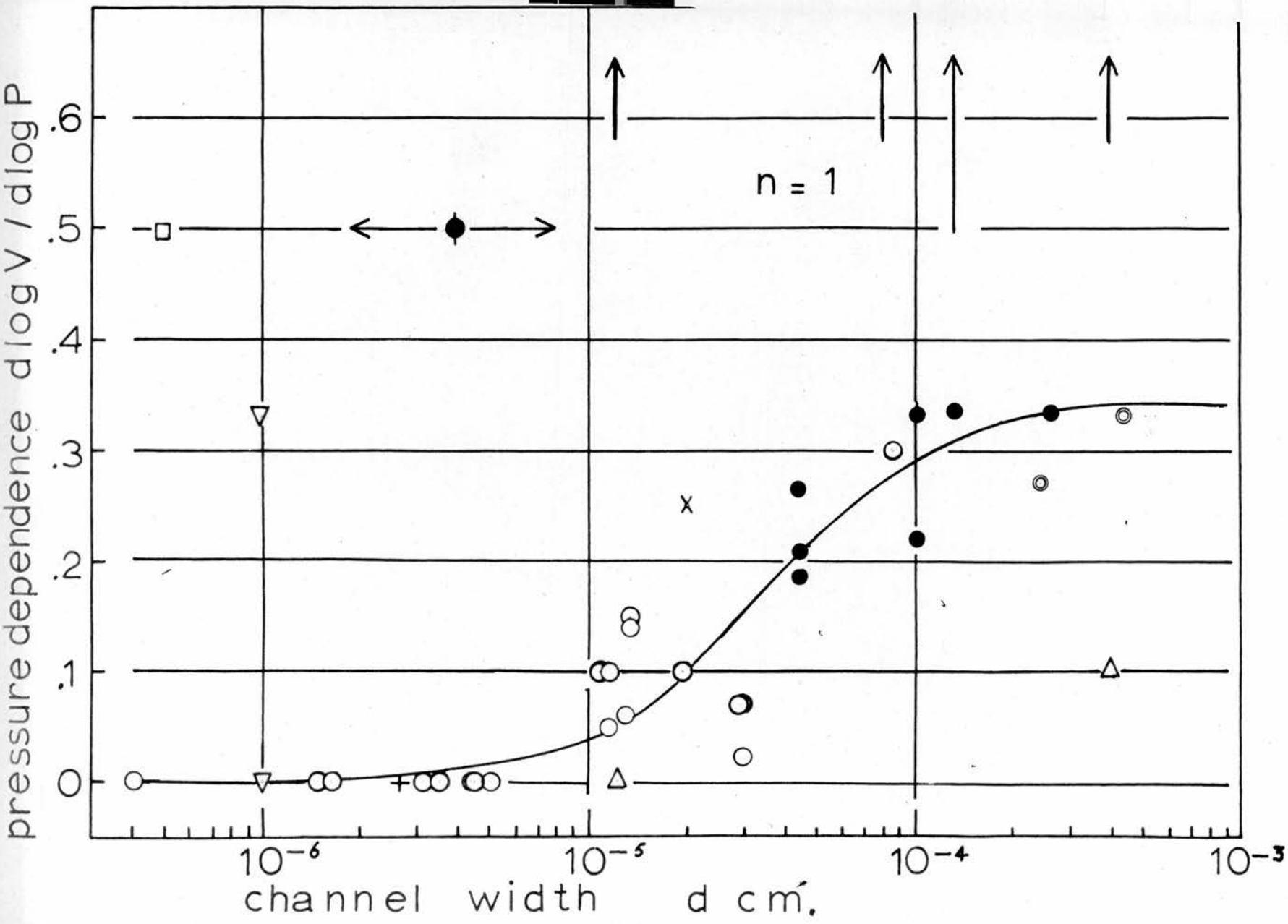
pressure dependence d log V / d log P
.6
.5
.4
.3
.2
.1
0
n = 1
10^{-6}
10^{-5}
10^{-4}
10^{-3}
channel width d cm.

△ Allen and Misener, (1939)., (high pressures).

○ Present author.

▽ Seki, (1962), (high pressures). $n = 0$.

● Hung, Hunt and Winkel, (1952) and Winkel, Delsing and Gorter, (1955).

◎ Swim and Rorschach, (1955).

□ Champeney, (1957)

▽ Seki, (1962). $n = 0.33$

↑ Arrows indicate measurements of n=1 by Allen and Misener (1939)., and Hammel and Keller, (1965).

Figure 68.

6.5 A regime resembling laminar flow of a classical liquid

Since this investigation has covered only certain aspects of flow in channels where $d < 10^{-4}$ cm it is only possible to make a few very speculative comments on flow in the range of sizes $d > 10^{-4}$ cm. In section 1, chapter 5, it was seen how a regime resembling laminar flow† of a classical fluid could arise due to poor thermal contact between reservoir and bath. When flow takes place under conditions of bad contact then the velocity v and hydrostatic pressure p are related by the equation

$$p - \Phi v = 0 \qquad (97)$$

where

$$\Phi = \frac{S^2 T A_2}{A_1 C(T)}$$

in which A_2 refers to the channel area, A_1 the contact area and the other constants are as previously defined.

Examination of figure (68) shows that if the points corresponding to values of n = 1, 0.5 and 0.3 (for $d = 10^{-6}$ cm) are ignored then there appears to be a fairly simple relation between n and d. This relation could be interpreted as implying that in channels where $d > 10^{-4}$ cm the mutual friction force is important in determining the relation between v and p but when $d < 10^{-5}$ cm then n = 0 and v is independent of p.

---

†Allen and Misener (1939) observed that for $p < 40$ dynes cm^{-2} at temperature $T \gtrsim 1.75°K$ there was a regime where $v \propto p$.

This approach may be an over simplification of the complex phenomena of superflow in narrow channels but measurements by van Alphen (1965) on flow through Vycor glass and jewellers rouge offer some support to the belief that thermal effects may give rise to values of $n > 0.3$. The experiments of Atkins (1951) with a capillary of diameter 81.5μ showed that v was proportional to $p^{1/3}$. Recent experiments by Bhagat and Mendelssohn (1961) have shown that for d = 89μ, v and p are related by

$$v = v_c - K \text{ grad } p .$$

They also found that K was a constant but depended on initial level difference. Recently Hammel and Keller (1965) have also observed a similar regime (n = 1) when d = 0.31μ, 2.29μ and 3.3μ but state that the v_s - p curves jumped about both from run to run and even during a single run. These latter authors do not as yet propose any explanation of their results and it is not clear whether their observations are related to those of Bhagat and Mendelssohn.

In attempting to explain the regime n = 1 Bhagat and Mendelssohn have discussed their results in terms of a superfluid eddy viscosity η_s. The term f_s in the thermohydrodynamic equation they replace by $\eta_s \nabla^2 v_s$ and the eddy viscosity is imagined as arising from the interaction of vortices in the superfluid. If we suppose that for some reason the thermal contact in these experiments is less good than the authors supposed we must enquire how

the initial height dependence can come about. Referring now to the adjoining figure the area of contact A_1 is given by

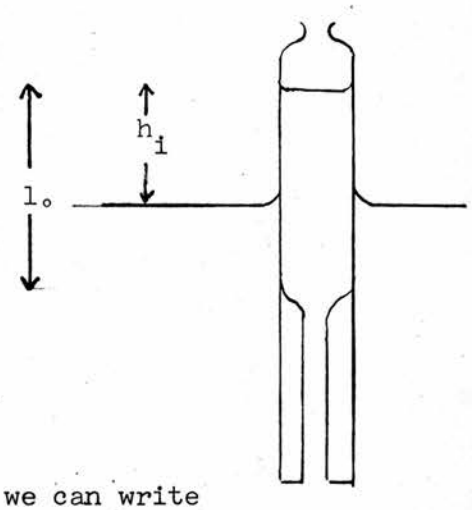

$$A_1 = \pi d(l_o - h_i)$$

$$= \xi (1 - h_i/l_o)$$

where ξ is a constant determined by the reservoir diameter.

In the case of thermally controlled flow we can write

$$v \propto (1 - h_i/l_o) \cdot p \ . \qquad (98)$$

Bhagat and Mendelssohn (1961), to describe their results, defined an effective viscosity η_{eff},

$$\eta_{eff} = \eta_s + \eta_n$$

and for the pressure dependent part of v (which they called v_p) wrote

$$v_p = - \frac{a^2}{8} \left[\left(\frac{\rho_n}{\rho}\right)^2 \frac{1}{\eta_n} + \left(\frac{\rho_s}{\rho}\right)^2 \frac{1}{\eta_s} \right] \text{grad } p \ .$$

At low temperatures

$$\left(\frac{\rho_n}{\rho}\right)^2 \ll \left(\frac{\rho_s}{\rho}\right)^2$$

and $\eta_s \sim \eta_n$ so we can write v_p as,

$$v_p \approx -\frac{a^2}{8}\left(\frac{\rho_s}{\rho}\right)^2 \frac{1}{\eta_s} \text{ grad } p \qquad (99)$$

i.e. $v_p \propto \frac{1}{\eta_s}$, p, by dropping the temperature dependent part. We see by comparing equation (98) and (99) that if the effect they observed was of thermal origin then η_s should depend on initial level difference as

$$\eta_s \propto \left(1 - \frac{h_i}{l_o}\right)^{-1} \sim 1 + \frac{h_i}{l_o} \quad . \qquad (100)$$

The quantity η_s should increase with h_i. Bhagat and Mendelssohn did observe η_s to increase with h_i but as $(h_i)^\beta$, where $\beta \sim 0.7$ and varied with temperature. Since we have no knowledge of the precise experimental procedure and also since the concept of an eddy viscosity gives a fairly satisfactory qualitative explanation of the regime n = 1 we can do no more than point out that thermal effects can probably cause a flow resembling classical laminar flow.

The complexity of flow in narrow channels is further emphasized by the recent observation of Hammel and Keller (1965) of a friction force whose magnitude is proportional to $(v_s - v_c)^{1.75}$. This force corresponds neither to mutual friction nor to thermal effects. Richards and Anderson (1965) have investigated flow through a pin-hole of size 15μ, observed slightly pressure dependent flow, a critical velocity of 27 cm sec^{-1} and flow rates which

depended on the vortex line density in the neighbourhood of the orifice. It is clear that there are a great many unsolved questions relating to superflow of liquid He II in narrow channels.

6.6 Summary

To facilitate the measurements described in this thesis the reservoirs were designed so that the magnitude of temperature differences between reservoir and bath were reduced to the point where the hydrostatic head equalled the total driving pressure. The efficacy of this procedure has recently been verified experimentally by Keller and Hammel (1965). The latter authors have also investigated flow from closed reservoirs where there is no thermal contact via the vapour phase, and measured the temperature differences which arise during the flow process. One interesting feature of their work was that when the flow caused a temperature difference of 32μ degree no critical velocity was observed but instead the flow velocity fell asymptotically to zero. This observation is not inconsistent with the discussion given in Chapter 5.1.

Evidence to support the transition to a flow regime where the flow velocity is independent of pressure has been recently obtained in an investigation by van Alphen et al (1965), who used both Vycor glass and jewellers rouge type superleaks.

There is much scope for further investigations of superfluid flow at temperatures in the range $1°K < T < T_\lambda$ and also for $T < 1°K$. It should be possible to use the dielectric property of He II to measure flow rates, and in the case of low temperature investi-

gations, $T < 1°K$, this would be an important advantage since it dispenses with the need for visual observations which in turn means that the flow vessel can be completely protected from incident radiation. This suggested method could also be adapted to investigate the oscillatory motion subsequent upon superflow.

Tab

Date	Number of wires in w-f-t	Half perimeter of wires after drawing q/2 cm	Period of oscillation τ sec	Area of reservoir + side arm A x 10^2 cm^2	Length of w-f-t cm
11.12.62	6000 (1)	47.7	3.9 (s)	8.46, 14.6	10.4
23. 1.63	6000 (2)	43.7	-	84.6 , 14.6	12.8
30. 1.63	6000 (2)	43.7	23.0 (l)	84.6 , 14.6	12.8
13. 2.63	6000 (3)	43.6	9.64 (s)[†] 2.36 (l)	84.0 , 14.8	7.8
15. 3.63	6000 (4)	41.9	13.06 (s)	83.2 , 14.0	4.4
10. 9.63	6502 (5)	43.1	17.53 (s)	84.0 , 14.8	9.9
24. 9.63	6502 (6)	45.0	10.7 (s)	84.0 , 14.8	11.05
8.10.63	6700 (7)	44.6	10.31 (s)	84.0 , 14.8	10.6
10.10.63	6600 (8)	47.0	15.51 (l) 6.41	84.0 , 14.8	9.6

ɔss- ıal v-f-t :m^2	Channel width d cm $2S_o\rho_s/\rho q$	Flow rate at zero pressure $\dot{x}$ div. sec^{-1}	Mean superfluid critical velocity v_c cm/sec $\dot{x}\, A\rho/\rho_s S_o$	Dependence of velocity on driving pressure $\frac{d \log v}{d \log p}$
0^{-3}	8.45×10^{-4}	0.725 (1) (1.25)*	7.0	0.3
	-	-	-	0.1
0^{-4}	1.91×10^{-5}	0.22 (1) (1.27)	10.3	0.1
0^{-4} 0^{-4}	1.15×10^{-5} 1.08×10^{-5}	2.96 (s)(1.25)	10.5 11.1	0.1
0^{-4}	3.49×10^{-6}	1.25 (s)(1.22)	14.35	0.0
0^{-4}	4.45×10^{-6}	0.24 (1)(1.17)	12.6	0.0
0^{-4}	1.33×10^{-5}	0.48 (1)(1.165)	8.07	0.14
0^{-4}	1.33×10^{-5}	0.54 (s)(1) (1.17)	9.24	0.15
0^{-3} 0^{-3}	2.88×10^{-5} 2.96×10^{-5}	1.67 (1)(1.17)	12.4 12.05	0.07

(continued on next page.....)

(continued.....)

Table 1

Date	Number of wires in w-f-t	Half perimeter of wires after drawing q/2 cm	Period of oscillation τ sec	Area of reservoir + side arm A x 10^2 cm^2	Length of w-f-t cm	Open cross-sectional area of w-f-t $S_o \rho_s/\rho$ cm^2	Channel width d cm $2S_o \rho_s/\rho q$	Flow rate at zero pressure $\dot{x}$ div. sec^{-1}	Mean superfluid critical velocity v_c cm/sec $\dot{x} A\rho/\rho_s S_o$	Dependence of velocity on driving pressure $\frac{d \log v}{d \log p}$
17.10.63	6000 (9)	42.9	10.98 (s)	84.0 , 14.8	9.8	4.84×10^{-4}	1.13×10^{-5}	0.466 (1) (1.165)	9.72	0.05
26.11.63	6600 (10)	44.2	9.78 (s)	83.98 , 14.78	9.2	5.74×10^{-4}	1.3×10^{-5}	0.652 (1) (1.19)	11.4	0.06
28.11.63	6600 (11)	43.8	10.60 (s)	83.98 , 14.78	9.6	5.1×10^{-4}	1.16×10^{-5}	0.655 (1) (1.18)	12.9	0.0
5.12.63	6600 (12)	43.0	17.31 (s)	83.98 , 14.78	9.4	1.87×10^{-4}	4.35×10^{-6}	1.44 (s) (1.195)	13.65	0.0
12.12.63	6600 (13)	42.4	11.0 (s)	15.01 , 4.04	9.75	1.31×10^{-4}	3.1×10^{-6}	1.0 (1) (1.16)	13.75	0.0
17.12.63	6600 (14)	40.7	15.12 (s)	15.01 , 4.04	9.2	6.55×10^{-5}	1.61×10^{-6}	0.439 (1) (1.18)	12.07	0.0
9. 1.64	6600 (15)	40.7	12.44 (s)	13.50 , 2.525	9.2	6.04×10^{-5}	1.48×10^{-6}	0.486 (1) (1.17)	13.05	0.0
16. 1.64	6600 (16)	47.0	2.14 (s) 6.0 (n)	1.63(6), 13.9 35.6 , 82	9.6	1.38×10^{-3} 1.49×10^{-3}	2.94×10^{-5} 3.16×10^{-5}	0.356 (1) (1.19)	11.1 10.25	0.02(4)
28. 1.64	6600 (17)	38.4	14.2 (s)	2.52(5), 0.81(8)	9.4	1.54×10^{-5}	4.01×10^{-7}	0.498 (1) (1.18)	9.8	0.0

(footnotes over page.....)

Footnotes to Table 1

† (s), (m) and (l) refer to small medium and large reservoir diameters respectively.

ø 1 division equals 4.6×10^{-2} cm, elsewhere 1.2×10^{-2} cm.

ẋ (1.25) refers to temperature at which $\dot{x}$ was measured.

T°K	$(T/T_\lambda)^{-\frac{1}{2}}$	$\exp {}^{\dagger}\Delta/k(\frac{1}{T_\lambda} - \frac{1}{T})$	$(\frac{T}{T_\lambda})^{-\frac{1}{2}}\exp\frac{\Delta}{k}(\frac{1}{T_\lambda} - \frac{1}{T})$	ρ_s/ρ
2.18	1.00	1.00	1.00	0.0
2.10	1.02	0.86	0.875	0.125
2.00	1.04	0.70	0.726	0.274
1.90	1.07	0.565	0.605	0.395
1.80	1.10	0.433	0.475	0.525
1.70	1.13	0.326	0.368	0.632
1.60	1.17	0.239	0.344	0.656
1.50	1.2	0.168	0.202	0.798
1.40	1.25	0.111	0.139	0.861
1.30	1.3	0.068	0.088	0.912
1.20	1.35	0.040	0.054	0.946

Calculation of ρ_s/ρ from equation (18) of 1.3

${}^{\dagger}\Delta/k$ taken as 8.6°K [obtained from neutron scattering data of Yarnell et al (1959) by interpolation to 1.2°K. The temperature dependence of Δ was neglected. Further, the contribution of phonons to ρ_n/ρ (about 2% at 1.2°K, see London, F (1954) p 100) was neglected in calculating ρ_s/ρ.]

Table 2

T°K	T/T_λ	$(T/T_\lambda)^{3/2}$	$(\frac{T}{T_\lambda})^{3/2} \exp\frac{\Delta^\dagger}{k}(\frac{1}{T_\lambda} - \frac{1}{T})$	ρ_s/ρ
2.18	1.000	1.000	1.000	0.000
2.10	0.964	0.945	0.814	0.186
2.00	0.918	0.875	0.612	0.388
1.90	0.872	0.813	0.460	0.540
1.80	0.826	0.759	0.328	0.672
1.70	0.780	0.693	0.226	0.774
1.60	0.734	0.630	0.150	0.850
1.50	0.689	0.575	0.096	0.904
1.40	0.643	0.513	0.057	0.943
1.30	0.596	0.456	0.031	0.969
1.20	0.550	0.408	0.016(6)	0.983

Calculation of ρ_s/ρ from equation (3) of 1.3

$\dagger\Delta/k$ taken as 8.6°K [See Table 2]

Table 3

$T\ ^{\circ}K$	T/T_λ	$(T/T_\lambda)^{5.6}$	ρ_s/ρ
2.18	1.000	1.000	0.000
2.10	0.964	0.814	0.186
2.00	0.918	0.630	0.370
1.90	0.872	0.456	0.544
1.80	0.826	0.346	0.654
1.70	0.78	0.252	0.748
1.60	0.734	0.178	0.822
1.50	0.689	0.123	0.877
1.40	0.643	0.087	0.913
1.30	0.596	0.056	0.944
1.20	0.550	0.035	0.965

ρ_s/ρ calculated from ~~equation (1) of 1.1~~ $\left\{1-\left(\frac{T}{T_\lambda}\right)^{5.6}\right\}$
after Andronikashvili (1946)

Table 4

Pore size (Diameter in μ)	Dimensional variation (μ)	Pore volume (% of total filter volume)α	Total cross-sectional* area of the pores (% of the filter area)β
.01	.002	75	62
.05	.003	76	63
.10	.008	77	64
.22	.02	77.5	64
.30	.02	78.5	65
.45	.03	80.5	66
.65	.03	82	68
.80	.05	83	68
1.2	.3	83	68
3.0	.9	85	70
5.0	1.2	86	71

Data provided by Millipore Filter Corporation

* Assuming the pores to be conical and that $\beta = 0.825\alpha$

Seki (1962)

Table 5

Superleak	d cm	σ
Millipore filter	1.2×10^{-4}	7
Millipore filter	5×10^{-6}	1.5
Wire-filled tube	1.3×10^{-5}	7
Wire-filled tube	1.2×10^{-5}	7
Wire-filled tube	4.4×10^{-6}	7
Wire-filled tube	4×10^{-7}	3

The functional dependence of v on T can be expressed as $v = k(1 - (T/T_\lambda)^{\sigma})$ where k is a constant.

Values of σ are given in the table.

Table 5

Legend of figures

Fig. 1 Excitation spectrum of liquid helium II.

Fig. 2 Schematic diagram of an annular superleak formed by pressing together two optically flat discs.

Fig. 3 Classical flow from an orifice.

Fig. 4 Feynman's model of superflow from an orifice.

Fig. 5 Apparatus for wire-winding.

Fig. 6 Steel drawing piece for attaching the wire-filled tubes to the winch.

Fig. 7 Channel width d as a function of final die size.
+ d from gas flow at nitrogen temperature.
o d from gas flow at room temperature.
x d from period of inertial oscillations.

Fig. 8 The length of a wire bundle at various stages during the draw process.

Fig. 9 Shows a photomicrograph of steel wires initially of diameter 0.006", drawn inside a copper-nickel tube.

Fig. 10 Shows copper wires initially 0.006" diameter, in a copper tube. Even though this tube was drawn down by an amount comparable with the other tubes large gaps remained. One possible explanation is that when the Poisson's ratio of tube and wires is the same the wires do not relax after passage of the tube through each die plate and consequently hexagonal deformation does not occur.

Fig. 11 Shows a photomicrograph of copper wires in a copper-nickel tube. These were used in the investigation. The channel structure was brought out by etching with nitric acid. The channels appear large because of the etching process.

Fig. 12 Similar to figure 11 but in this case the sample was diamond polished and the etching agent was ferric chloride.

Fig. 13 A schematic diagram of the gas flow cryostat used both for estimating channel size and also for flushing out the tubes with helium gas.

Fig. 14 An electron micrograph of a longitudinal section through a 4.5×10^{-5} cm size of Millipore filter.

Fig. 15 Mount for wire-filled tubes.

Fig. 16 Perspex apparatus for Millipore filters.

Fig. 17 Copper-glass apparatus for Millipore filters.

Fig. 18 Schematic diagram of reservoir and flow channels.

Fig. 19 Possible forms of $f(d)$.

Fig. 20 (a) Flow in a tapered channel.
(b) Another possibility for $f(d)$.

Fig. 21 Poiseuille flow in a tapered channel.

Fig. 22 Inertial oscillations.

Fig. 23 Apparatus designed to investigate pressure gradients within a superleak.

Fig. 24 Schematic diagram of helium cryostat.

Fig. 25 Open view of radiation shield.

Fig. 26 Gas handling system.

Fig. 27 Critical velocity and pressure index for channels of mean width ranging from 8.5×10^{-5} to 4×10^{-7} cm.

Fig. (28-36) Typical plots of level difference vs. time.

Fig. (37-41) Measurement showing how the level difference at an intermediate point along superleaks of size 4.5×10^{-6} cm and 8.5×10^{-5} cm varied with time.

Fig. (42-45) Measurements of mean flow velocity at temperatures between 1.2°K and the λ-point for $d = 1.2 \times 10^{-4}$ cm, 5×10^{-6} cm and 10^{-6} cm.

Fig. 46 The relation between v_c and d for the filters. Also shows comparison between values of v_c obtained from wire-filled tubes together with Seki's measurements on Millipore.

Fig. (47-50) Oscillatory motion of reservoir level for $d = 4.45 \times 10^{-6}$ cm and $d = 1.15 \times 10^{-5}$ cm.

Fig. 51 Damping of oscillations plotted as $\log_{10} \delta$ vs. 1/T.

Fig. 52 Velocity-temperature curve for wire-filled tube of size $d = 4 \times 10^{-7}$ cm.

Fig. (53-62) The v-T dependence of other superleaks. The reproducibility from run to run is exemplified in figure 55. Also at 1.2°K twelve level vs. time plots were made. These showed a standard deviation from the mean of 0.25% and a maximum deviation of 1.33%.

Fig. (63-66) The function $v\rho/\rho_s$ is plotted against temperature. For constant v_s this would be a straight line parallel to the temperature axis.

Fig. 67 ρ_n/ρ from tables 2, 3 and 4.

Fig. 68 The pressure index together with comparable data from Hung, Hunt and Winkel (1952), Winkel, Delsing and Gorter (1955), Wansink, Taconis, Staas and Reuss (1955), Allen and Misener (1939), Swim and Rorschach (1955).

References

Allen, J. F., Peierls, R. and Uddin, M. (1937) Nature 140, 62.

Allen, J. F. and Jones, J. (1938) Nature 141, 243.

Allen, J. F. and Misener, A. D. (1939) Proc. Roy. Soc. A172, 467.

Allen, J. F. (1963) Liquid Helium (New York and London: Academic Press).

Allen, J. F. and Watmough, D. J. (1965) Proc. IXth Int. Conf. on Low Temp. Phys. Columbus Ohio (to be published).

Allen, J. F. and Watmough, D. J. (1965) Proc. St. Andrews Symposium on Superfluid Helium (to be published).

Andronikashvili, E. (1946) J. Phys. U.S.S.R. 10, 201 also (1948) J. Expt. Theoret. Phys. U.S.S.R. 18, 424.

Atkins, K. R. (1948) Ph.D. Thesis, Cambridge.

Atkins, K. R. (1951) Proc. Phys. Soc. (London) A64, 833.

Atkins, K. R. (1950) Proc. Roy. Soc. (London) A203, 119.

Atkins, K. R. and Seki, H. (1957) Proc. Vth Int. Conf. on Low Temp. Phys. Madison.

Atkins, K. R. (1959) Liquid Helium Cambridge Monographs on Physics (Cambridge: University Press).

Bhagat, S. M. and Mendelssohn, K. (1960) Proc. VIIth Int. Conf. on Low Temp. Phys. Toronto.

Bhagat, S. M. and Mendelssohn, K. (1961) Cryogenics 2, 34.

Bowers, R., Brewer, D. F. and Mendelssohn, K. (1951) Phil. Mag. 42, 1445.

Bowers, R. and Mendelssohn, K. (1949) Nature 163, 870.

Chopra, K. L. (1957) Rev. Sci. Instruments 28, 146.

Champeney, D. C. (1957) Proc. Vth Int. Conf. on Low Temp. Phys. Madison.

Critchlow, P. (1960) Ph.D. Thesis, Oxford.

Daunt, J. G. and Mendelssohn, K. (1938) Nature 141, 911.

Daunt, J. G. and Mendelssohn, K. (1939) Proc. Roy. Soc. London A170, 439.

Daunt, J. G. and Mendelssohn, K. (1946) Nature, London 157, 829.

Edwards, M. H., McKirdy, A. S. and Woodbury, W. C. (1965) Proc. IXth Int. Conf. on Low Temp. Phys. Columbus Ohio (to be published).

Fairbank, H. A. and Wilks, J. (1955) Proc. Roy. Soc. A231, 545.

Feynman, R. P. (1955) Progress in Low Temperature Physics, Vol. I, Ch. II, Ed. C. J. Gorter, (North-Holland: Amsterdam).

Fineman, J. C. and Chase, C. E. (1962) Proc. VIIIth Int. Conf. on Low Temp. Phys. London.

Ginsburg, V. L. (1949) Dokl. Akad. Nauk. S.S.S.R. 69, 161.

Ginsburg, V. L. and Pitaevskii, L. P. (1958) Zh. Eksper. teor. Fiz. Vol. 34, No. 5, 1240.

Gorter, C. J. and Mellink, J. H. (1949) Physica 15, 285.

Hall, H. E. and Vinen, W. F. (1956) Proc. Roy. Soc. A238, 204.

Hammel, E. F. and Schuch, A. F. Proc. Vth Int. Conf. on Low Temp. Phys. Madison, Ed. J. R. Dillinger.

Hammel, E. F. and Keller, W. E. (1965) Proc. St. Andrews Symposium on Superfluid Helium (to be published).

Hung, C. S., Hunt, B. and Winkel, P. (1955) Physica 18, 629.

Kapitza, P. L. (1941) J. Phys. U.S.S.R. 4, 181.

Kapitza, P. L. (1962) J. Phys. U.S.S.R. 5, 59.

Keesom, W. H. and Keeson, A. P. (1936) Physica 3, 359.

Keesom, W. H. and MacWood, V. E. (1938) Physica 5, 737.

Keller, W. E. and Hammel, E. F. (1965) Cryogenics 5, 245.

Kuper, C. G. (1958) Physica 24, 1009.

Landau, L. D. (1941) J. Phys. U.S.S.R. 5, 71.

Landau, L. D. (1947) J. Phys. U.S.S.R. 8, 110.

Lin, C. C. (1963) Liquid Helium (New York and London: Academic Press).

London, F. (1938) Phys. Rev. 54, 947.

London, F. (1954) Superfluids Vol. II (New York: John Wiley and Sons).

London, F. (1938) Nature, 141, 643.

Manchester, F. D. and Brown, J. B. (1957) Can. J. Phys. 35, No. 4, 483.

Osborne, D. V. (1950) Proc. Phys. Soc. A63, 909.

Onsager, L. (1949) Suppl. Vol. VI, Series IX, Nuovo Cimento.

Raja Gopal, E. S. (1963) Ann. of Phys. 29, No. 3, 350.

Hung, C. S., Hunt, B. and Winkel, P. (1955) Physica 18, 629.

Kapitza, P. L. (1941) J. Phys. U.S.S.R. 4, 181.

Kapitza, P. L. (1962) J. Phys. U.S.S.R. 5, 59.

Keesom, W. H. and Keeson, A. P. (1936) Physica 3, 359.

Keesom, W. H. and MacWood, V. E. (1938) Physica 5, 737.

Keller, W. E. and Hammel, E. F. (1965) Cryogenics 5, 245.

Kuper, C. G. (1958) Physica 24, 1009.

Landau, L. D. (1941) J. Phys. U.S.S.R. 5, 71.

Landau, L. D. (1947) J. Phys. U.S.S.R. 8, 110.

Lin, C. C. (1963) Liquid Helium (New York and London: Academic Press).

London, F. (1938) Phys. Rev. 54, 947.

London, F. (1954) Superfluids Vol. II (New York: John Wiley and Sons).

London, F. (1938) Nature, 141, 643.

Manchester, F. D. and Brown, J. B. (1957) Can. J. Phys. 35, No. 4, 483.

Osborne, D. V. (1950) Proc. Phys. Soc. A63, 909.

Onsager, L. (1949) Suppl. Vol. VI, Series IX, Nuovo Cimento.

Raja Gopal, E. S. (1963) Ann. of Phys. 29, No. 3, 350.

Richards, P. L. and Anderson, P. W. (1965) Phys. Rev. Letters 14, 540.

Robinson, V. E. (1951) Phys. Rev. 82, Series 2, 440.

Rollin, B. V. and Simon, F. (1939) Physica 6, 269.

Seki, H. and Dickson, C. C. (1960) Proc. VIIth Int. Conf. on Low Temp. Phys. Toronto.

Seki, H. (1962) Ph.D. Thesis, Pennsylvania.

Staas, F. A. (1961) Ph.D. Thesis, Leiden. Flow phenomena of pure He^4 and He^4-He^3 mixtures in the He II region.

Swim, R. T. and Rorschach, H. E. (1955) Phys. Rev. 97, 25.

Tisza, L. (1938) Nature 141, 913.

Tisza, L. (1947) Phys. Rev. 72, 838.

van Alphen, N. M., Olijhoek, V. F. and de Bruyn Ouboter, R. (1965) Proc. St. Andrews Symposium on Superfluid Helium (to be published).

Vinen, W. F. (1957) Proc. Roy. Soc. A240, 114.

Vinen, W. F. (1957) Proc. Roy. Soc. A240, 128.

Vinen, W. F. (1957) Proc. Roy. Soc. A242, 493.

Vinen, W. F. (1957) Proc. Roy. Soc. A243, 400.

Vinen, W. F. (1963) Liquid Helium (New York and London: Academic Press).

Wansink, D. H. N., Taconis, K. W., Staas, F. A. and Reuss, J. (1955) Physica 21, 596.

Winkel, P., Delsing, A. M. G. and Poll, J. D. (1955) Physica 21, 332.

Winkel, P., Delsing, A. M. G. and Gorter, C. J. (1955) Physica 21, 312.

Yarnell, J.L., Arnold, G.P. & Bendt, P.J. and Kerr, E.C, (1959) Phys. Rev. 113, 1379